SCHOOL OF AMERICAN RESEARCH PRESS

ARROYO HONDO ARCHAEOLOGICAL SERIES

DOUGLAS W. SCHWARTZ
GENERAL EDITOR

ARROYO HONDO ARCHAEOLOGICAL SERIES

1
The Contemporary Ecology of Arroyo Hondo, New Mexico
N. Edmund Kelley

2
Prehistoric Pueblo Settlement Patterns: The Arroyo Hondo, New Mexico, Site Survey
D. Bruce Dickson, Jr.

3
Pueblo Population and Society: The Arroyo Hondo Skeletal and Mortuary Remains
Ann M. Palkovich

4
The Past Climate of Arroyo Hondo, New Mexico, Reconstructed from Tree Rings
Martin R. Rose, Jeffrey S. Dean, and William J. Robinson

PAST CLIMATE OF ARROYO HONDO

The publication of this volume
was made possible by a grant from the
NATIONAL SCIENCE FOUNDATION.

THE PAST CLIMATE OF ARROYO HONDO, NEW MEXICO, RECONSTRUCTED FROM TREE RINGS

Martin R. Rose
Jeffrey S. Dean
William J. Robinson

SCHOOL OF AMERICAN RESEARCH PRESS
ARROYO HONDO ARCHAEOLOGICAL SERIES, Volume 4

SCHOOL OF AMERICAN RESEARCH PRESS
Post Office Box 2188
Santa Fe, New Mexico 87504-2188
www.sarpress.sarweb.org

Douglas W. Schwartz, General Editor
Philip Brittenham, Director of Publications
Jane Kepp, Series Editor

Library of Congress Cataloging in Publication Data

Rose, Martin R.
The past climate of Arroyo Hondo, New Mexico, reconstructed from tree rings.

(Arroyo Hondo archaeological series ; v. 4)
Bibliography: p. 109
1. Arroyo Hondo site, N.M. 2. Dendroclimatology—New Mexico—Arroyo Hondo site. 3. Rain and rainfall—New Mexico—Arroyo Hondo site. 4. Paleoclimatology—New Mexico—Arroyo Hondo site. I. Dean, Jeffrey S., 1939– joint author. II. Robinson, William James, joint author. III. Title. IV. Series.
E99.P9R67 551.69789'56 80-21834
ISBN 0-933452-05-5

Library of Congress Catalog Card Number: 80-21834
International Standard Book Number: 978-0-933452-05-3 paper
First edition. Reprinted 2011.

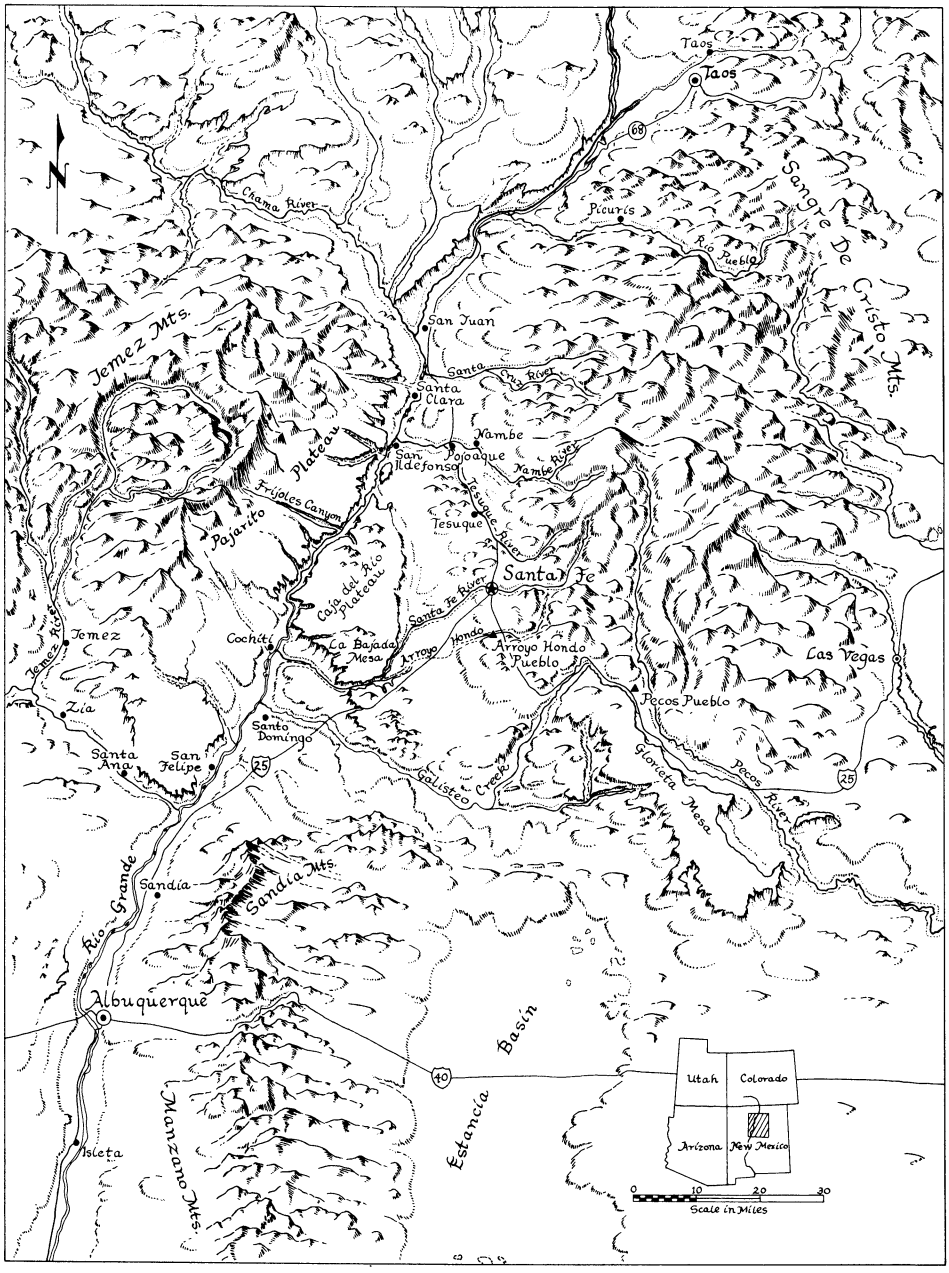

MAP 1. Location of Arroyo Hondo Pueblo in the northern Rio Grande region.

Foreword

Douglas W. Schwartz

Dendroclimatology, the study of the interrelationships between trees and climate, has entered a new age as the result of altered concepts, techniques, and equipment. This monograph clearly reflects the maturing sophistication of the discipline. The application of dendroclimatic methods to the wealth of tree-ring specimens from Arroyo Hondo Pueblo was fortunate for all concerned. For the authors of this volume, Arroyo Hondo provided the raw material necessary for the first attempt to "use archaeological tree-ring chronologies as a data base for quantitative reconstructions of climatic variables for the prehistoric period." To those of us involved in the archaeological interpretation of Arroyo Hondo Pueblo, this study offers a unique record of climatic variability: the reconstruction of annual and seasonal precipitation in inches from A.D. 985 to 1970.

The fourteenth-century town of Arroyo Hondo, located 4½ miles south of present-day Santa Fe, New Mexico (Map 1), was the focus of a multidisciplinary research project initiated in 1970 by the School of American Research. The project was designed to accomplish four main interrelated objectives:

1. provide ecological, regional, and chronological perspectives from which to understand the pueblo's sequence of change;
2. develop a detailed base of information about Pueblo culture in the northern Rio Grande region during the pivotal fourteenth-century period of large-settlement growth;

3. examine the causes and effects of the growth, change, and eventual decline of the pueblo;
4. use Arroyo Hondo Pueblo as a case study that could be combined with other archaeological, ethnographic, and historic data to examine the interplay of changes in population, resources, and culture in prehistoric agricultural communities.

The National Science Foundation supported excavation and laboratory work between 1971 and 1974 (grants GS-28001 and GS-42181), and interim results were published in three preliminary reports (Schwartz 1971, 1972; Schwartz and Lang 1973). At the end of fieldwork, a film entitled *The Rio Grande's Pueblo Past* was completed in collaboration with the National Geographic Society, illustrating the history of the project and presenting some initial conclusions. A subsequent National Science Foundation grant (BNS76-82510) provided support for the development and publication of the project results.

To document the project fully, a publication series of twelve volumes has evolved, eleven to present data and ideas on specific topics and the twelfth to synthesize the results and consider their broader implications. Although each of the first eleven volumes focuses on a particular set of data, each is also designed to stand independently as a contribution to northern Rio Grande archaeology. The final book in the series will place Arroyo Hondo Pueblo in historical perspective within the northern Rio Grande, integrate the contributions of the data volumes in terms of the culture and dynamics of the settlement, examine the interrelationships between population growth, resource use, and cultural change at Arroyo Hondo, and consider the cross-cultural implications of rapid growth in agricultural communities. The topics of the Arroyo Hondo volumes are contemporary ecology; site survey; skeletal and mortuary remains; dendroclimatology; palynology; faunal remains; paleoethnobotany and nutrition; bone, shell, and miscellaneous artifacts; lithic artifacts; ceramics; architecture; and project synthesis.

The dendroclimatological study reported in this volume provides significant insights into the prehistoric sequence of events at Arroyo Hondo Pueblo. So close is the correlation between the precipitation changes reflected by tree rings and the major developments seen in the archaeological record that we must infer a causal relationship between the two.

Arroyo Hondo Pueblo was established about A.D. 1300, when pre-

cipitation was increasing after a 50-year period of mostly below-average values. It may be that by making dry farming possible or by rejuvenating the spring in Arroyo Hondo Canyon below the pueblo, the increasing rainfall made this location attractive to settlers for the first time. Initially, a small group of farmers constructed an alignment of rooms along the edge of the canyon. The location selected was on a gently sloping piedmont at an elevation of 7,100 feet, immediately west of the foothills of the Sangre de Cristo Mountains. Emerging from the mountains and running southwest, the Arroyo Hondo cuts a gorge 125 feet deep and offers the best watered soils of the area (Kelley 1980). The site of the pueblo, in the past as at present, was surrounded by a piñon-juniper woodland that graded into ponderosa pine toward the mountains and into grasslands as the elevation dropped toward the south and west (Fig. 1). Thus, the settlers had ready access to the combined plant and animal resources of several ecological zones.

For most of the first 35 years of the existence of Arroyo Hondo Pueblo, precipitation remained above the long-term mean, and agriculture, the basis of the economy, probably was highly productive. Fields of corn, beans, and squash were planted in the farmland of the arroyo and probably on the piedmont around the village as well. The crops were supplemented by seasonally available wild greens, seeds, and nuts. Added protein was supplied by domesticated turkeys and at least 50 species of wild game, including jackrabbits, cottontails, mule deer, pronghorn antelope, and elk.

With this excellent ecological base and favorable climatic conditions, the pueblo grew to nearly a hundred times its original size in the first three decades of the 1300s. Adobe roomblocks were built at right angles to one another, forming open plazas that could be entered only by a single passageway. The settlement reached its greatest size around 1330, comprising 24 roomblocks constructed around ten wholly or partially enclosed plazas (Fig. 2). The population concentrated at the town by this time made Arroyo Hondo one of the larger communities in the region.

The roomblocks that composed the pueblo ranged from two to five rooms wide and up to fifteen rooms long. They were usually a single story on the exterior, stepping up to two stories near the central core. Internally, each block was divided into apartmentlike residence units of four or five interconnected ground-story rooms with related rooms on the second story. Rooms averaged about five square meters in floor

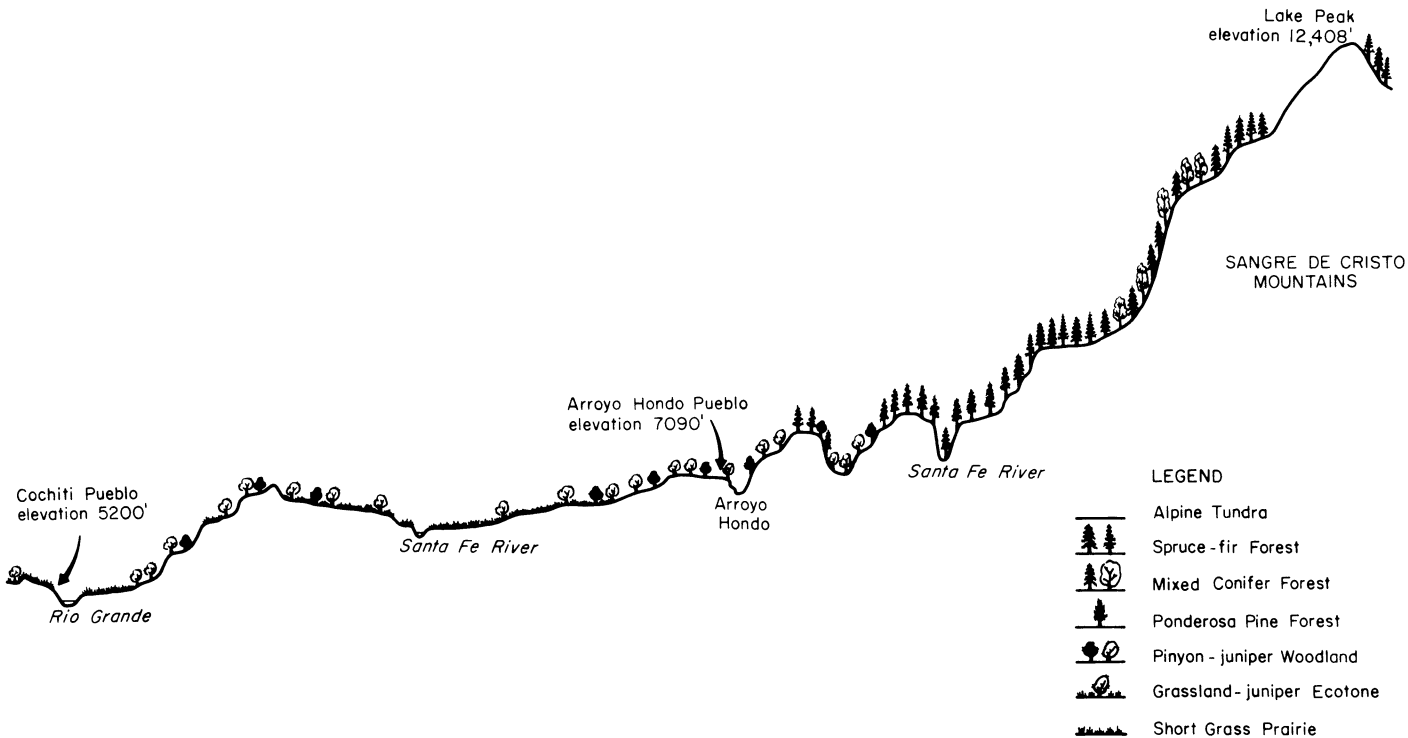

FIG. 1. Vegetation zones in a 38-mile transect from the Sangre de Cristo Mountains to the Rio Grande.

FIG. 2. Reconstruction of Arroyo Hondo Pueblo at about A.D. 1330.

area and were generally entered through hatchways in the roofs, which were built in standard Pueblo style, that is, with vigas, the major support beams, covered at right angles by smaller plank or pole latías. These roofing elements were the main source of tree-ring specimens recovered archaeologically.

Rooftops and plazas served as important adjuncts to the rooms and were used for cooking, food drying and processing, flint knapping, and pottery making. In some plazas and roomblocks were ceremonial kivas, while a larger kivalike structure located about 110 yards west of the pueblo probably served the whole community in a religious capacity. The material remains reflect a well-rounded, largely self-sufficient technology, and it is clear that the people at Arroyo Hondo prospered in the early 1300s.

Beginning about A.D. 1335, the pattern of precipitation shifted toward high annual variability, with severe droughts separated by brief wet intervals. The authors of this volume correctly predicted that this change would have required the residents of Arroyo Hondo to make major adaptations or even to abandon the pueblo temporarily. The archaeological record indeed shows that soon after A.D. 1335, the town's population began to decline even more dramatically than it had increased. The more recently built roomblocks were abandoned first, and the occupation contracted in the reverse order of the construction sequence. Some evidence of the economic hardships suffered at this time can be seen in the skeletal remains excavated at Arroyo Hondo. Nutritional stress indicated by bone pathologies probably was a major cause of the high infant mortality that characterized the pueblo's demography (Palkovich 1980). Although we cannot date the skeletal sample to discrete, short-term intervals within the Arroyo Hondo occupation sequence, it seems likely that mortality and the incidence of nutrition-related disease was highest during the droughts of the mid-1300s.

By about 1345, the pueblo was virtually abandoned. For the next 30 years, the ruined town was at most inhabited by a small remnant population, perhaps seasonally, and at times may have been vacant. Then, sometime during the 1370s, a second phase of settlement began in which a new town was built atop the ruins of the first. The resettlement coincided with a temporary return to high precipitation, but the new town did not reach its greatest expansion until the early 1400s, when the tree-ring data show a 10-year period of sustained high mois-

ture. Arroyo Hondo was once more on its way to becoming an active population center with extensive trade contacts, having grown to two hundred rooms organized in nine roomblocks around three plazas.

But the renewed growth did not continue, for soon after 1410, rooms were again being abandoned and demolished as population rapidly declined. Precipitation was also declining toward the lowest point in the 1,000-year tree-ring record, centered at A.D. 1420. Around that time, a catastrophic fire destroyed a large part of the village, and within a few more years the second and final occupation of Arroyo Hondo Pueblo came to an end.

The work of Rose, Dean, and Robinson contributes enormously to our understanding of the cultural dynamics of Arroyo Hondo Pueblo. Their approach to reconstructing climate from tree rings is much more than a simple translation of tree-ring widths into precipitation variability. Only a complex and exacting statistical analysis can produce the precision of result achieved in this study, which should prove invaluable to archaeologists throughout the Southwest.

References

KELLEY, N. EDMUND

1980 *The Contemporary Ecology of Arroyo Hondo, New Mexico*, Arroyo Hondo Archaeological Series, vol. 1 (Santa Fe: School of American Research Press).

PALKOVICH, ANN M.

1980 *Pueblo Population and Society: The Arroyo Hondo Skeletal and Mortuary Remains*, Arroyo Hondo Archaeological Series, vol. 3 (Santa Fe: School of American Research Press).

SCHWARTZ, DOUGLAS W.

1971 *Background Report on the Archaeology of the Site at Arroyo Hondo: First Arroyo Hondo Field Report* (Santa Fe: School of American Research).

1972 *Archaeological Investigations at the Arroyo Hondo Site: Second Field Report—1971* (Santa Fe: School of American Research).

SCHWARTZ, DOUGLAS W., AND RICHARD W. LANG

1973 *Archaeological Investigations at the Arroyo Hondo Site: Third Field Report—1972* (Santa Fe: School of American Research).

Contents

MAPS AND FIGURES

Maps

Figures

TABLES

Acknowledgments

The dendroclimatic analyses reported here could not have been accomplished without the support of several institutions. The National Science Foundation, through grants GS-247, 908, 2232, and 35086 to the Laboratory of Tree-Ring Research, supported the analysis of archaeological tree-ring material from the entire Southwest and the initial construction of the archaeological tree-ring chronologies on which the paleoclimatic reconstructions are based. Grant AFOSR 72-2406 from the Advanced Research Projects Agency financed the collection and analysis of samples from living trees that were used to extend the archaeological chronologies to the present. The Southwest Region and the Interagency Archeological Services Division of the National Park Service, through a series of six contracts, supported the Laboratory's Southwest Paleoclimate Project, which undertook the final data processing and analyses involved in the reconstruction of dendroclimatic variability from A.D. 680 to 1970 in the northern Southwest.

Many individuals contributed to various aspects of the work reported here. Among those who participated in the laboratory analyses of the samples and in data processing are Richard V. N. Ahlstrom, Dennie O. Bowden III, John W. Hannah, and Richard L. Warren. Invaluable consultation on the intricacies of dendroclimatic calibration, verification, and reconstruction was provided by T. J. Blasing, Harold C. Fritts, David M. Meko, Charles W. Stockton, and C. Larrabee Winter. Linda G. Drew, head of the Laboratory's Data Processing Section, played her customary crucial role in the data processing and analysis phases of the work. Mary Kathleen Klobnak prepared the final

versions of the illustrations that accompany this report. Finally, we are indebted to Douglas W. Schwartz, President of the School of American Research, for providing the stimulus for this study, our first attempt to use archaeological tree-ring chronologies as a data base for quantitative reconstructions of climatic variables for the prehistoric period.

Introduction

Excavations by the School of American Research at Arroyo Hondo Pueblo (LA 12), New Mexico, between 1970 and 1974 produced more than 1,000 tree-ring samples. These specimens, most of them charcoal fragments, were submitted to the Laboratory of Tree-Ring Research at The University of Arizona for dendrochronological dating. Species represented in the Arroyo Hondo collection are, in order of decreasing frequency, piñon *(Pinus edulis)*, ponderosa pine *(P. ponderosa)*, Douglas fir *(Pseudotsuga menziesii)* and true fir *(Abies* spp.), juniper *(Juniperus* spp.), cottonwood or aspen *(Populus* spp.), and nonconiferous shrub species (less than one percent). This distribution of species is consistent with the present environment of Arroyo Hondo Pueblo. The site is situated in the piñon-juniper forest on the west flank of the Sangre de Cristo Mountains (Map 1, Fig. 1), and ponderosa pine and Douglas fir could have been procured in the mountains only a few miles east of the site before these species were depleted by modern logging activities.

The tree-ring samples from Arroyo Hondo were subjected to standard dendrochronological dating procedures (Stokes and Smiley 1968), and more than 300 of the piñon, ponderosa, and fir samples were absolutely dated. The remaining specimens failed to yield dates because they were of unsuitable species, had too few rings to establish crossdating, or had ring series with characteristics that precluded dating. The 300+ dates form the basis for the calendric chronology of events in the construction history of the site.

A number of the dated tree-ring samples were measured to provide the ring-width data necessary to develop for the site a quantified com-

posite chronology suitable for dendroclimatic analysis. Data from specimens exhibiting a strong climatic signal (Fritts 1976) were incorporated into the special Arroyo Hondo dendroclimatic chronology, which extends from A.D. 982 through 1410. The selection, measurement, standardization, and merging procedures employed in building such a chronology are described by Stokes and Smiley (1968:55–61), Fritts (1976), and Fritts, Mosimann, and Bottorff (1969).

In addition to the Arroyo Hondo tree-ring material, the Laboratory of Tree-Ring Research has a large collection of tree-ring samples and quantified tree-growth data from other archaeological sites (Robinson, Harrill, and Warren 1973) and from living trees in the Santa Fe area. These data were used to construct a local Santa Fe dendroclimatic tree-ring chronology that is included in a spatial network of chronology stations that forms the basis for reconstructing paleoclimatic variability throughout most of the Southwest over the last 1,200 years (Dean and Robinson 1977). The Santa Fe chronology is used to broaden the time range and geographical scope of the Arroyo Hondo dendroclimatic analyses. The application of recently developed statistical techniques for quantifying the relationships between tree growth and climate (Fritts 1976) to the high quality tree-ring chronologies now available for the Santa Fe area provides the basis for reconstructing paleoclimate in the vicinity of Arroyo Hondo Pueblo. This is our first attempt to use archaeological tree-ring chronologies for quantitative reconstructions.

1
Dendroclimatology

The physiological processes that control tree growth are influenced by external environmental variables. Those variables that limit physiological processes also limit radial growth, producing a permanent record of their effects in the annual growth increment. Because climate is the primary limiting factor to growth in the arid Southwest, the sequence of narrow and wide rings in a southwestern tree-ring chronology is a partial record of year-to-year fluctuations in climate. Recent research in dendroclimatology, the subdiscipline of dendrochronology concerned with the interrelationships of tree growth and climate (Fritts 1976), has produced techniques for extracting some of the climatic information contained in tree-ring series. The application of these techniques to archaeological tree-ring chronologies, such as those available for the area around Arroyo Hondo, permits the quantitative reconstruction of some aspects of the paleoclimate of the localities represented by the chronologies.

Climatic influence on the growth of trees has been a major focus of attention throughout the 75-year history of dendrochronology. A postulated relationship between tree growth and weather first stimulated the astronomer Andrew Ellicott Douglass to study the rings of trees and to develop the science of dendrochronology. Douglass and his colleague Edmund Schulman, using trees from western North America, demonstrated a positive relationship between tree-ring widths and the rainfall of the winter preceding each growing season (Douglass 1914; Schulman 1956:39–51). Their studies led to the formulation of a model of the relationship between tree growth and environment that specified soil moisture held over from the winter into the spring grow-

ing season as the primary environmental control of tree growth. This model was widely accepted and used by archaeologists in their attempts to relate tree-ring records to prehistoric events.

In the 1960s, the conjunction of three factors revolutionized the study of dendroclimatology. First, investigators trained in biology and familiar with the physiological processes of tree maintenance and growth became active in dendrochronology. Second, multivariate statistical techniques capable of controlling many variables were applied to the problems of dendroclimatology. Third, electronic computers made possible the analysis of the large number of variables and the great quantities of data involved. Recent dendroclimatic research has been focused on the interactions of the many environmental variables that influence tree growth and has revealed the extreme complexity of the relationships involved. Two general approaches have been emphasized in the study of relationships between tree growth and environment: (1) multivariate analyses of the covariation of measures of radial growth and of the environment (Blasing 1975; Blasing and Fritts 1975, 1976; Fritts 1966, 1971, 1974; Fritts et al. 1971; Fritts, Smith, and Stokes 1965; Julian and Fritts 1968); and (2) physiological and growth studies of living arid-site trees that have been subjected to carefully measured and partly controlled environmental constraints (Brown 1968; Budelsky 1969; Fritts 1969; Fritts et al. 1965; Fritts, Smith, and Stokes 1965). The studies of living trees elucidate the ways in which external conditions impinge on the life processes of the trees to produce the relationships indicated by the statistical analyses.

This research has produced analytical techniques for determining the quantitative effects of various factors on the radial growth of trees. Application of these techniques has shown that in general, conifers growing under the limiting conditions of the lower forest border in the arid Southwest respond primarily to the precipitation and secondarily to the temperatures of the year prior to the growing season and of the growing season itself. Subordinate to this general response are climatic relationships that differ from species to species and from site to site. In effect, each species responds to conditions of different parts of the year preceding the growing season and therefore records in its growth rings climatic information slightly different from that recorded by each of the other species. Thus, in addition to the annual climatic information contained in tree-ring sequences, intra-annual (seasonal) variability in climate is preserved as well.

One result of this research has been the development of a new model of the relationships between tree growth and climate (Fritts 1976:231–38). Although far more complex than the residual soil moisture model, the new model holds much greater significance for paleoclimatic reconstructions based on dendrochronological data. In this model, the link between the previous year's climate and current growth is stored food reserves rather than holdover soil moisture. Conditions during the year that favor photosynthesis over respiration result in the production of surplus food, which is stored in the cells of the tree until needed for the tree's maintenance or growth. Much of this reserve is not used until the following spring when it is metabolized to supply the energy necessary for growth. During the growing season, arid-site conifers often produce no food except that used in respiration, and growth depends entirely on stored food (Fritts 1976:181). If the conditions of the previous year have not been conducive to food production, the lack of stored reserves limits growth, and a narrow annual ring is formed.

The studies of the responses of tree growth to various external factors and the models derived from them are the foundation for dendroclimatic reconstructions of past environmental conditions. Several techniques have been developed for extracting environmental information from long-range tree-ring series. The simplest uses the departures of tree growth from the long-term mean as measures of variability in precipitation and temperature over the period of dendrochronological record. This method was used by Fritts (1965) to reconstruct patterns of climatic variation throughout western North America from A.D. 1500 to 1940 and by Robinson and Dean (1969; Dean and Robinson 1977) to make similar projections for the Southwest from A.D. 680 to 1970. Other techniques permit the reconstruction of atmospheric pressure-pattern anomalies (Blasing 1975; Blasing and Fritts 1975, 1976; Fritts 1971; Fritts et al. 1971) and the estimation of past surface runoff (Stockton 1975; Stockton and Fritts 1971a, 1971b). Kemrer, Robinson, and Dean (1971) attempt to use differential seasonal climatic input into the growth of different species to identify intra-annual variations in the prehistoric climate of Mesa Verde, Colorado.

Two major assumptions underlie the attempted reconstruction of aspects of the paleoclimate of the Southwest in general and the Arroyo Hondo area in particular. First, we take the position that tree-growth response to climate was the same in the past as it is today. Several types of evidence support this assumption. The fact that a continuous 2,200-

year tree-ring chronology composed of thousands of overlapping ring sequences from at least five tree species can be constructed indicates that there has been no basic change in the growth-climate relationships of each species during the period of record. The lack of appreciable change in the elevational and environmental distributions of the various species during the last 2,000 years also indicates that there have been no fundamental changes in the ways in which the trees respond to climate. Finally, the statistical characteristics of modern tree-ring series do not differ significantly from those of the prehistoric chronologies.

Our second major assumption is that there has been no change in the type of climate prevalent in the Southwest during the 2,200-year period covered by the tree-ring chronologies. Schoenwetter (1962:191–94) presents the case in support of this assumption, and we do not argue it here. Suffice it to say that pollen studies, geological evidence, and plant and animal distributions lend strong support to this position. Given this assumption, the phenomena of concern to us are relatively short-term variations within the range of a single type of climatic regime.

The Arroyo Hondo study is the first attempt by the Laboratory of Tree-Ring Research to use archaeological tree-ring chronologies as a basis for quantitative rather than qualitative reconstructions of past climatic variability. This effort involves the application of statistical techniques developed by the Laboratory's dendroclimatic research program to the analysis of long tree-ring sequences that include material from archaeological sites. Two different approaches to quantitative dendroclimatic reconstruction have been developed. The more complex approach uses spatial grids of tree-ring chronologies and weather stations to establish networks of tree-growth–climate relationships that are used to reconstruct climatic variability for points within the boundaries of the grid. The simpler technique uses the relationships between tree-ring and weather data for a single locus as the basis for reconstruction. The second approach is employed in the Arroyo Hondo study because its greater simplicity is appropriate to an initial attempt to apply analytical techniques to different kinds of data. The method involves establishing a mathematical relationship between the two synchronous time series—the tree-ring chronologies and the weather records—for their period of overlap. The relationship is then used as a basis for estimating incremental values of one time series from the known values of the other. In this case, tree-ring data, which cover a

much longer time span than do weather records, are used as predictors of climatic values. This method is a complex one consisting of five distinct but interrelated steps (Fig. 3): (1) evaluation of tree-ring data; (2) evaluation of climatic data; (3) calibration of the tree-ring and climatic time series; (4) verification of the calibration; (5) retrodiction of past climatic values from the long-range tree-ring chronologies.

Four tree-ring series are used in the Arroyo Hondo study: a series from a group of living piñon trees on Glorieta Mesa, New Mexico; two archaeological series, one of them derived from Arroyo Hondo charcoal and the other from material from other prehistoric and historic sites in the Santa Fe area; and a composite climatic chronology created by merging the Santa Fe archaeological and Glorieta Mesa sequences. These chronologies must be evaluated with respect to the amount of climatic information they contain and to the homogeneity of the ring records through time. An important step in the evaluation process is ensuring that the chronologies contain a high percentage of climate-related variance. Living-tree chronologies are constructed from trees growing on sites with attributes known to enhance climate input into tree growth (Fritts 1976:17–19, 29–31). The degree of climatic sensitivity of these series is measured by correlating them with weather records from nearby locations. Climate-sensitive archaeological tree-ring chronologies are more difficult to achieve because the growth sites of the trees are unknown and growth-climate relationships cannot be checked against contemporary weather data. Samples included in such chronologies are carefully screened for conformance with a variety of statistical criteria that are known to reflect climate sensitivity in living trees (Dean and Robinson 1977, in press; Robinson and Dean 1969).

Before archaeological tree-ring series and sequences from living trees can be merged into long composite chronologies to be used for paleoclimatic reconstructions, they must be shown to represent the same statistical population. Otherwise, the relationship between modern tree growth and climate cannot be used as a basis for reconstructing climate from the part of the total chronology composed solely of archaeological materials. The equivalence of two series is tested by comparing their descriptive statistics and by evaluating the results of several statistical operations applied to the chronologies for their period of overlap. Ring series that survive these tests are merged into the long chronologies that form the data bases for quantitative paleoclimatic reconstructions.

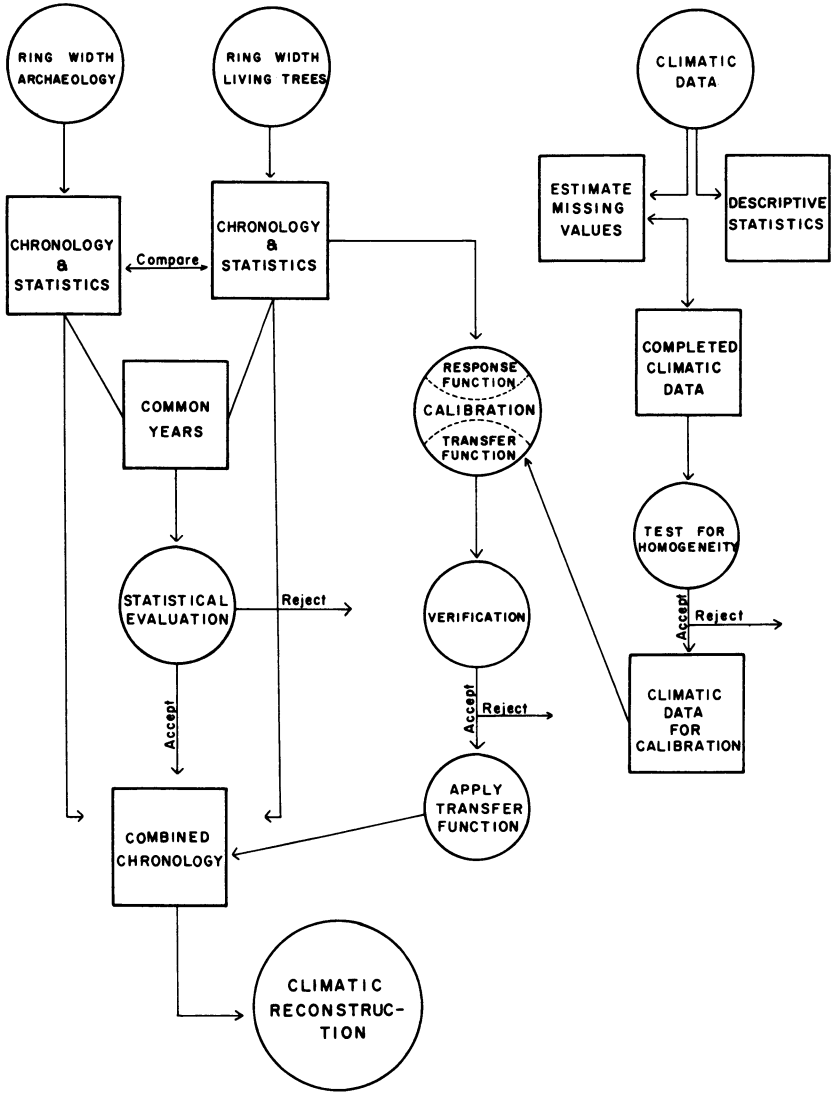

FIG. 3. Flow chart for Arroyo Hondo dendroclimatic analysis.

The next step—evaluation of the climatic data to be calibrated with the tree-ring series, in this case the weather record for Santa Fe—involves several operations. First, the general character of the precipitation and temperature records is assessed by means of their descriptive statistics. Second, gaps in the records—that is, months for which precipitation data or temperature data or both are unavailable—are eliminated by using linear regression analyses of weather data from nearby stations to estimate the missing Santa Fe values. The stations used for estimating missing Santa Fe values are carefully screened to determine which are the best predictors for Santa Fe. Third, the final Santa Fe precipitation and temperature series are tested for homogeneity (Fritts 1976:252–54; Kohler 1949). Once missing values have been estimated and series homogeneity has been established, the weather record is ready to be calibrated with the tree-ring series covering the same span of time.

Locality-level calibration (Fritts 1976:312–75), as applied in the Arroyo Hondo analyses, is a complex procedure involving the generation of equations that represent the relationships between tree growth at a particular site (Glorieta Mesa in this case) and the climate at a nearby weather station (Santa Fe). A fourteen-month "year" is used to approximate the time during which climate directly or indirectly affects tree growth. Various studies indicate that the fourteen-month interval beginning with June of the year prior to growth and ending with July of the current growing season includes the climatic variables that have the greatest effect on tree growth in the Southwest (Fritts 1970:93; 1976:238–41, 356). Average temperature and total precipitation values for each of these months yield a total of 28 climatic variables that are used in calibration. In addition, ring-width indices for each of the three years prior to the current ring are used to measure the effects of previous growth on current growth.

The relationship between climate and tree growth is expressed mathematically by a *response function* that consists of a series of coefficients used to estimate tree growth from climatic variables (Fritts 1976:318). The response function isolates the months in which precipitation or temperature or both affect tree growth and thereby indicates the climatic variables that can be reconstructed from the tree-ring data. Response functions are produced by extracting eigenvectors from the climatic data and relating the eigenvector-weighted climatic data to tree growth. Eigenvector-weighted data are superior to the original data

for three reasons: (1) being uncorrelated with one another, they facilitate the use of multiple regression analyses, (2) fewer eigenvectors than climatic variables can account for an equal amount of variation in tree-ring data, and (3) generally, fewer degrees of freedom are consumed in using eigenvectors.

The next step in the calibration process is the generation of a *transfer function* consisting of a different set of coefficients that are used to estimate climatic variables from ring indices (Fritts 1976:318). Locality-level calibration involves bivariate or multiple linear regression using tree-growth indices as predictors of climatic variables. Once regression equations are generated for the climatic variables, residuals are checked for autocorrelation. If autocorrelation is not statistically significant, the transfer function is used to retrodict climatic values for the months characterized by significant response function elements.

Verification of the retrodictions with data independent of those used to produce the response and transfer functions is necessary before the transfer function can be used to reconstruct aspects of prehistoric climate. Verification is accomplished by comparing reconstructed climatic values with actual values for time periods not used in the calibration procedure. In this study, climatic data for the period from 1917 to 1970 are used to calculate the Santa Fe–Glorieta Mesa response function. Santa Fe climatic data for the 1869–1916 interval are reserved for checking the accuracy of the reconstruction. The fit between the reconstruction for the 1869–1916 verification period and the actual data for the same period is evaluated with an array of statistical techniques. Only the variables whose reconstructions pass the rigorous verification tests are considered to be eligible for prehistoric climatic reconstruction.

In the reconstruction process, the transfer function is used to produce quantitative estimates of values for those climatic variables that the response function showed to be related to tree growth *and* that passed the verification tests. In the Arroyo Hondo case, two reconstructions are possible for the years from A.D. 985 through 1970: total precipitation for previous August through current July and total precipitation for current March through June.

2
Evaluation of Tree-Ring Chronologies

Four tree-ring chronologies are used in the paleoclimatic reconstruction for Arroyo Hondo. The first three are (1) the Arroyo Hondo site chronology (computer control number 708000), spanning the interval from A.D. 982 to 1410; (2) the Santa Fe archaeological chronology (799900), composed of prehistoric and historic materials covering the years from A.D. 878 to 1930; and (3) the Glorieta Mesa piñon chronology (343000), which includes the years from A.D. 1556 to 1972. The last two chronologies are merged to produce the fourth, the Santa Fe climatic chronology (700000, Dean and Robinson 1978:49–50).

The Arroyo Hondo site chronology is composed primarily of piñon samples but also includes six specimens of ponderosa pine in the interval from A.D. 1223 to 1385. The segment of the Santa Fe archaeological chronology corresponding to the period of occupation at Arroyo Hondo is almost all piñon. Making up the Glorieta Mesa chronology are samples collected in 1973 from living piñon trees at elevations of 7,100 to 7,200 feet. The collection site has sandstone parent material and is located on a south-facing slope that varies from 0° to 45°. The purely piñon segment of the Santa Fe archaeological chronology falls 121 years short of overlapping with the Glorieta Mesa piñon sequence. This gap is filled by ponderosa pine samples included in the Santa Fe archaeological chronology.

Tree-ring chronologies such as those used in the Arroyo Hondo study are produced by a series of operations that quantify dated ring-

width variability. Every ring in a wood or charcoal sample is assigned an absolute calendar-year date by the process of crossdating (Fritts 1976:20–23). Representative samples—that is, samples that have a high degree of ring-to-ring variability in width, that possess a large number of rings (preferably 100 or more), and that crossdate well—are selected for measurement. The rings of each sample are measured to the nearest 0.01 mm sequentially along a radius from the center to the periphery of the specimen. These ring-width measurements are then analyzed by a computer program (Fritts 1976:261–68; Fritts, Mosimann, and Bottorff 1969) that transforms them into standardized growth indices and calculates the descriptive statistics of each ring series. Standardized indices are produced by fitting a trend line to the sequentially arrayed ring-width values of a sample and then calculating the percentage departure of each ring-width value from the value of the trend line at that point. This procedure produces for each sample a series of indices with a mean of one and a unique standard deviation. Standardization enhances the amount of climate-related variance in each ring series by removing the effects of several variables, notably growth trend and mean ring width, that are related to factors peculiar to the growth of individual trees rather than to external climatic factors. It also makes the variance relatively constant throughout the length of the series. The statistical attributes of the standardized ring series are used (Dean and Robinson, in press) to select samples for inclusion in composite chronologies, each of which represents a single archaeological site, a localized area, or a stand of living trees. The indices chosen to represent a particular site, area, or stand are averaged to produce a composite chronology. The standardized indices of these chronologies are the quantitative tree-ring data used in the dendroclimatic analyses reported here.

Before these chronologies can be used for dendroclimatic analysis, their suitability for this purpose must be established. The dendroclimatic potential of the chronologies is assessed by comparing their statistical characteristics and frequency composition with corresponding attributes of chronologies known to possess high proportions of climate-related variability. The statistical and frequency attributes are also employed to evaluate the degree of similarity among the three chronologies used in the Arroyo Hondo study. Finally, analyses of the time and frequency variation in the Santa Fe archaeological and Glorieta Mesa piñon chronologies establish the statistical identity of these two time

series, which legitimizes the merging of the two to form the Santa Fe climatic chronology that is used for the climatic reconstructions.

EVALUATION OF DENDROCLIMATIC POTENTIAL

In an analysis of the statistical characteristics of 89 tree-ring chronologies from western North America, Fritts and Shatz (1975) discovered that the chronologies most suitable for climatic analysis had low first-order serial correlations, large standard deviations, and high mean sensitivities. Mean sensitivity *(ms)* is the mean percentage change from each measured ring value to the next (Douglass 1936:28; Fritts 1976:258). Mean sensitivity values range from zero when there is no difference from one ring to the next to two when adjacent values are zero and nonzero. This statistic measures high frequency variability, but its distribution, and therefore its power, is unknown.

The statistics presented in Table 1a show that all three chronologies are sensitive in that they possess low serial correlation coefficients, large standard deviations, and high mean sensitivity values. Mean values for the pertinent statistics calculated by Fritts and Shatz (1975: Table 2) are listed in Table 1b. Both ponderosa pine and piñon values are included because the Santa Fe archaeological and Arroyo Hondo chronologies include ponderosa pine samples. As is evident from Table 1a and 1b, the statistics of the three Santa Fe area chronologies are as good as or better than the mean values for "good" climatic chronologies. Therefore, we conclude that all three are suitable for the proposed dendroclimatic reconstructions.

Fritts and Shatz (1975) also employed digital filtering techniques (LaMarche and Fritts 1972) to evaluate the suitability of tree-ring chronologies for climatic analysis. Appropriately designed mathematical filters analyze the variability of time series such as tree-ring chronologies into various frequency components. To permit the comparison of two or more time series, the digital filters are designed to preserve the phase and amplitude characteristics in any frequency range of the time series. A low-pass filter is a set of numerical weights applied to a time series to produce a new series in which the low frequency variance is passed or retained and the high frequency variance is blocked out. Conversely, a high-pass filter produces a series in which the high frequency variance is retained, while the low frequency variance is blocked out.

TABLE 1.
Statistics of the tree-ring chronologies for their total lengths (s = standard deviation; s^2 = variance; Serial r = first-order autocorrelation; ms = mean sensitivity).

	Series			*Serial*	
	Mean	*s*	s^2	*r*	*ms*
	a. *Unfiltered Indices*				
Santa Fe Archaeological	1.0013	0.431	0.186	0.146	0.503
Glorieta Mesa	0.9938	0.396	0.157	0.349	0.416
Arroyo Hondo	0.9974	0.486	0.236	0.161	0.579
	b. *Mean Values of "Good" Chronologies (Fritts and Shatz 1975: Table 2)*				
Piñon		0.395		0.361	0.412
Ponderosa Pine		0.366		0.452	0.348
	c. *Intrachronology Variance Ratios*				
	High/Unfiltered		Low/Unfiltered		High/Low
Santa Fe Archaeological	0.6054		0.2210		2.7397
Glorieta Mesa	0.4962		0.3127		1.5866
Arroyo Hondo	0.6144		0.2525		2.4329

Fritts and Shatz (1975) separated each chronology in their study into high and low frequency components, and they subjected the unfiltered indices and the frequency components to correlation analyses. Ratios of unfiltered, high frequency, and low frequency variance components were calculated for each chronology. The chronologies best suited for dendroclimatic analyses possessed large ratios of high frequency variance to the variance of the unfiltered series, very small ratios of low frequency variance to the variance of the unfiltered indices, and large proportions of high to low frequency variance.

Low frequency variation results from the processes of tree growth, different stand histories, disease, fire, changes in competition, long-term climatic changes, or unknown factors. The amount of low frequency variability in a tree-ring chronology is controlled by using site selection criteria and sampling procedures designed to enhance high

frequency variability (Fritts 1976:17–19, 29–31). High frequency variability, especially the year-to-year changes in ring widths, is generally the result of climatic fluctuations. Intrachronology correlations of all frequency components are usually higher when climatic factors exert a greater influence on tree growth than do nonclimatic factors. In contrast, when the effects of nonclimatic factors on tree growth exceed the effects of climatic variables, low frequency variability increases, and the correlation of these components within sites decreases.

The application of filtering techniques and time series analysis in several fields and at various levels of sophistication is covered by Blackman and Tukey (1958), Brier (1961), Brillinger (1974), Box and Jenkins (1976), Holloway (1958), and Mitchell et al. (1966).

To compare the chronologies used in the Arroyo Hondo study with those found by Fritts and Shatz to be suitable for dendroclimatic analysis, we treated the total lengths of the Arroyo Hondo, Santa Fe archaeological, and Glorieta Mesa piñon chronologies independently with the low-pass and high-pass filters. For the purposes of this comparison, low frequency variability refers to periods greater than eight years in length, that is, to frequencies less than ⅛ cycle per year. High frequency variability is defined as periods less than eight years long, that is, as frequencies greater than ⅛ cycle per year. The eight year cutoff point between high and low frequency variability is arbitrary but is used to make the Arroyo Hondo study consistent with the earlier work of Fritts and Shatz. The intrachronology ratios of variance are listed in Table 1c. These data indicate that all three Santa Fe area chronologies fulfill the Fritts and Shatz (1975) variance ratio criteria for climatic sensitivity and suitability for dendroclimatic analysis.

Chronology Variance Component Characteristics

The descriptive statistics of the unfiltered and filtered tree-ring series (Table 1) indicate that all three chronologies are quite similar. Further evidence for evaluating the degree of similarity among the three chronologies is provided by those segments of the chronologies that overlap with one another. The Santa Fe archaeological and Arroyo Hondo chronologies overlap for the 429-year period from A.D. 982 to 1410; the Santa Fe archaeological and Glorieta Mesa chronologies overlap for the 375-year interval from A.D. 1556 to 1930. These combinations

create two pairs of overlapped chronology segments that can be compared with one another. The overlap periods are investigated in detail because the climate–tree-growth relationships established for the recent portion of the Santa Fe climatic chronology, composed primarily of the Glorieta Mesa living piñon trees, are to be used to retrodict climatic variability from the early portion of the Santa Fe climatic chronology, which is composed solely of archaeological samples.

To evaluate the variance component characteristics of the common periods, the overlapping segments of each chronology are treated with the high-pass and low-pass filters. The unfiltered and filtered values of each pair of chronology segments are correlated with one another using Pearson's product moment correlation coefficient (Blalock 1972:361–427). In addition, the following ratios are calculated for each chronology: (1) the variance passed by the high-pass filter to that in the unfiltered sequence, (2) the variance passed by the low-pass filter to that in the unfiltered series, (3) the variance passed by the low-pass filter to that passed by the high-pass filter, and (4) the variance passed by the high-pass filter to that passed by the low-pass filter.

Statistics for the overlap periods between the Santa Fe archaeological and Glorieta Mesa series and between the Santa Fe archaeological and Arroyo Hondo chronologies are presented in Table 2. All three versions of the Santa Fe archaeological and Glorieta Mesa time series—unfiltered, low-pass filtered, and high-pass filtered—have high positive correlations, indicating that a common environmental factor or set of factors has been limiting to both. This indication is substantiated by the multivariate response function for the Glorieta Mesa series discussed later.

The high correlations between the unfiltered Glorieta Mesa and Santa Fe archaeological series and between their high frequency components (Table 2a) imply microclimatic conditions common to both chronologies. The relatively high correlation between the low frequency components indicates similar responses to climatic variations greater than eight years in length and similar growth-site characteristics and histories. The inferences drawn from the data in Table 2a are supported by the ratios of intrachronology variances presented in Table 2c, which were computed from the variance values in Table 2b. Approximately 80 percent of the variance in both chronologies was passed by the low-pass and high-pass filters combined. Thus, it appears that the filters do not perfectly handle wavelengths representing about 20 per-

TABLE 2.
Statistics of the tree-ring chronologies for their overlap periods.

	Glorieta Mesa with Santa Fe (A.D. 1556–1930)	*Arroyo Hondo with Santa Fe (A.D. 982–1410)*
	a. *Interchronology Correlations (r)*	
Unfiltered Indices	0.615	0.740
High-Pass Filter	0.665	0.837
Low-Pass Filter	0.565	0.639
	b. *Actual Variance (s^2)*	
Unfiltered Indices	0.152 (GM) 0.198 (SF)	0.236 (AH) 0.193 (SF)
High-Pass Filter	0.075 (GM) 0.114 (SF)	0.145 (AH) 0.117 (SF)
Low-Pass Filter	0.046 (GM) 0.050 (SF)	0.060 (AH) 0.037 (SF)
	c. *Intrachronology Ratios of Variances*	
High-Pass Filter/ Unfiltered Indices	0.492 (GM) 0.575 (SF)	0.614 (AH) 0.605 (SF)
Low-Pass Filter/ Unfiltered Indices	0.304 (GM) 0.250 (SF)	0.252 (AH) 0.192 (SF)
Low-Pass/High-Pass	0.618 (GM) 0.436 (SF)	0.411 (AH) 0.318 (SF)
High-Pass/Low-Pass	1.618 (GM) 2.295 (SF)	2.435 (AH) 3.147 (SF)

cent of the variance in these chronologies, that is, periodicities centered around eight years.

Information about the overlap period of the Santa Fe archaeological and Arroyo Hondo series is also presented in Table 2. The filtered and unfiltered versions of both time series have high correlations, implying that the trees represented by the specimens in both chronologies were responding similarly to short-term and long-term climatic variation. Intrachronology variance ratios (Table 2c) indicate that both chronologies

have a large amount of high frequency variance, a small amount of low frequency variance, a small low/high frequency variance ratio, and a large high/low frequency variance ratio. The Arroyo Hondo chronology contains a slightly larger percentage of low frequency variance than does the Santa Fe archaeological series, producing the larger low/high frequency variance ratio and the smaller high/low frequency variance ratio.

These analyses show that the variance components of the Santa Fe archaeological, Glorieta Mesa, and Arroyo Hondo chronology overlap periods fall within the limits of previously determined standards that define climate-sensitive tree-ring series. Furthermore, these analyses reveal no significant differences between the Santa Fe archaeological and Glorieta Mesa and Arroyo Hondo chronologies for their periods of overlap and establish the basic identity of the three chronologies.

EVALUATION FOR CHRONOLOGY MERGING

Before the Glorieta Mesa and Santa Fe archaeological chronologies can be merged into a single, longer series to be used as the basis for the dendroclimatic reconstructions, it is necessary to demonstrate as far as possible that the two shorter series represent the same statistical population. The comparison of the descriptive statistics and variance components already presented indicates the fundamental similarity of all three Santa Fe area chronologies and strongly supports the hypothesis that they represent a single statistical population. Spectral analyses of the overlapping segments of the Santa Fe archaeological and Glorieta Mesa chronologies provide additional tests of this hypothesis.

The digital filters, variance ratios, and cross-correlation analyses reported above provide a general indication of the distribution of variance by frequency in the chronologies during the overlap periods. We used the filter analysis, which partitions the frequency domain into two *arbitrary* units, primarily to achieve comparability with previous research (Fritts and Shatz 1975). However, it is questionable whether this procedure divides the series into *natural* high and low frequency bands. To investigate the distribution of variance throughout the entire frequency domain, the time series technique of spectral analysis is used. LaMarche (1974) used spectral analysis to investigate frequency-dependent relationships of tree growth to climate along an ecological

gradient. Similarly, Stockton (1975:18) employed spectral analysis to evaluate the frequency domain of tree-ring series.

Spectral analysis is based on classic harmonic analysis, which involves decomposing a time series into a finite number of sinusoidals (harmonics) with variable periods (Mitchell et al. 1966:33). In contrast to classic harmonic analysis, spectral analysis assumes that the time series is composed of an infinite number of small oscillations spanning a continuous range of wavelengths. Spectral analysis is used to evaluate the nonrandomness of a time series, assuming minimal *a priori* knowledge about the nature of the nonrandomness. The simplifying assumption of weak stationarity, which states that each series has a constant mean and constant variance through time, is made (Jenkins and Watts 1968:149). This assumption appears to be reasonable because standardizing raw ring widths produces a series with a mean of one and relatively constant variance through time (Fritts 1976:260–67).

The first step in computing the variance (power) spectrum of a time series is calculation of the autocovariance function, a measure of persistence in time series. In order to compare the persistence structure of the two series, the autocovariance function is normalized to produce the autocorrelation function (Jenkins and Watts 1968:182).

The Autocorrelation Function

Estimates of the autocorrelation function are obtained by dividing the autocovariance estimates at lag k, $c_{xx}(k)$, by the estimate of the variance of the total series. Thus, the autocorrelation coefficient, $r_{xx}(k)$, is equal to $c_{xx}(k)/c_{xx}(0)$. The autocorrelation coefficient is a linear correlation coefficient between a time series and itself at different time intervals, or lags (offsets). The autocorrelation at lag zero, $r_{xx}(0)$, is the correlation between elements t, t_{+1}, t_{+2}, t_{+3}, . . . , $+ t_{+n}$ and themselves, with the result obviously equal to +1.0. The autocorrelation at lag one, $r_{xx}(1)$, is the correlation obtained when elements t, t_{+1}, t_{+2}, t_{+3}, . . . , $+ t_{+n}$ are matched with elements t_{+1}, t_{+2}, t_{+3}, t_{+4}, . . . , $+ t_{n+1}$. This procedure is carried out to a maximum lag, determined by the series length. Usually, the maximum lag depends on the requirement of statistical stability of the spectral estimates or on the need to investigate the amount of variance at a particular frequency. A general rule is that the maximum lag is 25 percent of the series

length (Jenkins and Watts 1968:290–91). As the number of lags is increased, $r_{xx}(k)$ is based on fewer and fewer observations, leading to an increase in variance and violation of the assumption that the autocorrelation value is from a long series. For this reason, little significance can be attached to high autocorrelation values at large lags, unless the corresponding series is very long.

The autocorrelation functions for the Santa Fe archaeological and Glorieta Mesa chronologies during the overlap period are presented in Figures 4 and 5. The expected, or mean, autocorrelation of a series of random numbers is zero, and the individual values plotted on the ordinate fluctuate above and below a horizontal line equal to zero. If the series is long and the maximum lag small, 10–25 percent of the series length, an approximate significance test for the autocorrelation values can be calculated. In this test, the null hypothesis is that the value of a particular autocorrelation coefficient equals zero. The alternative hypothesis is that the particular autocorrelation value is significantly greater than or less than zero. The standard deviation of a series is $1/\sqrt{n}$ (Jenkins and Watts 1968:188), and the 95 percent confidence

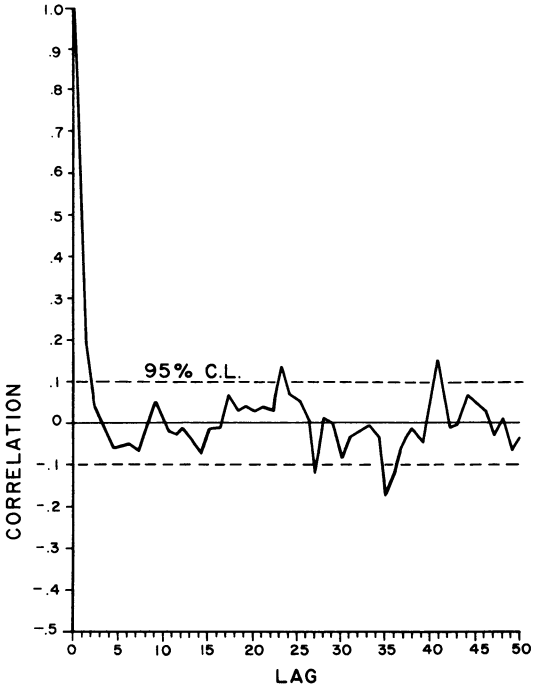

FIG. 4. Autocorrelation function of Santa Fe archaeological chronology: overlap period.

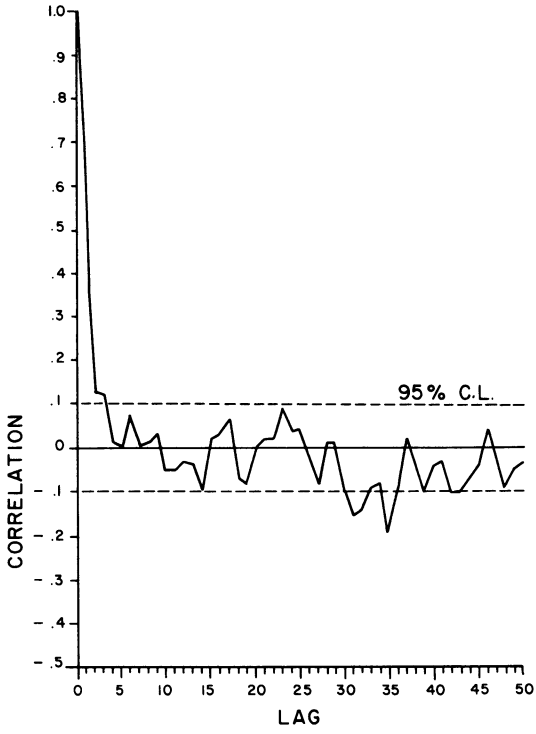

FIG. 5. Autocorrelation function of Glorieta Mesa piñon chronology: overlap period.

limits are approximately $\pm$ (1.96) $(1/\sqrt{n})$. The 95 percent confidence limits calculated for the two series (Figs. 4 and 5) are $\pm(1.96)\,(1/\sqrt{375})$, or $\pm.101$.

Neither chronology, therefore, contains appreciable persistence except at one year. This one-year persistence is ubiquitous in tree-ring series and is incorporated into the calibration developed later. The persistence indicated at higher lags (greater than circa 25 years) is unimportant because of its relation to the length of the overlap series. We conclude that the persistence structures of the overlapping segments of the Glorieta Mesa piñon chronology and the Santa Fe archaeological chronology are similar and that these chronologies may be combined.

The Variance Spectrum

To obtain the variance spectrum of an individual series, a Fourier transform is applied to the autocovariance function. This procedure transforms the series from the time domain into the frequency do-

main, and its main purpose is to extract the dominant periodic components, or harmonics. The spectrum provides a measure of the distribution of variance in the series from zero to the smallest frequency resolvable. The resolution of the spectrum is directly proportional to the maximum lag value used in computing the autocovariance function. The smallest resolvable frequency, the Nyquist frequency, is equal to the reciprocal of twice the distance (two years in this case) between successive observations, or 0.5 cycles per year (c.p.y.). The Nyquist frequency is a harmonic of the fundamental wavelength, which is equal to the length of the record (Jenkins and Watts 1968:19). If λ denotes the fundamental wavelength, $\lambda/2$ is the second harmonic, $\lambda/3$ the third harmonic, and so on, to the Nyquist frequency.

The spectral estimates obtained by the Fourier transform of the autocovariance function are smoothed by a weighting procedure in order to derive a consistent estimate of the final spectrum. Following the "window closing" technique of Jenkins and Watts (1968:280–82), progressively larger maximum lags are used in computing the autocor-

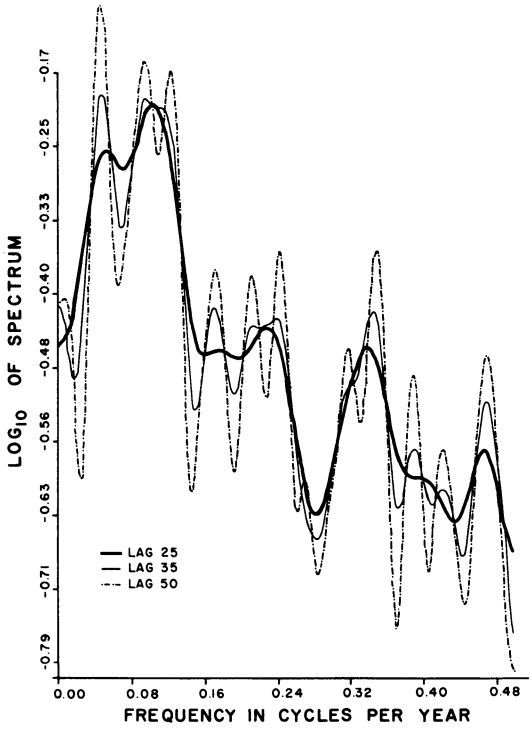

FIG. 6. Autospectra of Santa Fe archaeological chronology: overlap period.

relation functions, and hence the spectrum. In these analyses we use lags of 25, 35, and 50 years. The window closing procedure of focusing on increasingly narrow frequency bands emphasizes the more significant details of the spectrum. At small maximum lags (wide band widths) resolution is coarse, but the results are more stable statistically than those produced by using larger lags. Larger lags provide higher resolutions (smaller band widths), but the spectral estimates are generally less statistically stable. In the variance spectrum, various forms of nonrandomness appear differently. A pure sine or cosine wave is represented by a sharp peak at the appropriate frequency. A nonsinusoidal periodicity is manifested by a peak at the basic wavelength and by peaks at wavelengths corresponding to higher-order harmonics. Quasi periodicities are represented by broad humps spanning long ranges of frequencies.

The $\log_{10}$ values of the smoothed spectral estimates for the chronologies are plotted as functions of frequency in Figures 6 and 7. Plotted in this manner, the values show relative changes in variance, and the confi-

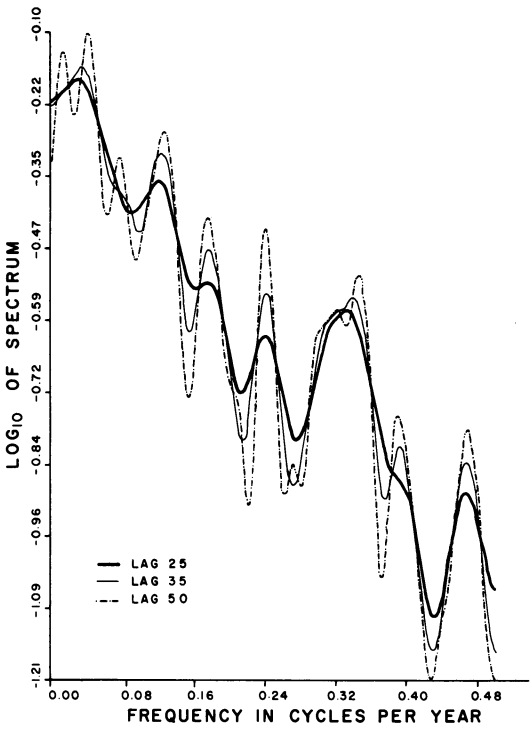

FIG. 7. Autospectra of Glorieta Mesa piñon chronology: overlap period.

dence intervals are represented as a single band for all frequencies (Jenkins and Watts 1968:254–55). The autospectra in the two figures are presented for maximum lag values of 25, 35, and 50 years, and those computed from the autocovariance function with the largest maximum lag exhibit the most variability.

Persistence in a time series occurs when each value is influenced by its immediate predecessors; large values tend to follow large values and small values tend to follow small values. Persistence is indicated when the variance is not randomly distributed. In the autospectra of a random series the variance is evenly distributed at all frequencies, with the spectral estimates clustering about a horizontal line. The autospectra of both chronologies, especially the Glorieta Mesa series, show a concentration of variance at low frequencies. There is a dropoff at very low frequencies in the Santa Fe archaeological chronology, possibly because it is composed of shorter ring series than the Glorieta Mesa sequence. In general, the autospectra of both chronologies appear to be fairly similar.

Cross-Spectral Analysis

Cross-spectral analysis is used to compare the relationship between the two series at different frequencies. Instead of the autocovariance and autocorrelation functions, which are used in the analysis of single series, cross-covariance and cross-correlation functions are computed (Jenkins and Watts 1968:324–25). The cross-correlation function defines the linear dependence of the values of one series on those of the other (Fig. 8). Both positive and negative lags are necessary for the computation of the cross-correlation function because it is an odd function. Comparisons are made at all possible lags as one series is lagged with respect to the second and then as the second is lagged with respect to the first. Unlike the autocorrelation function, which is calculated using the variance of the entire series, the cross-correlation function uses only the variance of the common points.

The standard error of estimate for a cross-correlation value is approximately $1/\sqrt{n}$, as it is for the autocorrelation function (Jenkins and Watts 1968:338). Therefore, the 95 percent confidence limits for Figure 8 are $\pm.101$. The cross-correlation between the two series at different lags illustrates their similarity in persistence structure and shows phase relationships. If the two series were out of phase, the maximum

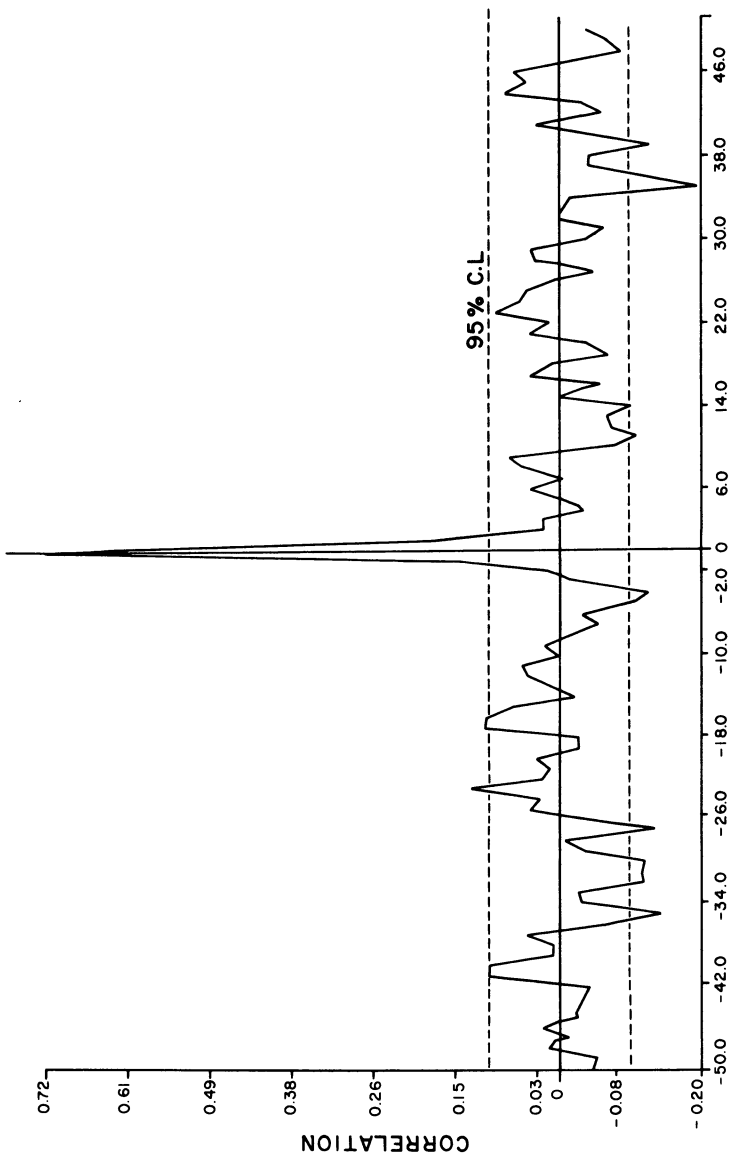

FIG. 8. Cross-correlation function between Santa Fe archaeological chronology and Glorieta Mesa piñon chronology: overlap period.

cross-correlation would occur at lags other than zero. Such an out-of-phase relationship is not indicated by Figure 8.

Cross-spectral estimates are obtained by Fourier transform of the cross-covariance function. The cospectral estimates (Fig. 9) express the amplitude of the in-phase periodic components of the two series (Jenkins and Watts 1968:343). Positive values, as in Figure 9, represent in-phase variations in the same direction, while negative values indicate in-phase variations in opposite directions. In this case, the maximum values in the cospectrum occur between 0.08 and 0.16 c.p.y. and at approximately 0.34 c.p.y. The quadrature spectrum (Fig. 9) expresses amplitudes of components in the two series that are 90° out of phase, that is, the variations are similar but precede or follow one another (Jenkins and Watts 1968:343). While both positive and negative values are present in Figure 9, they are all very near zero, indicating that there is no out-of-phase component.

A measure of the degree of association between the two series at any frequency is provided by the coherency squared, $K^2_{12}(f)$ (Amos and Koopmans 1963; Jenkins and Watts 1968; Koopmans 1974). Coherency squared is the frequency domain analog of the squared correlation coefficient and varies between zero and +1.0. A value of zero indi-

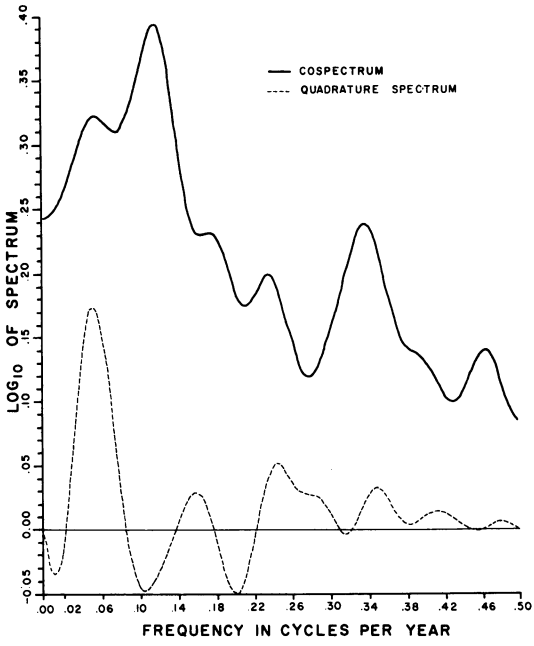

FIG. 9. Cospectrum and quadrature spectrum of Santa Fe archaeological chronology and Glorieta Mesa piñon chronology: overlap period.

cates that the two series are uncorrelated at a particular frequency, while a +1.0 indicates that they are exactly correlated. Jenkins and Watts (1968:379) note that apart from smoothing, the variance of the coherency, $\sqrt{K_{12}^2(f)}$, is identical to that of the ordinary correlation coefficient. Confidence intervals for the coherency spectrum are constructed by using the transformation, $Y_{12} = \text{arctanh } |K_{12}(f)|$, because the variance of the spectrum is independent of frequency (Jenkins and Watts 1968:379–80, 403). The confidence interval is represented by a constant band on the Y scale; therefore, the estimate $Y_{12}(f)$ is plotted rather than the coherency itself. The coherency values and their 95 percent confidence intervals for maximum lags of 25, 35, and 50 years are plotted on the *transformed* scale in Figure 10. The coherence between the two series is high except at very low frequencies. Again, the estimates based on the smallest lag exhibit the most stability.

The cross-spectral analyses of the overlapping segments of the Glorieta Mesa and Santa Fe archaeological chronologies reveal no significant differences between these two tree-ring series. This evidence indicates that the Glorieta Mesa and Santa Fe archaeological series represent a single statistical population and can safely be combined into a longer composite series.

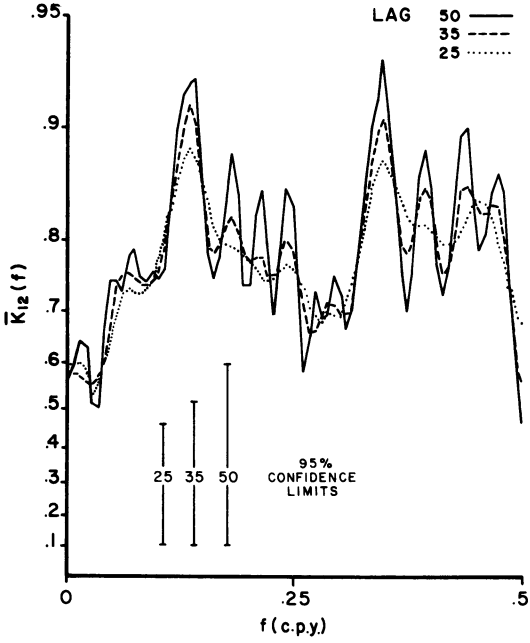

FIG. 10. Coherency squared for Santa Fe archaeological chronology and Glorieta Mesa piñon chronology: overlap period.

SUMMARY OF CHRONOLOGY EVALUATIONS

The dendroclimatic potential of the Santa Fe archaeological, Arroyo Hondo, and Glorieta Mesa tree-ring series was evaluated against statistical criteria for "good" dendroclimatic chronologies as developed by Fritts and Shatz (1975). Both the descriptive statistical attributes and the variance component characteristics of all three Santa Fe area chronologies equaled or surpassed the Fritts and Shatz criteria. Therefore, all three chronologies are suitable for dendroclimatic analysis.

Comparison of the descriptive statistics and variance component attributes of the total lengths of the Santa Fe area chronologies indicated a basic similarity among all three series that was evaluated further by analyzing the variance component characteristics of the segments of these chronologies that overlap with one another. These analyses established the fundamental identity of all three chronologies for the periods of overlap, a result that provides additional support for the suitability of the chronologies for the proposed Santa Fe area climatic reconstructions. This result also implies that the three chronologies can be used interchangeably in the reconstructions.

In order to merge the Santa Fe archaeological and Glorieta Mesa piñon ring series into a single chronology to be used in the reconstructions, it was necessary to establish that both series represent a single statistical population. Although the statistical and variance component comparisons provided strong support for this hypothesis, it was further evaluated by means of spectral and cross-spectral analyses of the frequency structure of overlapping segments of the two chronologies. These analyses established the statistical identity of the two series.

All analyses indicated that the Santa Fe archaeological, Arroyo Hondo, and Glorieta Mesa chronologies are derived from the same statistical population. Therefore, the archaeological and living tree chronologies are merged to produce a continuous Santa Fe climatic chronology spanning the period from A.D. 982 to 1970. The descriptive statistics of the Santa Fe climatic chronology (mean sensitivity = 0.473, serial correlation = 0.183, standard deviation = 0.410) compare favorably with the Fritts and Shatz (1975) criteria. The Santa Fe climatic chronology, like its component series, is climatically sensitive and suitable for use in reconstructing aspects of past climatic variability.

Because there are no visual or statistically significant differences between the Arroyo Hondo and Santa Fe climatic chronologies and

because all three chronologies are interchangeable, the Santa Fe climatic chronology is used to reconstruct Arroyo Hondo paleoclimate. Thus the Arroyo Hondo chronology per se is not used from this point on in the analysis.

3
Evaluation of Santa Fe Climatic Data

Another step in the reconstruction of paleoclimatic variability at Arroyo Hondo is to describe and evaluate the range of variation of the modern Santa Fe climatic data that are to be calibrated with the Glorieta Mesa tree-ring series. Our analysis of the climatic data has three main objectives. First, the nature of annual climatic variability near Santa Fe is specified by the descriptive statistics of the precipitation and temperature time series. Second, regression analyses of data from nearby weather stations are used to estimate values for the months for which Santa Fe data are not available. Third, the two time series are tested for homogeneity in order to isolate changes in the data that might adversely affect the results of the calibration and verification operations.

The climatic data for Santa Fe and the other stations used in this study are published annually, with monthly summaries of the observations, by the United States Department of Commerce, National Oceanic and Atmospheric Administration, Environmental Data Service. Earlier versions of the climatological summaries for New Mexico were prepared by the New Mexico State Engineer Office in cooperation with the New Mexico Interstate Stream Commission and the United States Department of Commerce Weather Bureau. Of the many climatological variables presented in these reports, we use only two in our dendroclimatic analyses, mean monthly temperature and total monthly precipitation. Although the Santa Fe weather record runs from 1850 to

the present, we use only the data representing the interval from 1869 through 1971 for calibration and verification. Apparent anomalies in the data cast doubt on the reliability of the first 20 years of the record. In addition, differences between the recording procedures employed by the United States Army Post Surgeons before 1871 and those subsequently used by the Signal Corps (1871–1891) and the Weather Bureau call into question the comparability of the two segments of the record. For these and other reasons, we delete the first 20 years of the record as potentially unreliable. Post-1971 climatic data are not used because the Glorieta Mesa tree-ring series ends in that year.

DESCRIPTIVE STATISTICS

Descriptive univariate statistics that specify the degree of sample variability indicate the limitations of and potential problems in the weather data. The descriptive statistics also provide a basis for comparing the weather records from the stations used in the bivariate and multivariate statistical analyses. Statistics computed include the median, mean, standard error of the mean (SE), 95 percent confidence interval of the mean, variance (s^2), standard deviation (s), skewness, kurtosis, and coefficient of variation (c.v.) (Nie et al. 1975). The statistics are calculated by month for the mean temperature and total precipitation series (Tables 3 and 4). Graphs of the monthly mean, standard deviation, skewness, kurtosis, and the coefficient of variation are shown in Figures 11 and 12.

Figure 11 shows a smooth transition from one month to the next in mean monthly temperature. Variance is greatest during the cooler months of the year, whereas values tend to cluster more tightly around the mean during the warmer months. The deviation of values from the mean is small for all months (Table 3, Fig. 11). The coefficient of variation, or the mean divided by the standard deviation, expresses variability independent of the size of the mean. It is smallest during the warmer months and largest during the cool months.

Distributions of mean temperature values for February and November are slightly negatively skewed, indicating that the most extreme observations lie to the left of the mean, with most of the values clustered slightly to the right of it (Table 3, Fig. 11). The January and December distributions are approximately normal, while those for March through

TABLE 3.
Descriptive statistics of Santa Fe temperature (degrees F.), A.D. 1869–1970.

	Median	*Mean*	*SE*	*95% Confidence Interval*	s^2	*s*	*Kurtosis*	*Skewness*	*Range*	*c.v.*	*N*
January	29.1	29.2	.36	28.5–30.0	13.1	3.6	−0.8	−.1	21.8–36.3	12.4	102
February	33.4	33.1	.38	32.3–33.8	14.8	3.8	−0.1	−.4	23.1–41.0	11.6	102
March	39.2	39.3	.33	38.7–40.0	11.1	3.3	1.8	.7	32.2–53.2	8.5	102
April	47.3	47.5	.29	46.9–48.1	8.5	2.9	2.7	.9	40.8–59.9	6.2	102
May	56.2	56.4	.27	55.9–56.9	7.3	2.7	2.2	.3	48.9–66.6	4.8	102
June	65.8	65.8	.24	65.4–66.3	5.9	2.4	2.7	.9	60.6–76.6	3.7	102
July	69.6	69.5	.20	69.1–69.9	4.1	2.0	1.2	.4	64.6–76.7	2.9	102
August	67.7	67.9	.19	67.5–68.2	3.5	1.9	0.8	.6	63.9–74.5	2.8	101
September	61.2	61.7	.22	61.2–62.1	4.9	2.2	0.8	.4	55.8–69.2	3.6	101
October	50.9	50.9	.24	50.4–51.3	5.7	2.4	0.7	.2	45.2–58.5	4.7	102
November	39.4	39.2	.32	38.6–39.9	10.2	3.2	0.0	−.4	29.2–45.2	8.1	102
December	30.9	30.8	.38	30.0–31.5	14.3	3.8	−0.5	.0	21.9–39.8	12.3	100

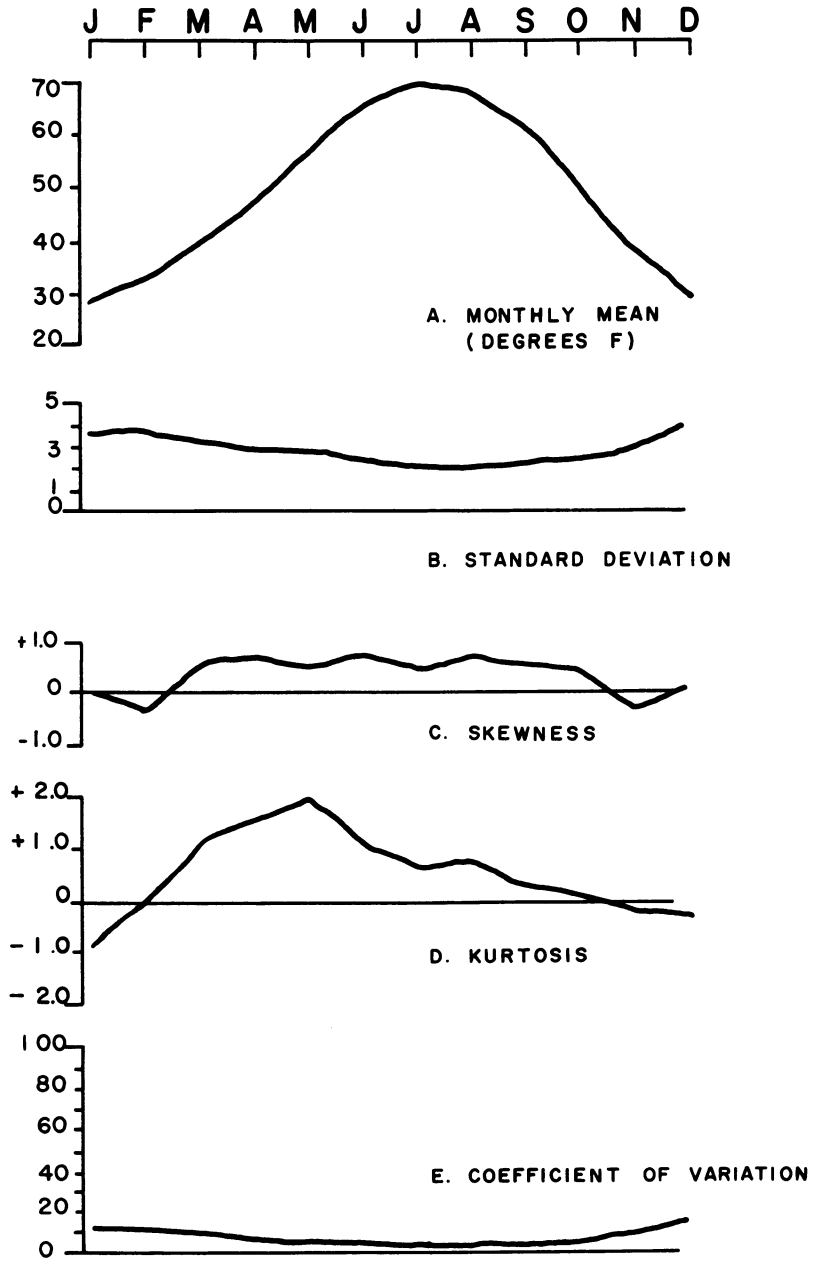

FIG. 11. Descriptive statistics of Santa Fe temperature.

October are slightly positively skewed. This skewing indicates that a few extreme monthly mean values lie to the right of the mean, with the rest of the values clustered slightly to the left. Figure 11 also shows that the distributions for January, November, and December are slightly flatter (platykurtic) than a normal (mesokurtic) distribution, while the values for February mean temperature are normally distributed. Mean temperature values for March through October are leptokurtic (peaked) to varying degrees.

In contrast to temperature, precipitation exhibits marked fluctuations in many characteristics (Fig. 12). Mean monthly precipitation increases gradually from November through June, increases abruptly in July and August, and decreases gradually in September and October. The coefficient of variation indicates that the mean monthly totals are variable during all months except late summer and early fall (Table 4). Precipitation values are much more skewed than their temperature counterparts, and all in a positive direction. The positive nature indicates extreme values to the right of the mean monthly totals, with most of the values clustered to the left of the mean. The monthly values of the kurtosis statistic denote varying degrees of peakedness, with the leptokurtic extremes associated with the months of February, April, June, and November.

ESTIMATION OF MISSING VALUES IN WEATHER RECORDS

The Santa Fe climatic record is characterized by a problem common to meteorological series: rainfall and temperature measurements are missing for a few individual months scattered throughout the series. Therefore, it is necessary to estimate the missing precipitation and temperature values to produce a complete time series suitable for analysis. This estimation is done by relating the Santa Fe series to climatic records from nearby stations that have data for the appropriate months. The relationships are established by means of simple linear regression equations with regression lines fitted to scattergrams of paired variates by the least squares method (Spiegel 1961:220). Three nearby stations with long records—Albuquerque, Pecos, and Taos—are tested to determine which are the best predictors of the Santa Fe data. The stations having the highest correlations with the Santa Fe temperature and precipitation records are used to estimate the missing values and the others are rejected.

TABLE 4.
Descriptive statistics of Santa Fe precipitation (inches), A.D. 1869–1970.

	Median	*Mean*	*SE*	*95% Confidence Interval*	s^2	*s*	*Kurtosis*	*Skewness*	*Range*	*c.v.*	*N*
January	0.47	0.64	.05	0.53–0.72	0.28	0.53	3.71	1.66	0.00–3.02	83.02	102
February	0.65	0.72	.05	0.63–0.81	0.21	0.45	0.36	0.85	0.01–1.99	63.11	102
March	0.70	0.78	.05	0.69–0.87	0.22	0.47	−0.22	0.64	0.01–2.06	59.90	102
April	0.71	0.89	.08	0.73–1.06	0.69	0.83	6.21	2.00	0.00–4.82	93.01	102
May	0.99	1.26	.11	1.04–1.47	1.18	1.09	1.93	1.33	0.01–5.58	86.61	102
June	0.75	1.12	.10	0.93–1.32	0.96	0.98	0.72	1.13	0.01–4.26	87.49	102
July	2.18	2.43	.14	2.16–2.71	1.94	1.39	0.32	0.79	0.40–6.91	57.32	102
August	2.09	2.35	.12	2.12–2.59	1.47	1.21	0.87	0.93	0.36–6.28	51.46	102
September	1.24	1.51	.11	1.29–1.74	1.31	1.15	1.69	1.23	0.01–5.37	75.67	102
October	0.95	1.09	.09	0.92–1.27	0.79	0.89	0.74	1.02	0.00–4.19	81.14	102
November	0.54	0.65	.06	0.53–0.76	0.36	0.60	5.56	1.77	0.00–3.39	92.60	102
December	0.56	0.73	.06	0.62–0.84	0.31	0.56	0.25	0.99	0.00–2.27	77.10	102

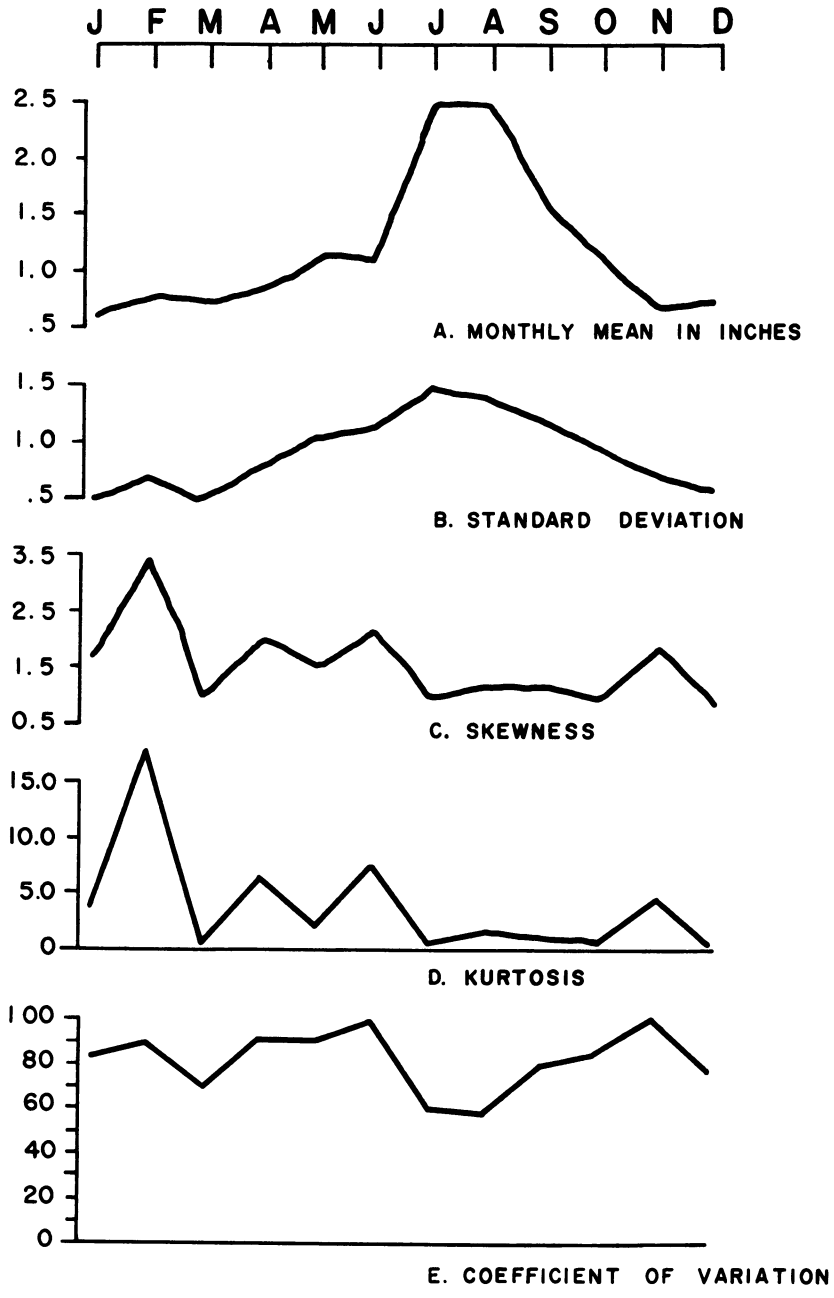

FIG. 12. Descriptive statistics of Santa Fe precipitation.

The correlation and regression information for the three pairs of stations (Santa Fe–Albuquerque, Santa Fe–Pecos, Santa Fe–Taos) is presented in Tables 5–7. These tables show that Santa Fe mean monthly temperature values are most highly correlated with those from Albuquerque. Linear regression equations establishing the nature

TABLE 5.
Correlation and regression statistics for Santa Fe (Y) and Albuquerque (X) climate.

	Correlation		*Regression*		
	r	r^2	*Y Intercept*	*Slope*	*N*
			a. *Temperature*		
January	.927	.860	−2.106	0.916	78
February	.943	.889	−4.653	0.954	78
March	.909	.827	−2.143	0.892	77
April	.886	.785	−0.808	0.880	77
May	.830	.689	8.804	0.741	78
June	.706	.499	19.248	0.633	78
July	.806	.650	14.148	0.716	78
August	.726	.527	22.670	0.599	78
September	.826	.683	15.007	0.682	78
October	.872	.760	5.090	0.807	78
November	.833	.693	3.160	0.821	78
December	.899	.808	−4.173	0.992	78
			b. *Precipitation*		
January	.697	.485	0.288	0.924	99
February	.139	.019	0.710	0.269	99
March	.424	.180	0.538	0.593	99
April	.681	.464	0.456	0.870	99
May	.739	.545	0.556	1.165	99
June	.687	.471	0.677	0.780	97
July	.483	.233	1.417	0.708	98
August	.343	.118	1.765	0.482	99
September	.668	.446	0.590	1.019	99
October	.760	.578	0.518	0.735	99
November	.729	.531	0.334	0.858	100
December	.521	.272	0.454	0.634	98

TABLE 6.
Correlation and regression statistics for Santa Fe (Y) and Pecos (X) climate.

	Correlation		*Regression*		
	r	r^2	*Y Intercept*	*Slope*	*N*
			a. *Temperature*		
January	.895	.802	6.168	0.795	26
February	.911	.829	5.439	0.842	25
March	.886	.785	12.500	0.693	27
April	.801	.642	11.009	0.794	32
May	.713	.508	23.628	0.603	28
June	.674	.454	17.360	0.755	29
July	.713	.508	31.580	0.564	28
August	.704	.495	30.414	0.567	25
September	.798	.636	14.567	0.784	22
October	.784	.615	22.291	0.574	22
November	.847	.717	11.608	0.711	22
December	.850	.723	−2.620	1.067	25
			b. *Precipitation*		
January	.886	.784	0.154	0.741	49
February	.621	.386	0.276	0.584	48
March	.644	.414	0.402	0.412	51
April	.875	.766	0.204	0.744	51
May	.795	.631	0.218	0.910	52
June	.800	.640	0.242	0.797	50
July	.476	.227	0.788	0.523	51
August	.609	.371	0.966	0.427	49
September	.801	.642	0.439	0.626	44
October	.763	.582	0.418	0.658	49
November	.822	.675	0.223	0.684	51
December	.761	.579	0.199	0.766	49

of the monthly relationships allow prediction of the missing Santa Fe values. For the month of November, Santa Fe temperature values are slightly better correlated with those from Pecos, the difference between the Albuquerque and Pecos *r* values being only 0.014. This difference is tested to determine whether it is statistically significant, following

TABLE 7.
Correlation and regression statistics for Santa Fe (Y) and Taos (X) climate.

	Correlation		*Regression*		
	r	r^2	*Y Intercept*	*Slope*	*N*
			a. *Temperature*		
January	.864	.746	10.313	.763	70
February	.865	.749	9.889	.750	70
March	.834	.696	8.007	.818	69
April	.748	.560	11.070	.779	69
May	.786	.617	9.933	.840	70
June	.734	.538	15.133	.792	70
July	.522	.272	27.524	.615	70
August	.645	.416	24.573	.647	70
September	.589	.346	23.990	.630	70
October	.656	.431	12.097	.790	70
November	.675	.455	13.132	.706	70
December	.791	.626	8.353	.827	70
			b. *Precipitation*		
January	.638	.407	0.206	.607	69
February	.562	.316	0.288	.583	69
March	.588	.346	0.354	.532	69
April	.763	.582	0.087	.884	69
May	.587	.345	0.510	.664	69
June	.739	.546	0.398	.847	67
July	.427	.183	1.156	.641	68
August	.529	.280	1.329	.473	69
September	.698	.487	0.400	.904	69
October	.736	.542	0.375	.696	69
November	.651	.424	0.205	.694	70
December	.626	.391	0.313	.649	68

the method outlined by Spiegel (1961:269–72). The correlation coefficients are converted to z scores, or standard normal variates, and tested for a significant difference at the .01 level using a two-tailed test. As Table 8 shows, the difference is not statistically significant at the specified level, and therefore the Albuquerque estimation equation is

retained. Because all Albuquerque–Santa Fe monthly temperature correlations are higher than those for Taos–Santa Fe, the Taos regression equations are rejected for purposes of estimation.

Interstation correlations and regression statistics are also obtained for total monthly precipitation (Tables 5–7). The results show precipitation values from Pecos to be the best independent variables for estimating missing Santa Fe values. For the month of July, however, the correlation between the Santa Fe and Albuquerque precipitation values is slightly higher than the Santa Fe–Pecos correlation, the difference between the r values equaling 0.006. This difference is tested in the same manner as that between the November temperature correlation coefficients (Table 9). The difference is not significant at the .01 level; therefore, the July values from Pecos are used in the estimation procedure. All the Santa Fe–Pecos monthly correlations are higher than the corresponding correlations for Santa Fe and Taos, allowing us to reject the Taos estimates. Because a complete temperature and precipitation series from Pecos is needed for the analysis of relative homogeneity, the Santa Fe–Pecos linear regression computations are reversed, and missing Pecos meteorological values are estimated from the Santa Fe data. This procedure is possible because none of the missing values at either station occur during the same months.

TABLE 8.
Test for difference between Albuquerque–Santa Fe and Pecos–Santa Fe correlation coefficients for November temperature.

Albuquerque–Santa Fe	$r = .833$	$N = 78$
Pecos–Santa Fe	$r = .847$	$N = 22$

Level of Significance: .01

Null hypothesis (H_0): $z_1 = z_2$
Alternate hypothesis (H_1): $z_1 \neq z_2$
The null hypothesis will be rejected if $z > 2.58$ or < -2.58.

$$z_1 = 1.197$$
$$z_2 = 1.244 \qquad z = -0.183$$
$$r_{(z_1 - z_2)} = 0.257$$

The null hypothesis is accepted because -0.183 is not greater than 2.58 nor less than -2.58. There is no significant difference between the two correlation coefficients.

TABLE 9.
Test for difference between Albuquerque–Santa Fe and Pecos–Santa Fe correlation coefficients for July precipitation.

Albuquerque–Santa Fe	$r = .483$	$N = 98$
Pecos–Santa Fe	$r = .476$	$N = 51$

Level of Significance: .01

Null hypothesis (H_0): $z_1 = z_2$
Alternate hypothesis (H_1): $z_1 \neq z_2$
The null hypothesis will be rejected if $z > 2.58$ or < -2.58.

$$z_1 = .526$$
$$z_2 = .518 \qquad z = .046$$
$$r_{(z_1 - z_2)} = .177$$

The null hypothesis is accepted because .046 is not greater than 2.58 nor less than −2.58. There is no significant difference between the two correlation coefficients.

ANALYSIS OF SERIES HOMOGENEITY

Homogeneity of meteorological data means that "it offers uniform representativeness of the data for conditions in rather large geographical areas" (Mitchell et al. 1966). A data series is considered homogeneous if it can be regarded as a sample drawn from a single population. If a series is not homogeneous, adjustments must be made so that statistical estimates will be valid estimates of population parameters (Thom 1966).

Heterogeneity can be introduced into meteorological time series by a variety of factors. For many years, instrument location, exposure, and observational standards were determined by day-to-day operational requirements, which were often highly variable. Changes in instruments, their location and exposure, observational techniques, and landscaping, along with urban growth and human-induced environmental changes, can drastically affect series homogeneity.

Relative homogeneity refers to the comparability between several time series. Tests for relative homogeneity can be made graphically or, if necessary, with more objective statistical analyses. In this study, the graphic tests for relative homogeneity of the temperature and pre-

cipitation series demonstrate that the records are homogeneous, so further statistical tests are not applied. Seasonal values of temperature and precipitation are examined for relative homogeneity using CUTE (cumulative temperature analysis) and DMASS (double mass analysis of precipitation series) computer programs at the Laboratory of Tree-Ring Research.

From the annual values of monthly or seasonal temperatures from a pair of weather stations, CUTE calculates the mean and standard deviation for each station and the yearly differences and cumulative differences between stations. A plot of the progressive sums of the differences is then examined for abnormalities indicating heterogeneity. When the series are homogeneous, the plotted points fall along a straight line, but when heterogeneity is present, the slope of the line changes. This analysis is done for all combinations of the Albuquerque, Pecos, and Santa Fe temperature series for years common to both stations. Initially, various combinations of months are used as "seasons," but for all stations involved, the months of July, August, and September are combined, as are the months from November to February. Plots of the cumulative temperature differences are presented in Figures 13 and 14. Graphic screening with the CUTE program indicates that the Albuquerque–Santa Fe temperature records are homogeneous for the estimation period. That is, the slope of the plotted line does not change significantly through time.

The DMASS program performs a double mass analysis on two precipitation series, following the method outlined by Kohler (1949). Basically, seasonal precipitation values for the station under test and those for comparative stations are plotted against one another in the form of cumulative sums. Screening the July to September and November to February Pecos–Santa Fe precipitation by the DMASS program indicates that the precipitation records from the two stations are relatively homogeneous because the slopes of the lines remain constant (Figs. 15, 16).

The analyses described in this chapter indicate that the Santa Fe precipitation and temperature data are suitable for dendroclimatic analysis. The statistical attributes of the weather data characterize the annual Santa Fe climatic variability that is to be related to Glorieta Mesa tree growth. Tests for homogeneity show both the precipitation and temperature time series to be free of time-dependent anomalies that could warp the results of the calibration and verification analyses.

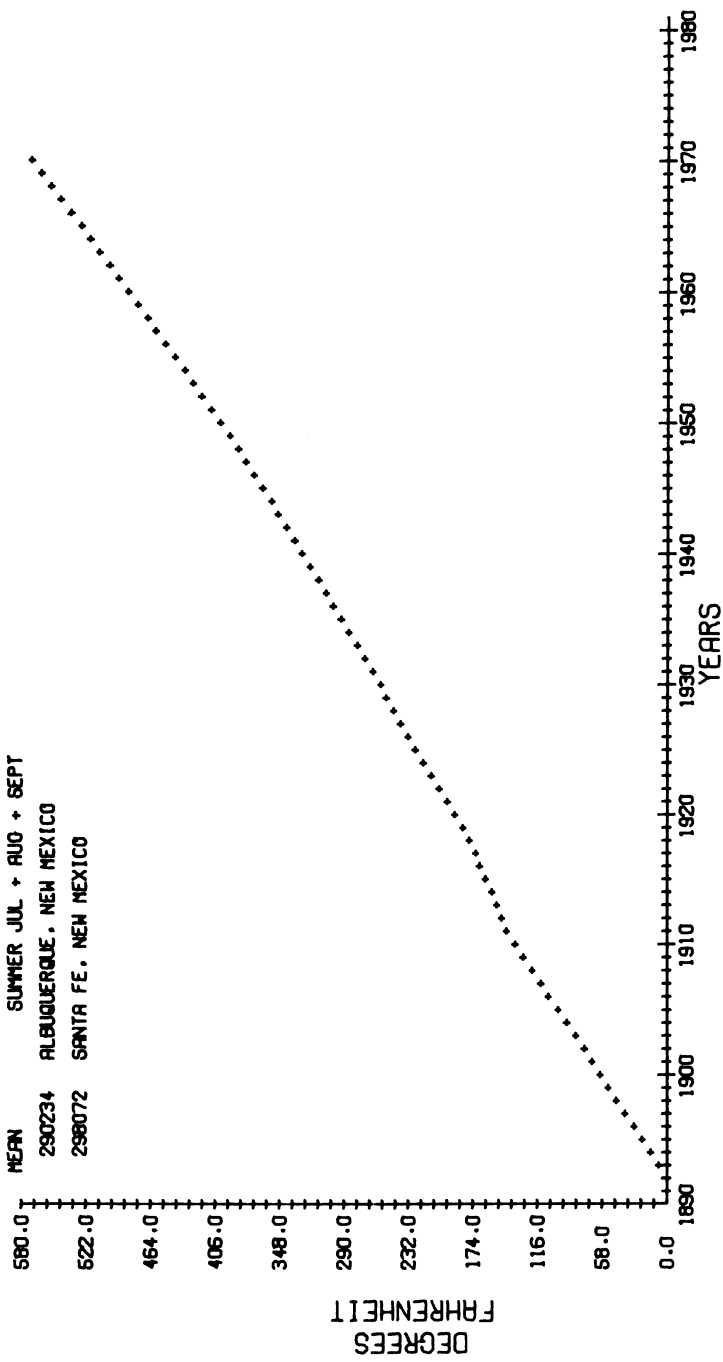

FIG. 13. CUTE analysis of July–September temperature, Santa Fe and Albuquerque.

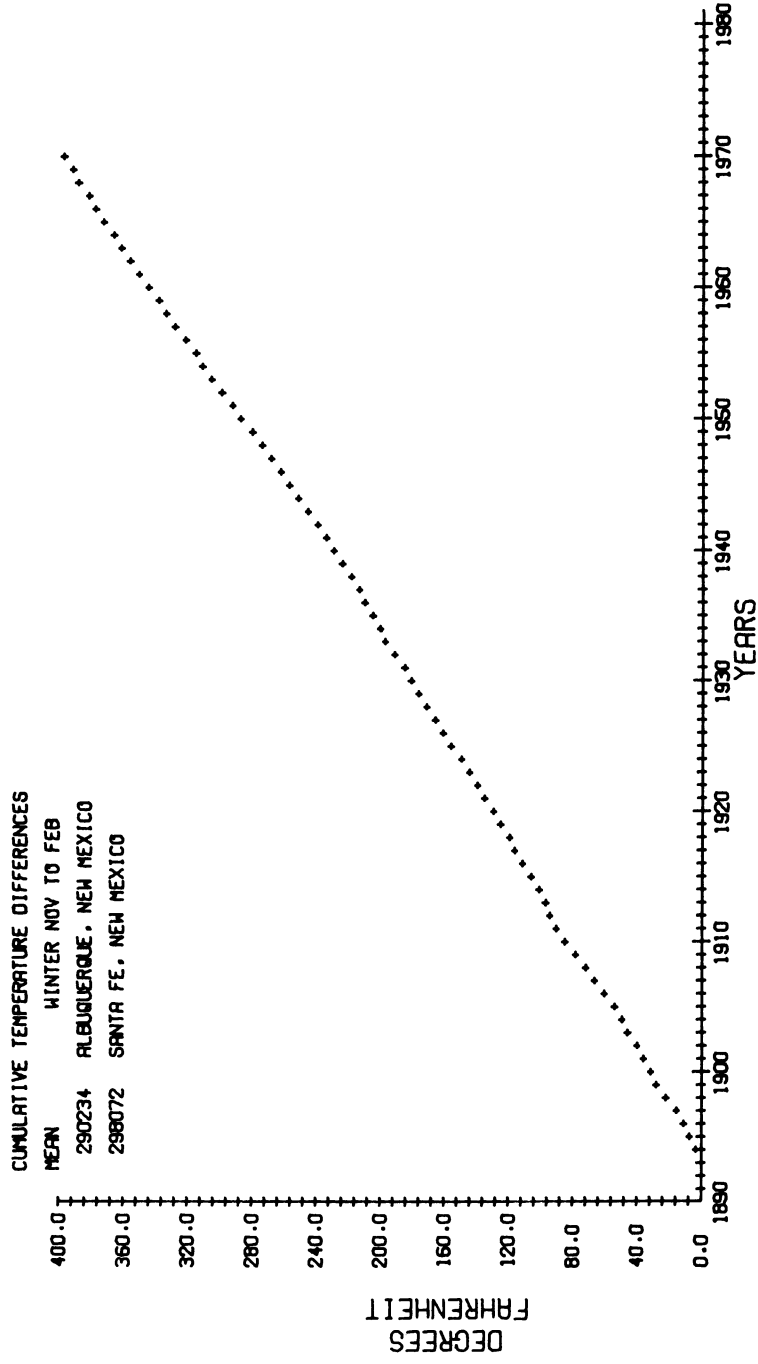

FIG. 14. CUTE analysis of November–February temperature, Santa Fe and Albuquerque.

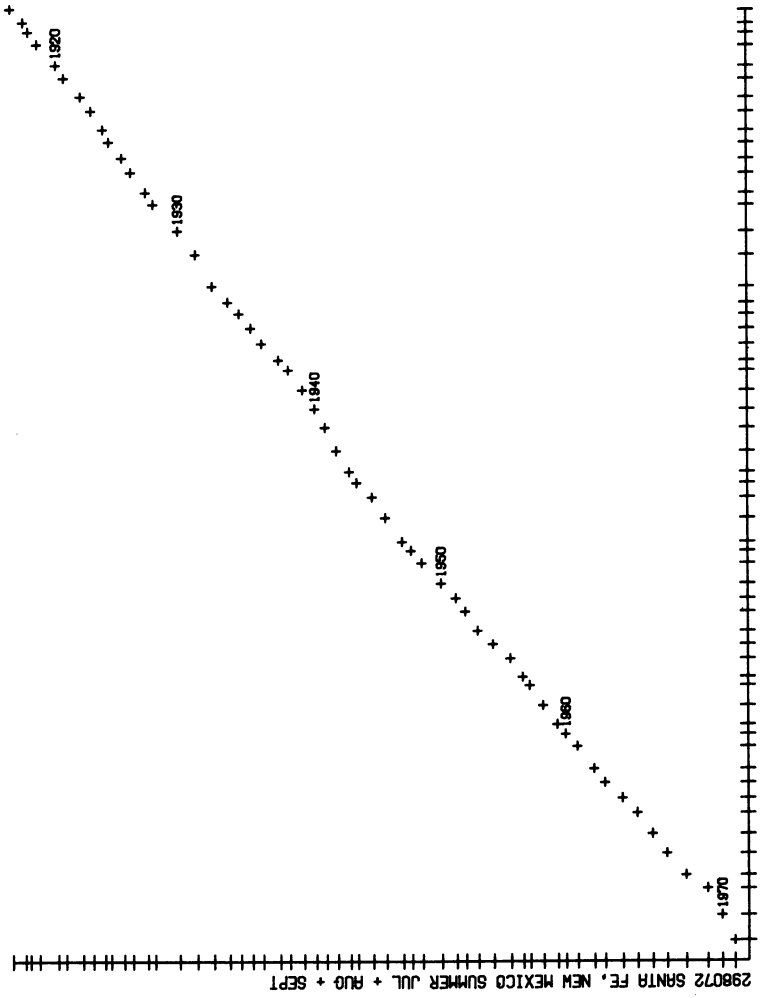

FIG. 15. DMASS analysis of July–September precipitation, Santa Fe and Pecos.

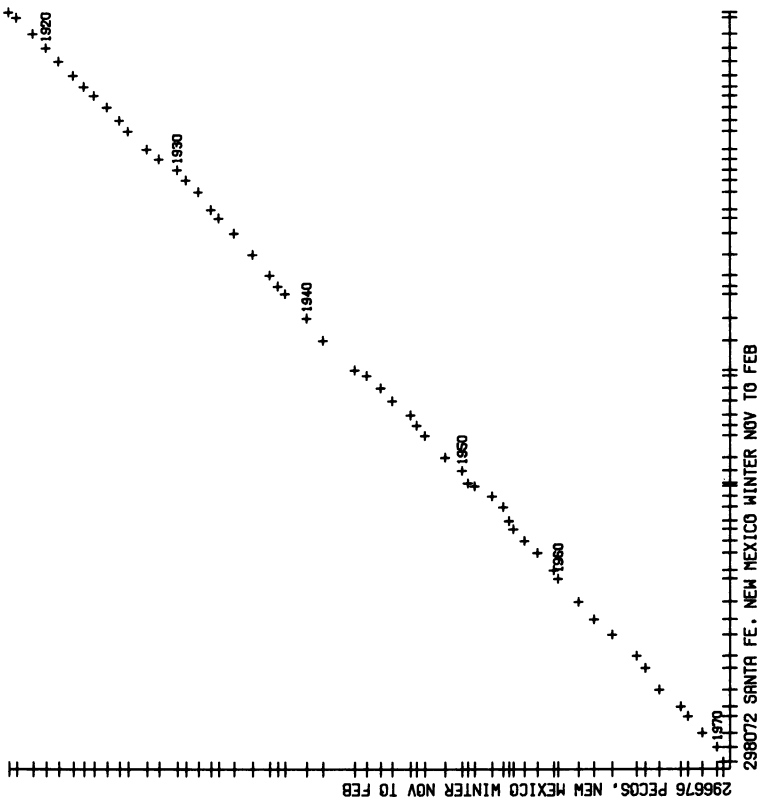

FIG. 16. DMASS analysis of November–February precipitation, Santa Fe and Pecos.

4
Calibration of Tree-Ring and Climatic Time Series

Previous dendroclimatological research used the technique of stepwise multiple regression, in which a small set of independent variables is selected from a larger set (Fritts 1962; Fritts, Smith, and Stokes 1965:111–17). The matrix of simple correlation coefficients between the independent variables (temperature and precipitation) and the dependent variable (tree-ring indices) is examined to determine which are most highly correlated. The independent variable most highly correlated with the dependent variable is entered into the regression equation first. Then, the remaining independent variable that has the highest correlation with the residual variance is entered, followed by the next most highly correlated, and so on. This operation is carried out as long as the amount of variance reduced is significant.

A problem with this technique, however, is that high intercorrelations among the independent variables may prohibit significant variables from being entered into the equation. The order of variables in the equation also can change as independent variables highly correlated with ones already in the equation are used. This occurs because the significance of each regression coefficient is tested at each step, and insignificant variables are removed from the equation. Another problem with stepwise multiple regression is that interrelationships among correlated variables combined linearly to create a vector variable require the

estimation of a large number of parameters. A combination of p variables has a total of $(p^2 - p)/2 + 2p$ parameters to estimate (Cooley and Lohnes 1971:96). The 28 climatic variables used in the present analysis—14 months of temperature and 14 months of precipitation— would require the estimation of 378 parameters $[(28^2 - 28)/2 + 2(28)]$.

The problems inherent in stepwise multiple regression analysis are avoided by transforming the variables into uncorrelated analogs, which is done by principal components analysis (Fritts 1976:352–63). The uncorrelated (geometrically orthogonal) variables are called eigenvectors. A p element vector variable of uncorrelated elements (eigenvectors) requires the estimation of only 2(28), or 56, parameters: the means and variances of the 28 climatic variables. A vector variable of uncorrelated elements also yields an unambiguous statistical relationship between any element and the dependent variable. The relationship of each element of the vector variable to the dependent variable is independent of any other element's relationship to it (Harris 1975).

THE RESPONSE FUNCTION

Principal components analysis is a multivariate technique used to examine relationships within a set of variables (Harris 1975). The components, linear combinations of the original variables, describe the correlation structure of the original data set and make it possible to account for most of the variability with a smaller number of uncorrelated variables. It is considered to be a data reduction technique because it reduces the dimensions of the original data matrix. Primarily, however, it provides uncorrelated variables that represent the dominant patterns in the data and that are used in multiple linear regression. Thus, problems caused by multicollinearity are eliminated.

Normalization of Climatic Data

The climatic data used in the calibration procedure are mean monthly temperature measured in degrees Fahrenheit and total monthly precipitation measured in inches for the 14-month period prior to and concurrent with the growing season. These two time series are not directly comparable because they are coded in nonequivalent units, inches and

degrees Fahrenheit, and because their means and variances differ. To achieve comparability, the data are transformed (normalized) into standard normal variates or z scores (Snedecor and Cochran 1967:35). The series mean is subtracted from each value and the result divided by the standard deviation of the series to produce a z score. The z scores for a set of data have a mean of zero and a standard deviation of one. Normalizing reduces the nonequivalent variability in different data sets to a uniform scale, which permits the direct comparison of the data. Normalized temperature and precipitation data for the 14-month periods ending in 1924, 1951, and 1954 are presented in Figures 17, 18, and 19.

Eigenvectors

To circumvent the problems caused by intercorrelations within the normalized climatic time series, principal components analysis is used to create new sets of uncorrelated (orthogonal) variables called eigen-

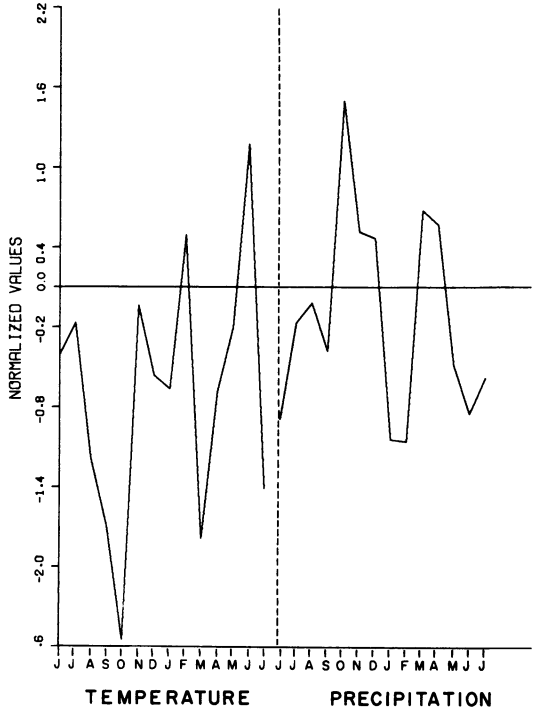

FIG. 17. Normalized temperature and precipitation for 14-month period ending in 1924.

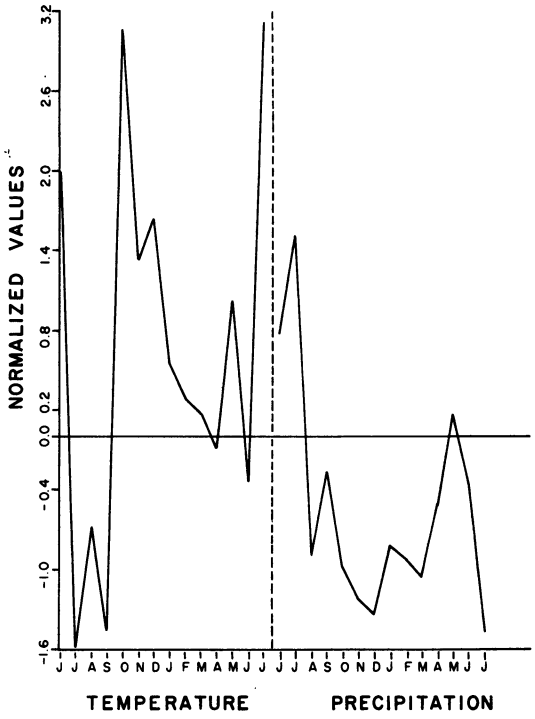

FIG. 18. Normalized temperature and precipitation for 14-month period ending in 1951.

vectors. In principal components analysis, eigenvectors are derived from the matrix of correlation coefficients among the independent variables by a mathematical procedure that is discussed by Ayres (1972), Cooley and Lohnes (1971), Harris (1975), and Tatsuoka (1974). The first few eigenvectors usually represent most of the variability in the data; the subsequent ones represent minor variations. This makes it possible to use a subset of the total set of eigenvectors in further statistical analysis.

The first eigenvector is the linear combination of original variables that most efficiently discriminates the cases in the sample, in this study 14-month "years." It is the one accounting for the largest amount of sample variance, subject to the constraint that the sum of the squares of the elements equals one. As an example, the sum of the squared values in Table 10 equals 1.00, neglecting rounding error. The second eigenvector is the linear combination of the original variables accounting for the largest amount of residual sample variance, subject to the restrictions that the total of the squared elements equals one and that the eigenvector is uncorrelated with the first principal component.

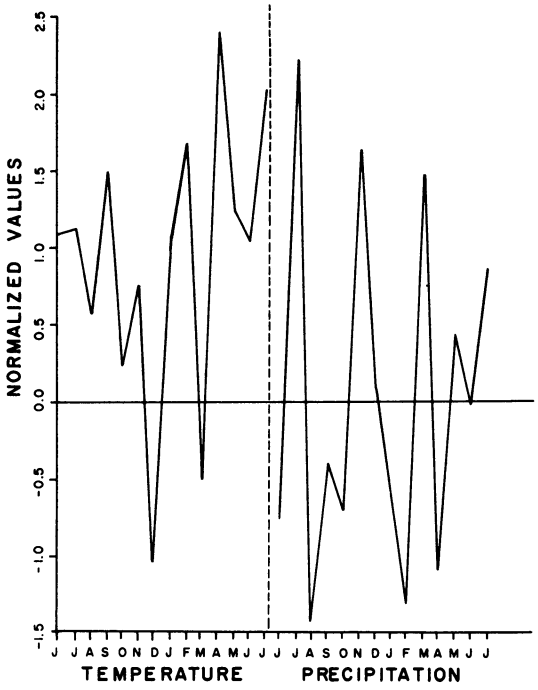

FIG. 19. Normalized temperature and precipitation for 14-month period ending in 1954.

TABLE 10.
Elements of eigenvector 1 for 14-month "year."

	Temperature		*Precipitation*	
	Elements 1–14	*Elements²*	*Elements 15–28*	*Elements²*
June	.3041	.0925	−.1280	.0164
July	.1769	.0313	.0471	.0022
August	.2203	.0485	−.1229	.0151
September	.3448	.1189	−.1901	.0361
October	.3660	.1296	−.2678	.0717
November	.0558	.0031	.0967	.0094
December	.2244	.0504	−.1727	.0298
January	.2133	.0455	.0513	.0026
February	.0893	.0080	.0966	.0093
March	.1114	.0124	.0570	.0033
April	.1994	.0143	−.1391	.0194
May	.1384	.0192	.0733	.0054
June	.1300	.0169	−.1600	.0256
July	.3611	.1304	−.0861	.0074
			Sum of squares =	.9747

Each successive eigenvector accounts for as much variance as possible in the original data, subject to the condition that it be uncorrelated with previous ones. When the original variables are highly intercorrelated, the first few eigenvectors account for a high percentage of the variance. The remaining eigenvectors account for little variance and can be disregarded for most purposes. The uncorrelated nature of the eigenvectors eliminates complication in interpreting the way each year's values on a set of variables affect or are affected by other variables.

Associated with each eigenvector is an eigenvalue, which represents the variance accounted for by each component. Eigenvalues for the eigenvectors extracted from the Santa Fe climatic data are presented in Table 11. The proportion of the variance explained by a particular eigenvector is obtained by dividing its eigenvalue by the sum of all the eigenvalues and multiplying by 100. Table 11 shows that the first eigenvector accounts for 10.531 percent of the variance, that the first twenty account for 93.134 percent of the variance, and that all 28 eigenvectors account for 100 percent of the variance in the original data.

Each eigenvector contains elements that express the relative importance of each of the original variables and that can be used in describing the mode of behavior the eigenvector represents. Each eigenvector contains as many elements as there are original variables, in this case 28. The elements of the 28 climatic variables for the first three eigenvectors are presented in Table 12 and plotted in Figures 20, 21, and 22. For example, the first eigenvector represents a type of year in which climate was either warmer and drier or cooler and wetter than normal. The actual signs of the elements of an eigenvector are not important, for all could be multiplied by -1.0. What is important is the pattern represented by the elements of an eigenvector. That is, for certain variables the elements are opposite in sign and differ in magnitude, or possibly they have similar signs and are large or small.

Eigenvector Amplitudes

Multiplying the transpose of the eigenvector matrix by the matrix of normalized climatic data creates a new matrix of values referred to as amplitudes (Equation 1). The amplitude matrix contains in uncorrelated form the same information as the matrix of normalized climatic data.

TABLE 11.
Eigenvalues for Santa Fe climatic data matrix for calibration period, A.D. 1917–1970.

Eigenvector	*Eigenvalue*	*Variance (%)*	*Cumulative %*
1	2.94877	10.531	10.531
2	2.65160	9.470	20.001
3	2.08745	7.456	27.457
4	1.98876	7.103	34.560
5	1.77079	6.324	40.884
6	1.64129	5.862	46.746
7	1.56017	5.572	52.318
8	1.35319	4.833	57.150
9	1.25068	4.467	61.617
10	1.18741	4.241	65.858
11	1.11543	3.984	69.842
12	1.07245	3.830	73.672
13	0.94325	3.366	77.037
14	0.84516	3.018	80.056
15	0.77236	2.758	82.814
16	0.65811	2.350	85.165
17	0.62407	2.229	87.393
18	0.58459	2.088	89.481
19	0.53588	1.914	91.395
20	0.48692	1.737	93.134
21	0.39583	1.414	94.548
22	0.33106	1.182	95.730
23	0.29451	1.052	96.782
24	0.25815	0.922	97.704
25	0.25489	0.910	98.614
26	0.18142	0.648	99.262
27	0.11386	0.407	99.669
28	0.09272	0.331	100.000

TABLE 12.
Eigenvector elements for first three eigenvectors for 14-month "year."

	Temperature			*Precipitation*		
	1	2	3	*1*	2	3
June	.3041	−.1795	.0174	−.1280	−.3846	−.1891
July	.1769	.0517	.3573	.0471	−.1199	−.3566
August	.2203	.1388	.2507	−.1229	−.0287	−.0459
September	.3448	.1366	.1773	−.1901	−.0268	−.0702
October	.3660	.0388	−.1476	−.2678	−.1083	.1487
November	.0558	.3229	−.3920	.0967	−.3487	.1343
December	.2244	.0388	−.0589	−.1727	.1432	.0636
January	.2133	−.0162	−.2348	.0513	.1890	.2562
February	.0893	−.1298	−.0944	.0966	.0316	.1727
March	.1114	.4169	−.0073	.0570	−.2207	.2622
April	.1994	.0419	.0650	−.1391	−.2658	−.1018
May	.1384	.0795	−.0212	.0733	−.1556	.0929
June	.1300	.0950	.1049	−.1600	.2072	.1289
July	.3611	−.0830	−.2016	−.0861	.2538	.2539

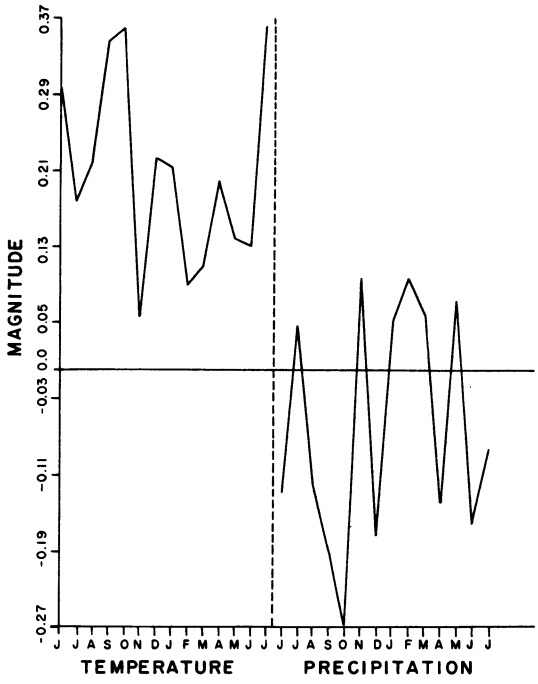

FIG. 20. Eigenvector 1 of Santa Fe climate.

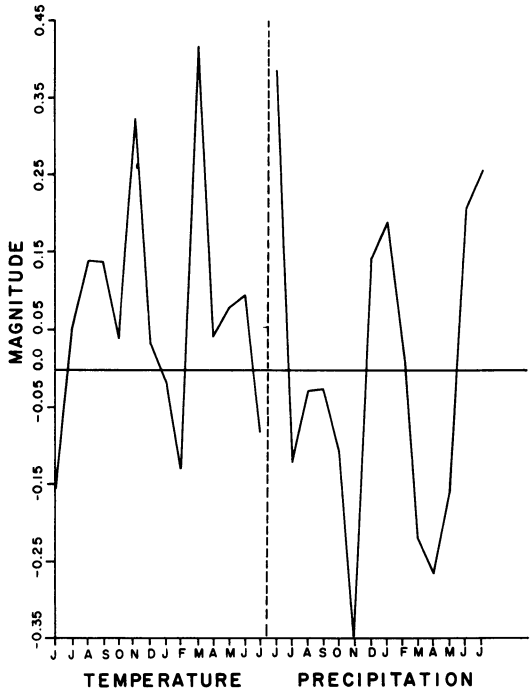

FIG. 21. Eigenvector 2 of Santa Fe climate.

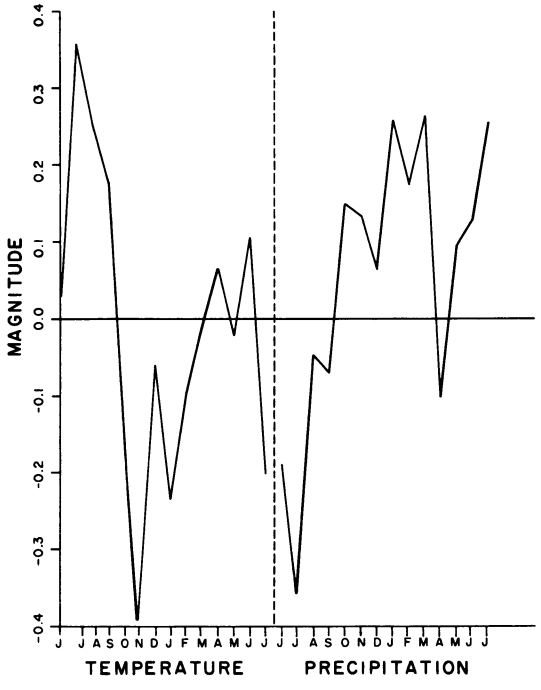

FIG. 22. Eigenvector 3 of Santa Fe climate.

Capital letters in Equation 1 symbolize matrices, while the subscripts before and after the capital letters are the numbers of rows and columns, respectively.

$$ {}_{p}X_{n} = {}_{p}E'_{m}{}_{m}F_{n} \tag{1} $$

where the subscripts
p = number of important eigenvectors (in this study, 20),
n = number of years (54), and
m = number of variables (28).

The transpose of the eigenvector matrix is denoted ${}_{p}E'_{m}$, and ${}_{m}F_{n}$ is the original climatic data matrix.

For each eigenvector, there is a value (amplitude) associated with each year from 1917 to 1970 for which climatic data are used. Each year's amplitude expresses how closely the temperature and precipitation of that year resemble the eigenvector. When the amplitude for a year is large and positive, the climate of that year resembles the positive form of the eigenvector; when the amplitude is large and negative, the climate resembles the inverse form. A small amplitude indicates that the year's climate is unlike the eigenvector. The amplitudes associated with the first three of the 28 eigenvectors are presented in Figure 23. The first series (Fig. 23a) has extreme amplitudes at 1924 (negative) and 1954 (positive). Thus, the climate of the 14-month year ending in 1924 resembles the inverse of the first eigenvector, while the climate of 1954 resembles it directly. The third amplitude series (Fig. 23c) has a large negative value for 1951, indicating that the climate of the 14-month period ending in that year resembles the inverse of the third eigenvector.

The plot of the normalized temperature and precipitation values for the 14-month year ending in 1924 (Fig. 17) resembles the inverse form of the first eigenvector (Fig. 20), as would be expected on the basis of the year's large negative amplitude (Fig. 23a). Conversely, the normalized climatic data for 1954 (Fig. 19) resemble the positive form of the first eigenvector (Fig. 20), as predicted by the large positive amplitude (Fig. 23a). In addition, the normalized climatic data for 1951 (Fig. 18) resemble the inverse of the third eigenvector (Fig. 22).

Unlike the "factors" of factor analysis, the orthogonal eigenvectors are closely related to the original variables. Knowledge of each year's amplitude for all the eigenvectors, combined with the knowledge of the

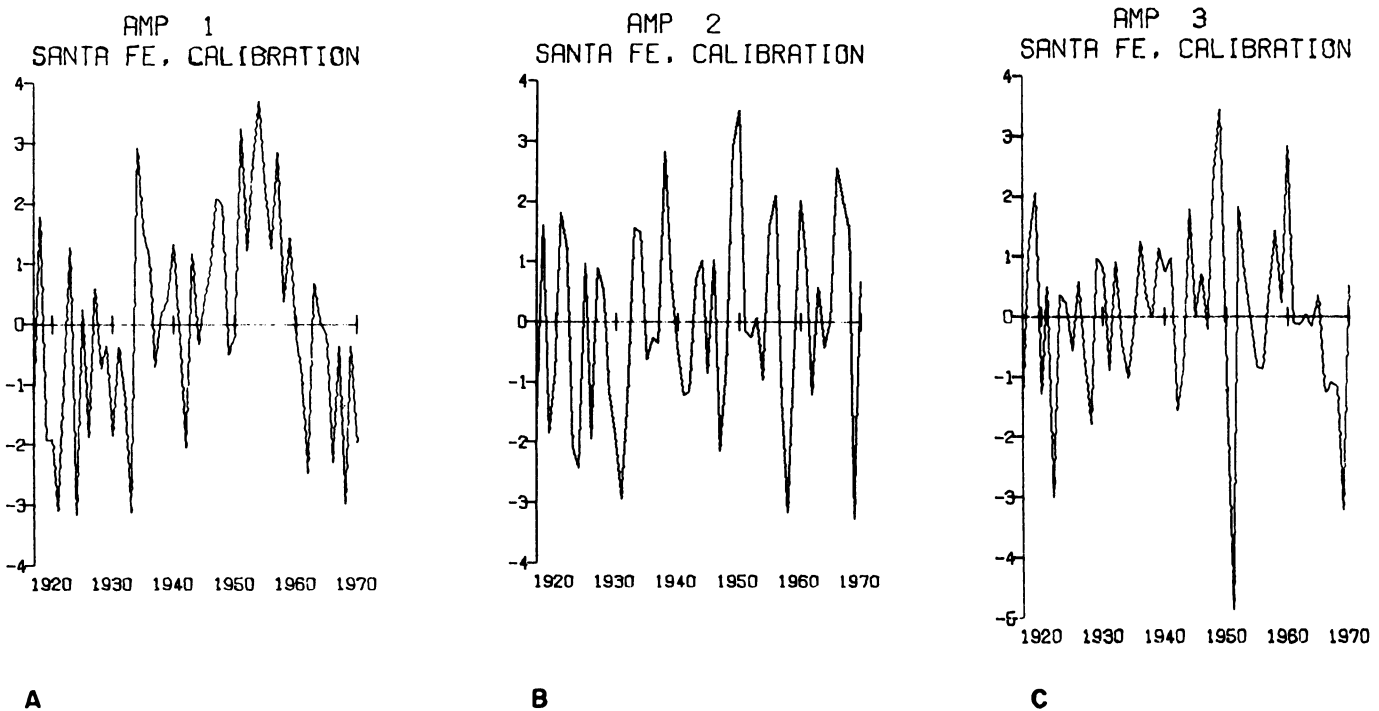

FIG. 23. Amplitude series for eigenvectors 1–3, Santa Fe climate.

elements, or coefficients, defining the relative importance of each original variable in the eigenvector, is sufficient to reproduce the exact values of each of the 28 climatic variables for every year. Just as eigenvectors are linear combinations of the original variables, it is also possible to define each of the original variables in terms of the eigenvector elements (Harris 1975:25).

Eigenvector Amplitudes and Regression

Because the eigenvectors are uncorrelated with one another, they satisfy the assumption of "independence" in the independent variables used in multiple linear regression procedures. An additional advantage is that it may be possible to use a smaller number of eigenvectors to achieve a predictive accuracy equal to that provided by a larger number of the original climatic variables. Furthermore, fewer degrees of freedom may be consumed. The amplitudes, because they represent the climatic data, can be used in the regression procedure to predict ring-width variability. Symbolically this is denoted by

$$ {}_1\hat{P}_n = {}_1R_p X_n \qquad (2) $$

where subscripts are the same as in (1) and
${}_1\hat{P}_n$ = row vector of predicted ring widths,
${}_1R_p$ = row vector of regression coefficients, and
${}_pX_n$ = amplitude matrix.

The regression coefficients in this equation indicate the relative importance of each eigenvector in predicting ring-width values. However, because entities in the real world do not behave in an uncorrelated manner, it is desirable to have a way of expressing these relationships with respect to the original climatic data. It is simple to convert the regression coefficients in (2) to new ones expressing the relationships in terms of the original climatic variables. Substituting the extended notation for the amplitudes (1) into equation (2) yields

$$ {}_1\hat{P}_n = {}_1R_p E'_m F_n. \qquad (3) $$

The addition of parentheses around the E and F matrices in (3) would designate regression with the amplitudes, identical to Equation (2). However, using the associative principle of multiplication, $[A(BC) =$

$(AB)C$], it is possible to multiply the R and E' matrices to create a new set of coefficients, ${}_1T_m$, which can be multiplied by the matrix of normalized climatic data.

$$ {}_1\hat{P}_n = {}_1T_m F_n \qquad (4) $$

$$ \text{where } {}_1T_m = {}_1R_p E'_m. $$

The T matrix is referred to as a response function whose elements can be interpreted in terms of the importance of the original climatic variables, mean monthly temperature or total monthly precipitation, relative to the width of the annual ring.

Because of autocorrelation, lagged ring-width indices for a number of prior years, three in this case, are often included as additional predictors in the regression equation. These lagged indices are denoted as ${}_1Z_3$, with the associated regression coefficients ${}_1R^*_3$. Ring indices can then be estimated by including these additional variables, ${}_1R^*{}_3Z_n$, in the equation. If significant autocorrelation is present, inclusion of prior growth values usually results in improved prediction. The residuals are then checked mathematically to determine whether their distribution through time is random. This is necessary to determine if the significance tests associated with the regression procedure are valid. In this analysis, residual autocorrelations were computed for lags of one to ten years and were found to be not significant at the .05 level.

Confidence limits for elements of the response function are calculated from their standard errors, which are derived from the standard errors for the elements of ${}_1R_p$ (Fritts 1976:365). This relationship is expressed by

$$ {}_mS_m = {}_mE_p U_p U_p E'_m \qquad (5) $$

where

${}_pU_p$ is the diagonal matrix of standard errors of elements of ${}_1R_p$, and

${}_mS_m$ is the symmetrical matrix whose diagonal elements are standard errors of the elements of ${}_1T_m$, the response function.

In this procedure, the distribution of the square of the errors to each standard error is proportional to the square of the elements of the eigenvector (Fritts 1976:365). Confidence limits for each element in the response function equal the square root of the product of each

diagonal element of the symmetrical matrix ($_mS_m$) multiplied by the F-value associated with V_1/V_2 degrees of freedom. V_1 equals the number of significant elements of $_1R_p$, and V_2 is the effective sample size minus the number of significant regression coefficients in $_1R_p$ and $_1R^*_3$, minus two more degrees of freedom. Effective sample size normally equals the length of the observation period if significant residual autocorrelation is absent. As mentioned earlier, this is the case for the Glorieta Mesa piñon response function, in which residual autocorrelation is not significant at the .05 level.

The Glorieta Mesa Piñon Response Function

The response function for Glorieta Mesa piñon, at four steps, is illustrated in Figures 24–27. The F-value at each step is presented at the top of each figure, in addition to the amount of variance in ring-width indices "explained" by the linear combination of climatic variables (PCL). The square of the correlation coefficient (R^2) is also listed in Figures 24–27. The R^2 value denotes the percentage of the variance in ring widths that is statistically explained by the linear combination of variables, including prior growth. In the response function in this study, the difference between PCL and R^2 can be regarded as the amount of variance explained by prior growth at a lag of one year. The vertical lines in the figures are the 95 percent confidence intervals used to test for significance.

The changing shape of the response function in Figures 24–27 indicates that as more eigenvector amplitudes are included in the regression equation, the predictions become more accurate, and finer details of the function emerge. Termination of the regression procedure occurs when the F-ratio for the variable being added to the equation is less than one. Using the F-ratio in such a capacity is using it not as a significance test but as a measure of the amount of variance reduced relative to the error variance (Fritts 1976:368). When the former is less than the latter, nothing is gained by including the variable as a predictor in the equation. If necessary, a larger F-ratio can be used as a stopping criterion. For instance, if 3.00 had been used, the calculation of the response function would have terminated after the seventh step, with 63.1 percent of the variance explained (Fig. 26). Continuing the calculation to the tenth step, with an F-ratio of 1.01

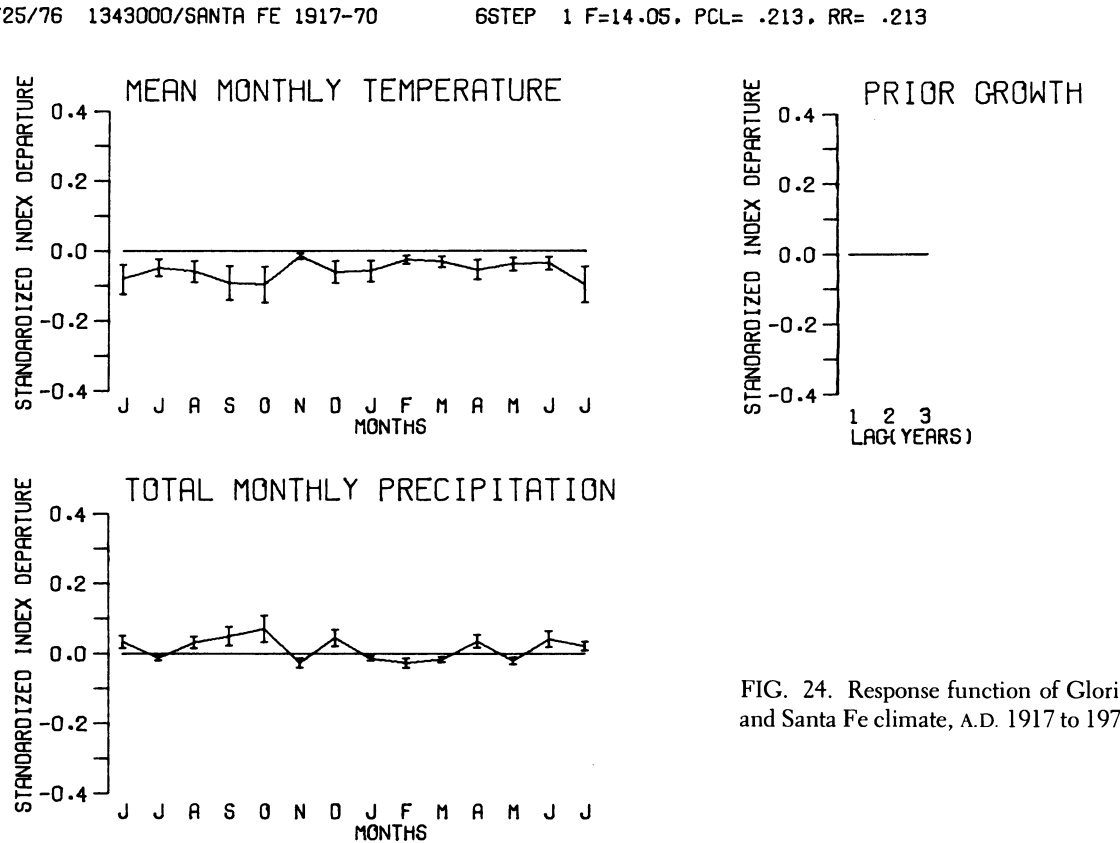

FIG. 24. Response function of Glorieta Mesa chronology and Santa Fe climate, A.D. 1917 to 1970, step 1.

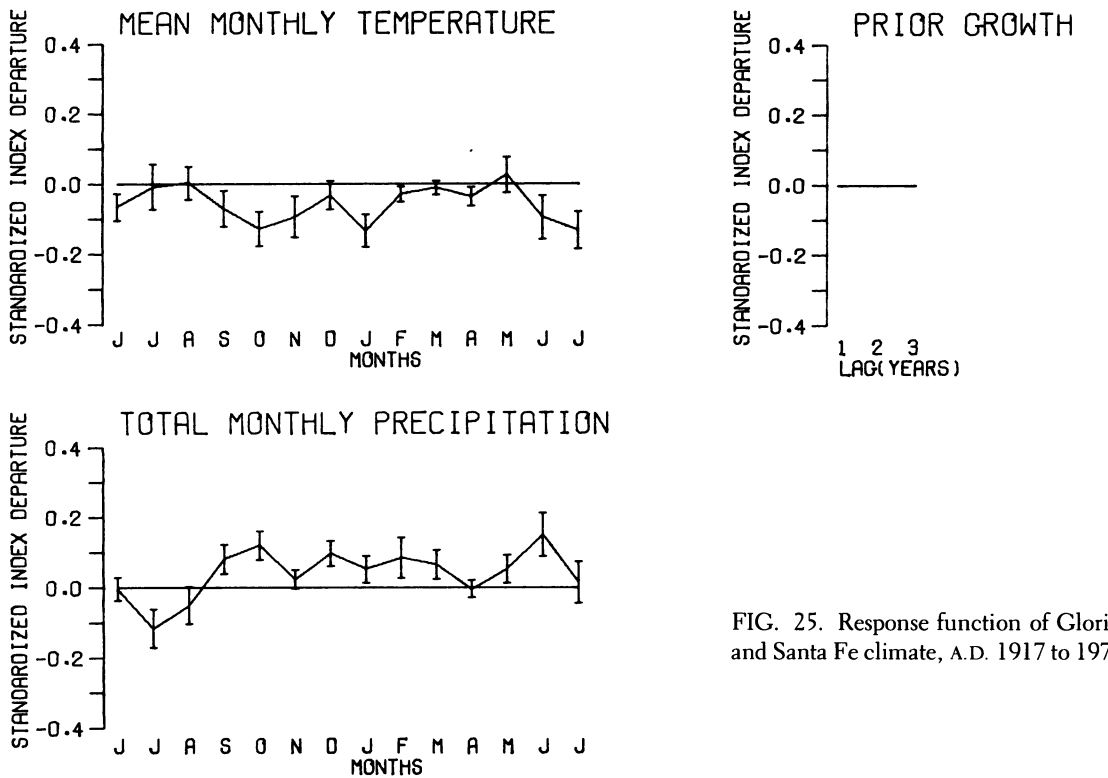

FIG. 25. Response function of Glorieta Mesa chronology and Santa Fe climate, A.D. 1917 to 1970, step 3.

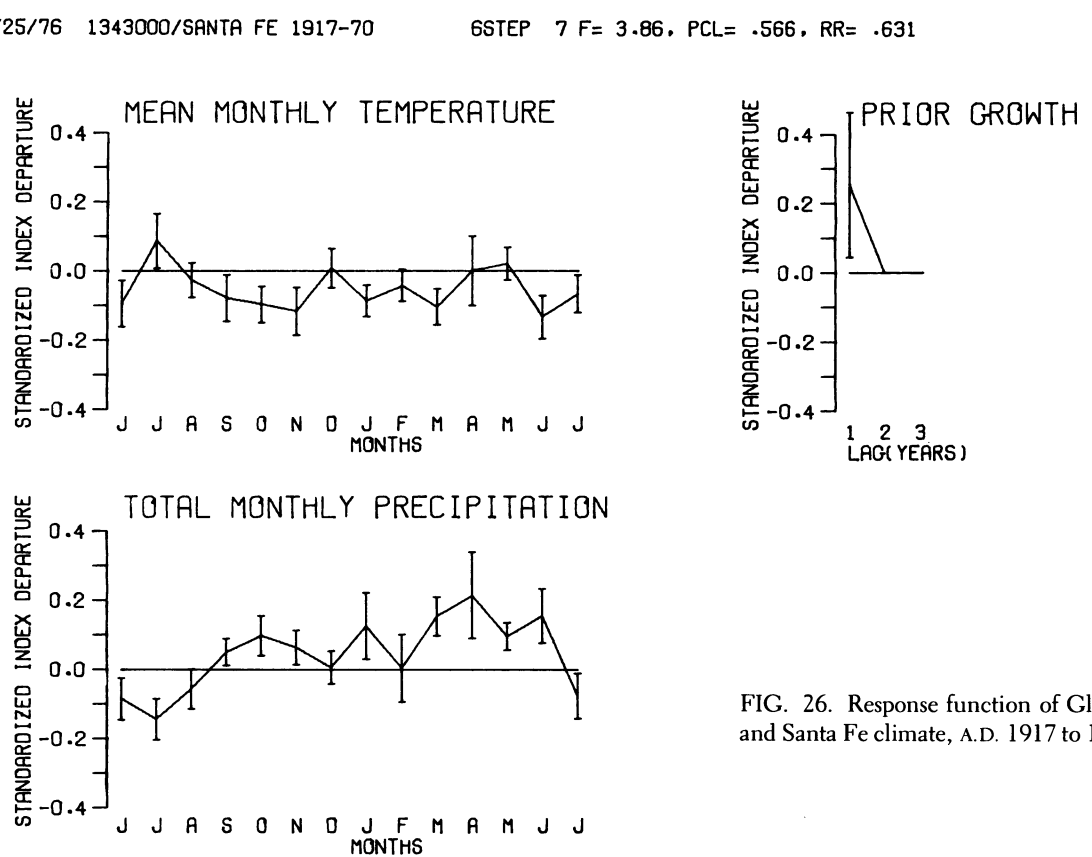

FIG. 26. Response function of Glorieta Mesa chronology and Santa Fe climate, A.D. 1917 to 1970, step 7.

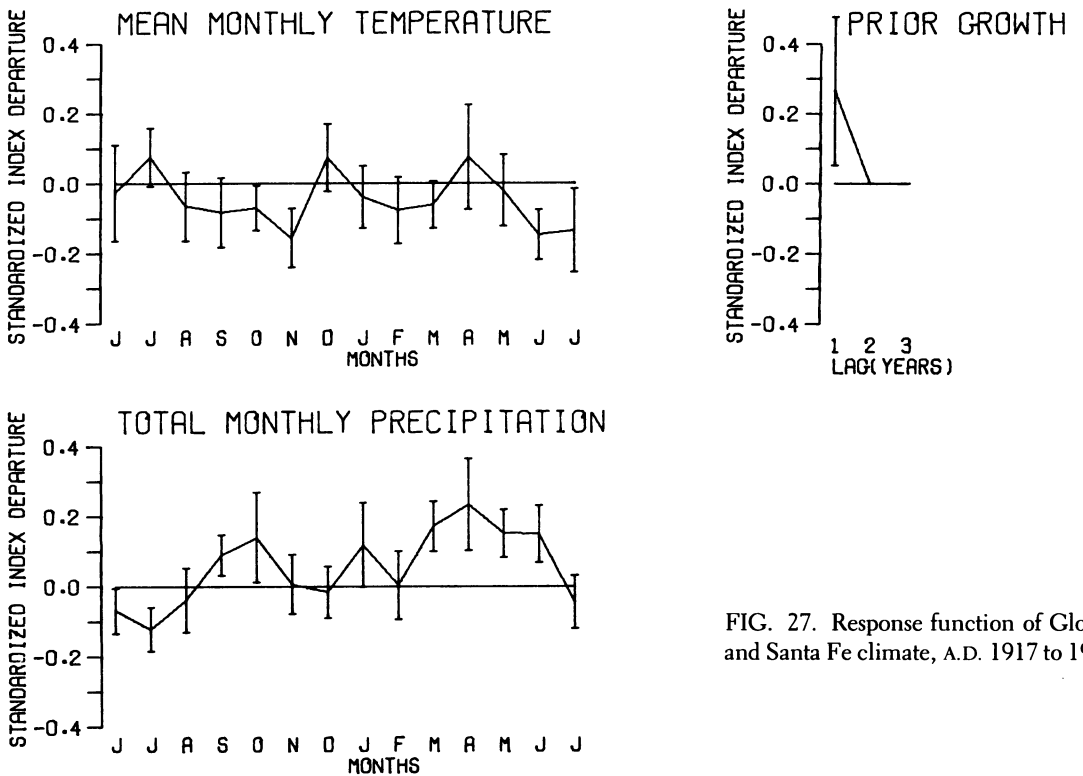

FIG. 27. Response function of Glorieta Mesa chronology and Santa Fe climate, A.D. 1917 to 1970, step 10.

and an R^2 of 66.3 percent, results in an increase of only 3.2 percent in explained variance (Fig. 27).

Other research (Fritts 1976:370) has demonstrated that the regression coefficients used in stepwise linear regression with actual climatic data do not coincide with elements of the response function, that is, results of regressing actual climatic data and regressing eigenvector amplitudes are not always the same. In general, results with actual data are not as stable as those obtained with the principal components technique used in conjunction with multiple linear regression, especially when elements of the original data matrix are highly intercorrelated.

In the Glorieta Mesa piñon response function (Fig. 27), some of the significant elements associated with a particular month are positive, while others are negative. A significant positive value indicates a positive (direct) relationship between the climatic variable and ring width; a significant negative value denotes a negative (inverse) relationship between the climatic variable and increases in ring width.

For example, the response function (Fig. 27) shows that below-average monthly temperatures during prior November and current June and July are associated with increased ring width. This relationship is denoted by the diagram in Figure 28. Only two of the significant elements of the response function exhibit an inverse relationship

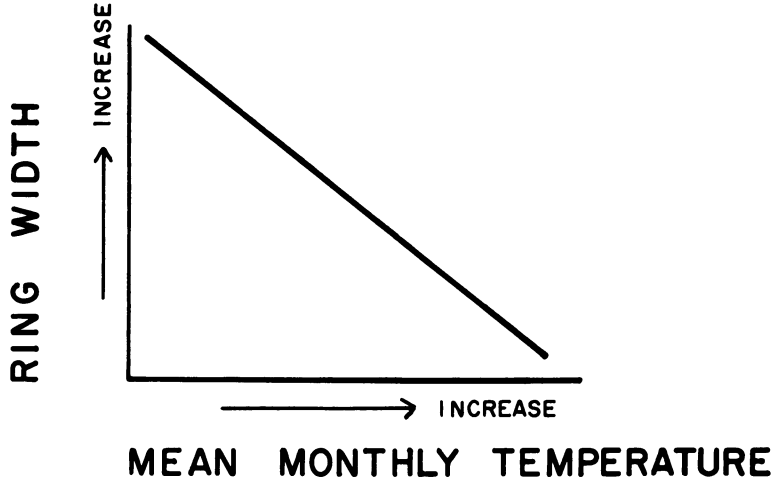

FIG. 28. Schematic diagram of inverse relationship in response function.

of total monthly precipitation to increased ring width. Below-average total precipitation for prior June and July is related to increases in ring width. In contrast, above-average monthly precipitation values for the prior September and October and the current January, March, April, May, and June are directly related to increased growth. The positive relationship is presented in simplified form in Figure 29.

Other climatic factors and months, if necessary, can be used in predicting ring-width variability if there are theoretical reasons for doing so. For instance, Fritts, Smith, and Stokes (1965) observed that radial growth in piñon trees on Mesa Verde, Colorado, began in early June and ended in late July or August. On the chance that Glorieta Mesa piñon growth might be affected by late summer weather, a response function was generated for this series that included the months of current August and September. However, the response to temperature and precipitation was not significant, and this response function is not used here.

THE TRANSFER FUNCTION

In contrast to the response function, which is used to predict tree-ring indices from eigenvector-weighted climatic data, the transfer function provides a basis for retrodicting climatic data from tree-ring

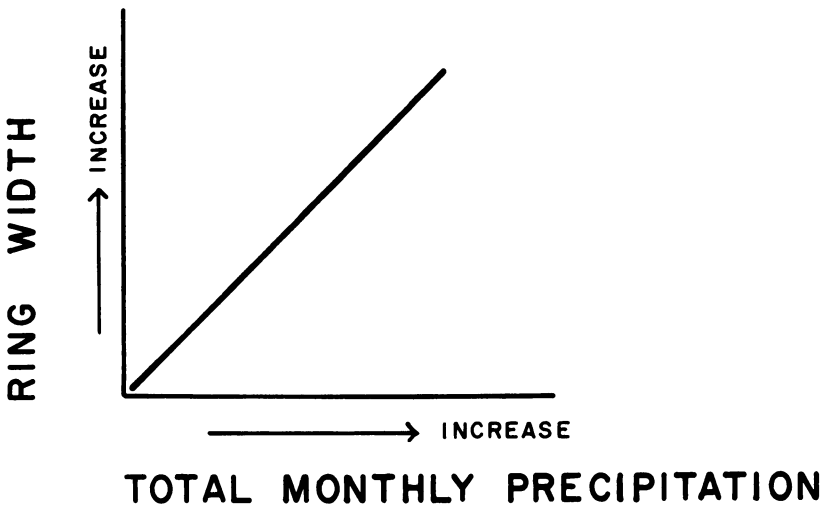

FIG. 29. Schematic diagram of direct relationship in response function.

values. The response function specifies several significant relationships between tree growth and climate in the Santa Fe area (Fig. 27). Total precipitation of prior August through current July, of prior September and October, of current January, and of current March through June are directly related to ring width, while prior June and July precipitation is inversely related to tree growth. Mean temperatures of prior October and November and of current June and July are inversely related to ring width. These variables are potentially reconstructable by applying the transfer function to the index values of the Santa Fe paleoclimatic tree-ring chronology.

Production of a transfer function, which translates ring-width variability into climatic variability, is a matter of multiple regression. The independent variables are ring indices for a given year, the three years preceding it, and the two years following it. Indices for six years are used to retrodict climatic values (the dependent variables) because of lags in the responses of southwestern conifers to climatic variation (Fritts 1976:25–28). Apart from the direct effects on tree growth of the weather of the preceding and current years that are specified by the response function, indirect effects link tree growth to the weather of the prior three and the two following years. Weather conditions influence needle production (Fritts et al. 1965:106–07), which in turn affects the amount of photosynthetic area available to the trees. Trees with photosynthetic area increased by favorable climatic conditions are more efficient and produce more food to be metabolized for radial growth. Conversely, trees with photosynthetic capacity reduced by unfavorable climatic conditions produce less food than might be expected from the amount of water actually available. Because piñons generally replace some needles each year (Fritts 1976:188), climatic effects on photosynthetic capacity are manifest in ring growth for up to three years. For these reasons, we use ring-width data for the three years prior to growth as climatic predictors. Similarly, because the effects of one year's climate on photosynthetic capacity persist for about three years, the two years following the target year for climatic retrodiction are incorporated in the regression analyses. The inclusion of these two years improves the retrodiction by more than five percent over a reconstruction based only on the three prior years and the current year. Note that this procedure cannot be reversed: climatic data for following years cannot be used to predict tree growth.

The Regression Equations

To transform ring-width index variability into climatic information, a multiple regression procedure is used, which fits a hyperplane, rather than a line as in bivariate regression, to the multidimensional data by the least squares technique. This technique minimizes the sum of the squared residuals and maximizes the correlation of the observed and predicted values. Preceding, current, and following ring-width indices are used as predictors of the climatic variables in these analyses. Precipitation and temperature values are considered to be potentially reconstructable only for those months or groups of months that have significant response function elements. The multiple regression equation used to predict climatic values from the ring-width indices is of the form

$$\hat{Y} = a + b_1X_1 + b_2X_2 \ldots + b_NX_N \qquad (6)$$

where

$\hat{Y}$ is the predicted climatic value,
a is the constant (y-intercept),
b's are the unstandardized regression coefficients,
X's are the values of the independent variables, the ring width indices, and the
N subscripts denote the number of independent variables included as predictors.

The b's in Equation (6) are partial regression coefficients (Nie et al. 1975:330) that represent the expected change in the dependent variable with a one-unit change in one of the independent variables, with the other independent variables held constant or otherwise controlled. The partial regression coefficient is equal to the simple bivariate regression coefficient (unstandardized) between the dependent variable and the residuals of the independent variable in question, from which the effects of the other independent variables have been removed. The strategy in the multiple regression procedure is the same as in bivariate regression: to select the constant and regression coefficients that minimize the sum of the squared residuals.

The equations that express the relationships between the tree-ring indices and the climatic variables that the response function indicated

to be important to tree growth (Equations 7–13) are presented in Table 13. Although the regression equations include variables specified by the response function, they cannot be indiscriminately used to retrodict past climatic values from the tree-ring data. First, the accuracy of the equations must be assessed.

Evaluation of the Regression Equations

The total variability in the dependent variable Y, denoted SS_y and expressed as $\sum_{i+1}^{N} (Y_i - \overline{Y}')^2$, can be separated into two parts. One is the sum of squares explained by the multiple regression hyperplane. This component, denoted SS_{reg}, is given by the equation $\sum_{i=1}^{N} (Y'_i - \overline{Y})^2$, where i equals the ith observation, Y_i denotes the predicted Y value, and $\overline{Y}$ is the mean of all the Y observations. The second component is the sum of squares not explained by the regression hyperplane. This component, denoted SS_{res}, is calculated as $\sum_{i=1}^{N} (Y_i - \overline{Y}')^2$, which is the sum of the squared residuals between the actual and the predicted values. Explained and residual variance are used in assessing the accuracy of the regression equations. The ratio of the SS_{reg} to the total sum of squares (SS_y) equals R^2 and is the percentage of the total variation in Y that is explained by the independent variables in the regression equation.

Several methods are used to evaluate the accuracy of the multiple regression equations in Table 13. The following statistics are calculated for the equations: the multiple correlation coefficient (R), the square of the multiple correlation coefficient (R^2), the overall F-ratio and its significance, the standard error of the estimate (*S.E.*), the F-ratio and its significance for each independent variable, a non-parametric runs test, and the Durbin-Watson statistic (D).

The multiple correlation coefficient (R) and its square (R^2) provide general measures of the accuracy of the equations (Nie et al. 1975). Multiple R expresses the simple correlation between the observed and the estimated values of the dependent variable, and R^2 equals the percentage of variation in the dependent variable that is explained by the independent variables. Both statistics (Table 14) indicate potentially good equations for several variables (especially those represented by Equations 7, 9, 10, 11, and 13) and reveal the equation for January precipitation (Equation 8) to be extremely poor.

TABLE 13.
Regression equations (7–13) for calibration period, A.D. 1917–1970.

Equation	Climatic Variable	Current Year t	+	t-1	+	t-2	+	t-3	+	t+1	+	t+2	+ Constant
	Precipitation	Coefficients											
(7)	March–June	2.4024		−.3551		−.3615		−.4863		−.3357		−.6632	3.3282
(8)	January	0.2069		−.0816		.1611		−.1254		−.1918		.0191	0.6176
(9)	August–July	4.1266		.2639		−.9343		−.7998		−.9493		−.5518	12.1914
(10)	Prior June–July	−0.9008		.7702		.7302		−.9407		−.5780		−.5840	4.9235
(11)	Prior Sept.–Oct.	1.1831		.6704		−.0892		−.2469		−.3814		.4746	0.9930
	Temperature												
(12)	June–July	−1.0587		−.3539		.0854		.0476		−.2515		.1003	69.4489
(13)	Prior Oct.–Nov.	−2.0700		−.3096		.4279		−.2200		.9280		−.9232	47.4259

TABLE 14.
Tests of accuracy of regression equations.

Equation	*Climatic Variable*	*Mult. R*	SS_{reg}/SS_y (R^2)	*Overall F-Ratio*	*Significance*	*S.E.*
	Precipitation					
(7)	March–June	0.65	0.43	5.86	0.000	1.379
(8)	January	0.27	0.07	0.60	0.730	0.472
(9)	August–July	0.69	0.47	6.99	0.000	2.063
(10)	Prior June–July	0.49	0.24	2.40	0.042	1.579
(11)	Prior Sept.–Oct.	0.53	0.28	3.01	0.014	1.279
	Temperature					
(12)	June–July	0.46	0.21	2.12	0.068	1.278
(13)	Prior Oct.–Nov.	0.55	0.30	3.32	0.008	1.767

Level of Significance = .05

The fit of each multiple regression equation to the data is objectively tested with the F-ratio of the SS_{reg}/k divided by $SS_{res}/(N-k-1)$, where k is the number of independent variables, and N is the sample size (Roscoe 1969). The F-ratio has degrees of freedom k and $(N-k-1)$. In certain tree-ring series the degrees of freedom are reduced by decreased effective sample size. Decreases in effective sample size occur when significant autocorrelation is present in the series, and one value is constrained by other values. Because autocorrelation is not significant in the Santa Fe area chronologies used in this study, sample size corrections are not necessary.

Once the overall F-ratios and degrees of freedom are determined, the null hypothesis is tested at the 0.05 level of significance. In this case, the null hypothesis is that the multiple correlation coefficient is zero in the population from which the sample is derived. The F-ratio and significance data in Table 14 indicate that the null hypothesis can be rejected for five of the seven equations (Equations 7, 9, 10, 11, and 13). Thus the amount of climatic data variance explained by the tree-ring indices is significant for total precipitation from current March through June ($R^2=0.43$), for the twelve-month year from prior August through current July (0.47), for prior June and July (0.24), and for

prior September and October (0.28), and for the mean temperature of prior October and November (0.30). The null hypothesis cannot be rejected for Equations (8) and (12), which represent two of the climatic variables that the response function indicates to be potentially reconstructable. Thus, current January precipitation and current June–July temperature are rejected for reconstruction because the amount of variance calibrated by tree growth is not significant.

Rejection of the null hypothesis for the five dependent climatic variables (Equations 7, 9, 10, 11, and 13) indicates that one or more of the regression coefficients associated with the independent variables (tree-ring indices) in these equations is significantly larger than zero. In order to discover which of the independent variables accounts for the greater part of the variance in the dependent variables, it is necessary to test the significance at the 0.05 level of the individual coefficients. This is accomplished by using the F-ratio and its significance for each regression coefficient to test the null hypothesis that the regression coefficient associated with each independent variable equals zero. The manner in which the F-ratio is computed depends on the type of regression design used. In the regression strategy employed here, in which variables are added one at a time, the change in the square of the multiple correlation coefficient is regarded as reflecting the variation in the dependent variable that can be attributed to the added independent variable. The computation of the F-ratios for this regression method is presented by Blalock (1972:397–400), Draper and Smith (1966), and Kerlinger and Pedhazer (1973). The F-ratios associated with each independent variable (Table 15) indicate that current ring width *(t)* alone accounts for most of the calibrated variance, with the addition of lagged values only slightly improving the amount of variance explained.

In multiple regression analysis, the fitting of the regression hyperplane by the least squares method minimizes the sum of the squared residuals and maximizes the correlation of the observed and predicted values. Thus, if the assumptions of multiple regression analysis are met, the residuals are independent of the predictor variables, they have a mean of zero, and the residual variance is the same throughout the range of Y values. These qualities provide additional tests of the accuracy of the regression equations.

On the basis of visual inspection of the 1917 to 1971 calibration period, the residuals for Equations (7) through (13) appear to lack linear

TABLE 15.
F-ratio and significance for regression coefficients.

Equation	*Climatic Variable*	*t*	*t−1*	*t−2*	*t−3*	*t+1*	*t+2*	*Constant*
				F-Ratio				
	Precipitation							
(7)	March–June	27.08	0.62	0.64	1.30	0.52	2.30	21.51
(8)	January	1.72	0.28	1.08	0.74	1.44	0.02	6.33
(9)	August–July	35.69	0.15	1.89	1.57	1.84	0.71	128.92
(10)	Prior June–July	2.90	2.21	1.97	3.70	1.17	1.36	35.90
(11)	Prior Sept.–Oct.	7.64	2.55	0.05	0.39	0.78	1.37	2.23
	Temperature							
(12)	June–July	6.12	0.71	0.04	0.02	0.34	0.06	10905.21
(13)	Prior Oct.–Nov.	12.25	0.29	0.54	0.16	2.40	2.72	2660.03
				Significance				
	Precipitation							
(7)	March–June	.000	.436	.430	.261	.476	.136	.000
(8)	January	.196	.600	.304	.395	.236	.899	.015
(9)	August–July	.000	.698	.175	.217	.181	.403	.000
(10)	Prior June–July	.095	.144	.167	.060	.286	.249	.000
(11)	Prior Sept.–Oct.	.008	.117	.833	.536	.383	.247	.142
	Temperature							
(12)	June–July	.017	.403	.840	.905	.564	.806	.000
(13)	Prior Oct.–Nov.	.001	.596	.465	.689	.128	.106	.000

trends and higher-order interactions and to support the accuracy of the regression equations. Mathematical tests provide additional bases for evaluating the residuals. The standard error of the estimate (S.E.) is the standard deviation of the residuals and is an absolute measure of explained variation. Because there are no instances of an unexpectedly large number of data points lying outside the range of the appropriate S.E. values (Table 14), none of the equations can be rejected on the basis of this statistic.

If the regression equations are accurate, there should be no significant autocorrelation in the residuals. A nonparametric runs test provides a test for residual autocorrelation (Blalock 1972; Hollander and Wolfe 1973; Roscoe 1969). The residuals are dichotomized by sign, positive or negative, and left ordered with respect to time. A run is defined as a sequence of values with the same sign that is bounded by values of the opposite sign or by the end of the data set. The null hypothesis is that the number of observed runs is typical of a random distribution. The two-tailed alternative hypothesis is that the number of runs is not random. The one-tailed alternative hypothesis is that there are either too many or too few runs. If the number of runs is large, the null hypothesis is not rejected. In the one-tailed test, positive z values indicate more runs than average, while negative values denote fewer than the average number of runs. The runs test, using the 0.05 level of significance, is applied to the differences between the actual and predicted values for the calibration period. In no case were we able to reject the null hypothesis that the runs are randomly distributed (Table 16). This result indicates a lack of autocorrelation in the residuals and provides further evidence for the accuracy of the equations.

We also used the Durbin-Watson statistic (Durbin and Watson 1951; Wesolowsky 1976) to test for first order autocorrelation among the residuals for the calibration period. The statistic is defined as the sum of the squared differences between the residuals of adjacent cases divided by the sum of the squared residuals.

$$D = \frac{\sum_{i=2}^{N} (e_i - e_{i-1})^2}{\sum_{i=1}^{N} e^2} \tag{14}$$

According to Wesolowsky (1976), the distribution of D is complex because it depends on the observed values of the independent variables in the sample. Therefore an exact test for significance is not available.

TABLE 16.
Tests of residual autocorrelation in the regression equations.

Equation	Climatic Variable	RUNS TEST: Positive Residuals	Negative Residuals	Total Runs	Expected Runs	Expected SD	Z-Score	Probability of ≥ Z	DURBIN-WATSON STATISTIC
	Precipitation								
(7)	March–June	25	29	31	28	3.619	1.008	.157	2.10
(8)	January	24	30	24	28	3.594	−0.881	.189	1.96
(9)	August–July	27	27	26	28	3.369	−0.412	.340	1.88
(10)	Prior June–July	24	30	31	28	3.594	1.067	.143	2.09
(11)	Prior Sept.–Oct.	23	31	31	27	3.558	1.150	.125	2.32
	Temperature								
(12)	June–July	29	25	22	28	3.619	−1.479	.070	1.91
(13)	Prior Oct.–Nov.	30	24	22	28	3.594	−1.438	.075	1.72

Level of Significance = .05

Null hypothesis that number of observed runs is typical of random distribution is accepted in all cases.

Durbin and Watson (1951) define lower (d_L) and upper (d_U) boundaries that, when exceeded by a D value, permit a definite decision. If $D>d_U$, autocorrelation is absent; if $D<d_L$, autocorrelation is significant; if $d_L \leq D \leq d_U$, the test is inconclusive. The null hypothesis is that the autocorrelation coefficient equals zero. The alternative hypothesis is that the coefficient is greater than or less than zero. A significance level of 0.01 is used in this test. The D values for all seven equations (Table 16) are greater than the upper boundary for six independent variables at the 0.01 level ($d_U = 1.63$). Thus none of the equations can be rejected on the basis of excessive first order autocorrelation among the residuals.

Summary of Regression Evaluations

The accuracy of the regression equations relating tree growth to seven climatic variables was evaluated in several ways. Statistics pertaining to the general fit of the regression hyperplane to the data (R, R^2, F-ratio) revealed that two of the equations (8 and 12) are unsatisfactory for reconstruction because the independent variables do not account for a significant amount of variance in the dependent variables. In terms of this criterion, the five other equations are acceptable, although two (7 and 9) are manifestly superior to the remaining three. Analysis of the residuals provided further tests of the accuracy of the equations. Visual inspection, the standard error of the estimate, a nonparametric runs test, and the Durbin-Watson statistic indicated that all seven equations are acceptable.

The evaluations of the regression equations produced the following results. The two equations, January precipitation and June–July temperature, that failed the F-ratio significance test are rejected for reconstruction. The five remaining equations—March–June precipitation, prior August–current July precipitation, prior June–July precipitation, prior September–October precipitation, and prior October–November temperature—survived all the tests and thus appear to be acceptable for climatic reconstruction.

5
Verification

The evaluations of the multiple regression equations for the calibration period (1917–1971) indicate that five climatic variables can potentially be reconstructed from tree-ring indices. The next step is to verify the results of the equations obtained for the calibration period. In the verification procedure, climatic data independent of those used in the calibration process are used to check the accuracy of the mean and variance of the reconstructed (estimated) climatic values. Actual precipitation and temperature measurements from Santa Fe for the period from 1869 to 1916 are checked against the values estimated for this verification period by the multiple regression equations. Several objective statistical techniques are used to determine the success of the reconstructions, including the *t*-test, the product mean statistic, Pearson's product moment correlation coefficient, and the reduction of error statistic.

THE t-TEST FOR DIFFERENCES OF MEANS

Differences between the means of the actual climatic data of the calibration and verification periods are tested for significance. If the means are found not to be significantly different, further verification steps may proceed. The *t*-test for comparing the means of independent samples from populations with common variance is used. The assumption of common variance is checked with an *F*-ratio at the .01 level of significance. For all five climatic variables, the null hypothesis

of no significant differences in variance is accepted, and therefore the pooled variance estimate is used in calculating the t statistic. Table 17 presents the t statistic, the degrees of freedom, and the two-tailed probability associated with obtaining a value greater than or equal to the t value, ignoring the sign. The null hypothesis is rejected if the two-tailed probability for H_0 is less than .05. In all instances the null hypothesis is accepted (Table 17), which indicates that there are no significant differences between the mean of the calibration period climatic data and the mean of the verification period data.

Next, the t-test for paired samples is used to determine if statistically significant differences exist between the means of the actual and estimated climatic values within the verification period alone. These means are tested with a two-tailed test at the .05 level, and inequality is the only alternative hypothesis tested. Table 18 shows that all the probabilities of obtaining the observed values are greater than .05. No significant differences in means are indicated, and therefore the mean is correctly reconstructed.

THE PRODUCT MEAN STATISTIC

Differences between the estimates and the actual values of the verification period are tested with the product mean statistic (Fritts 1976:331–32), which takes into account the signs and the magnitudes of departures of the actual and estimated values from the mean of the calibration period. Residuals are computed separately for the departures of the actual and estimated values. Products of the departures are obtained and summed with respect to sign. Positive values denote correct estimation of the difference from the mean: (+ actual) (+ estimate) = + product, (− actual) (− estimate) = + product. Negative values denote incorrect estimates: (+ actual) (− estimate) = − product, (− actual) (+ estimate) = − product.

Differences between the means of the positive and negative ranks are tested with the t statistic. If the actual t value is greater than the critical value, the difference is significant. A significant positive product mean "indicates a tendency for both actual and estimated departures from the average value to be large when the sign is correctly estimated and to be small when the sign is incorrectly estimated" (Fritts 1976:332).

TABLE 17.

t-Test for difference between means of observed climatic values, calibration and verification periods.

Climatic Variable	*Period*	*N*	*Mean*	*s*	*S.E.*	*F*	*Prob.*	*Pooled Variance Est.* *t*	*d.f.*	*Prob.**	*Separate Variance Est.* *t.*	*d.f.*	*Prob.**
Precipitation													
(7) March–June	Verif.	48	3.9017	1.607	.232	1.14	.647	−.85	100	.397	−.85	100	.395
	Calib.	54	4.1830	1.717	.234								
(9) August–July	Verif.	48	13.5346	3.257	.470	1.49	.163	.36	100	.718	.36	91	.721
	Calib.	54	13.3217	2.673	.364								
(10) Prior June–July	Verif.	48	3.6917	1.440	.208	1.39	.248	.93	100	.355	.94	100	.350
	Calib.	54	3.9998	1.700	.231								
(11) Prior Sept.–Oct.	Verif.	48	2.5423	1.540	.222	1.18	.555	−.26	100	.792	−.26	96	.793
	Calib.	54	2.6196	1.417	.193								
Temperature													
(13) Prior Oct.–Nov.	Verif.	48	44.8198	2.423	.350	1.49	.160	−.95	100	.345	−.94	91	.351
	Calib.	54	45.2343	1.986	.270								

Level of significance (*F*-ratio) = .0

Level of significance (*t*-test) = .05

Null hypothesis: Verification period mean = calibration period mean.
Alternate hypothesis: Verification period mean ≠ calibration period mean.

*Prob: The probability is for the occurrence of a value equal to or greater than the *t* value, ignoring the sign. A two-tailed test is appropriate to the set of hypotheses because it is not assumed that *t* will be either positive or negative.

TABLE 18.

t-Test for difference between means of observed and estimated values for the verification period, A.D. 1869–1916.

Climatic Variable	*Mean*	*SD*	*S.E.*	*Difference in Means*	*SD*	*S.E.*	*t*	*d.f.*	*Two-tail Probability*	*Results*
Precipitation										
(7) March–June (Obs.)	3.9017	1.607	.232	−.2489	1.249	.180	−1.38	47	.174	Accept
March–June (Est.)	4.1505	1.064	.154							
(9) Aug.–July (Obs.)	13.5346	3.257	.470	.2685	2.702	.390	0.69	47	.495	Accept
Aug.–July (Est.)	13.2661	1.776	.256							
(10) Prior June–July (Obs.)	3.6917	1.440	.208	.1705	1.675	.242	0.71	47	.484	Accept
Prior June–July (Est.)	3.3512	0.768	.111							
(11) Prior Sept.–Oct. (Obs.)	2.5423	1.540	.222	.0518	1.531	.221	0.23	47	.816	Accept
Prior Sept.–Oct. (Est.)	2.4905	0.624	.090							
Temperature										
(13) Prior Oct.–Nov. (Obs.)	44.8198	2.423	.350	−.5813	2.778	.401	−1.45	47	.154	Accept
Prior Oct.–Nov. (Est.)	45.4011	0.981	.142							

Level of significance = .05

Null hypothesis: Mean of observed = mean of estimated.
Alternative hypothesis: Mean of observed ≠ mean of estimated.

When the sign is wrongly estimated but the difference from the mean is small, it indicates that conditions were average, and the reconstruction is still regarded as accurate. Table 19 presents the average product means for the positive and negative categories, their standard deviations, t values, and the critical t values at the .05 level.

The actual and estimated departures of March–June precipitation for both the calibration and verification periods tend to be large when the sign is correctly estimated and small when it is not, as indicated by the average product means and the significant t values (Table 19). Similarly, the actual and estimated departures of August–July precipitation for both periods tend to be larger with correct sign estimation and smaller when the sign is incorrectly estimated. The t values are larger than the critical values (Table 19) and hence are significant. The reconstructions of the other three climatic variables (Equations 10, 11, and 13) pass the product mean test for the calibration period in that their actual t values exceed the critical t value. However, for the verification period, all three have t values smaller than the critical value (Table 19), which indicates that there are no significant differences between the positive and negative average product means. Based on the results of the product mean test of the verification period data, June–July precipitation, prior September–October precipitation, and prior October–November temperature are rejected for reconstruction. Only March–June and August–July precipitation are accepted for reconstruction.

THE CORRELATION COEFFICIENT AND THE REDUCTION OF ERROR STATISTIC

Pearson's product moment correlation coefficient expresses the relationship between the actual and estimated values of both the calibration and verification periods. For the calibration period, it is equal to the multiple correlation coefficient (R). It is possible to obtain a high correlation between actual and estimated values and yet to have an inaccurate reconstruction. This happens when the two time series increase and decrease simultaneously but have different means. The potential difference between the means is tested by the reduction of error statistic (Lorenz 1956). For the calibration period this statistic

TABLE 19.
Product mean test for calibration and verification periods.

Climatic Variable	*Period*	*Average Product Mean* +	*Average Product Mean* −	*Standard Deviation* +	*Standard Deviation* −	*t*	*Critical t*	*d.f.*	*Results*
Precipitation									
(7) March–June	Calib.	.8340	−.1082	0.8229	.1410	5.3931	2.01	52	Accept
	Verif.	.9440	−.2657	0.9211	.2103	4.0085	2.02	46	
(9) August–July	Calib.	.9215	−.1921	1.1482	.2158	3.8240	2.01	52	Accept
	Verif.	.9598	−.2792	1.2017	.2898	2.9796	2.02	46	
(10) Prior June–July	Calib.	.8622	−.2384	1.4624	.3111	2.4395	2.01	52	Reject
	Verif.	.6143	−.5882	0.7834	.6411	0.1211	2.02	46	
(11) Prior Sept.–Oct.	Calib.	.9024	−.2664	0.8961	.2487	3.8843	2.01	51	Reject
	Verif.	.6663	−.4823	0.6583	.4688	1.1059	2.02	46	
Temperature									
(13) Prior Oct.–Nov.	Calib.	.9741	−.2719	1.2082	.2544	3.2554	2.01	52	Reject
	Verif.	.5861	−.6871	0.7210	.7371	0.4599	2.02	46	

equals the square of the correlation coefficient (R^2). The reduction of error statistic (R.E.) is calculated as

$$R.E. = 1 - SSR/SSM \tag{15}$$

where
SSR is the sum of the squared differences between the actual data and the estimates, and
SSM is the sum of the squared differences of the actual data from the mean of the data used in the calibration period.

The limits of this statistic range from plus one, denoting perfect fit between the means, to minus infinity. Positive values of the R.E. statistic are tested in the same way as the square of the Pearson's *r* (Blalock 1972, Freund 1969). Sizable negative values indicate no agreement and are treated as zero. Fritts (1976) points out that this test is very rigorous when applied to independent data sets used for verification and that any value greater than zero can be considered encouraging. Its disadvantage, however, is that the effect of several accurate predictions can be offset by one large difference.

The correlation coefficients and R.E. statistics associated with the potentially reconstructable variables (Equations 7 and 9) are given in Table 20. All reconstructions that are rejected on the basis of the product mean statistic (Table 19) also have small correlation coefficients and negative values for the R.E. statistic, and they are not included in the table. The *r* and R.E. values for March to June precipitation change little from the calibration to the verification period; therefore, values of this variable are reconstructed using the Santa Fe climatic chronology. A plot of the actual and estimated values of

TABLE 20.
Correlation coefficients and reduction of error statistics for calibration and verification periods.

Climatic Variable	*Calibration*		*Verification*	
	r	*R.E.*	*r*	*R.E.*
Precipitation				
March–June	.654	.3085	.629	.2587
August–July	.698	.3735	.558	.1170

current March–June precipitation for the verification and calibration periods is shown in Figure 30. The plot of the time series for total 12-month precipitation (August–July) for the verification and calibration periods is presented in Figure 31. From the calibration to the verification period, the correlation coefficient for 12-month precipitation decreases from 0.698 to 0.558, the R.E. statistic from 0.3735 to 0.1170. However, both r values are large and the R.E. values are positive.

Prior September–October precipitation provides an example of a potential reconstruction that is rejected on the basis of the verification procedure. Although the correlation between the actual and predicted values for the calibration period is 0.527, it drops to 0.216 for the verification period. Similarly, the R.E. statistic is 0.054 for the calibration period and −0.565 for the verification period. The plot of prior September–October precipitation (Fig. 32) illustrates the differences between the calibration and verification periods in terms of the actual and estimated values for this variable.

In summary, only two of the climate–tree-growth relationships indicated by the response function analysis to be potentially reconstructable have survived various testing techniques. Statistical tests of the regression equations for two of the variables—January precipitation and current June–July mean temperature—show that these relationships account for an insignificant amount of variance. In addition, the verification procedures eliminate precipitation of prior June–July and prior September–October and mean temperature of prior October–November. We are left, then, with annual precipitation (previous August through current July) and spring precipitation (March through June of the current ring year) as the variables that can be dendroclimatically reconstructed for the Santa Fe area.

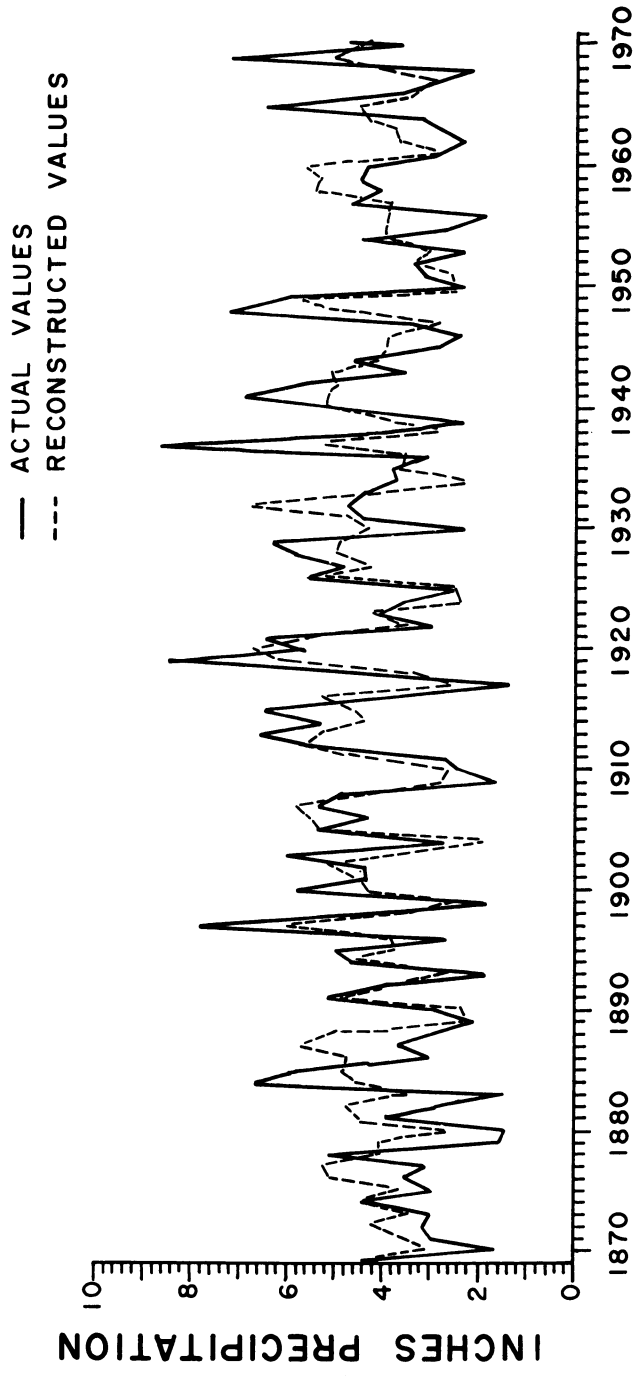

FIG. 30. Actual and reconstructed values of current March–June precipitation for calibration and verification periods.

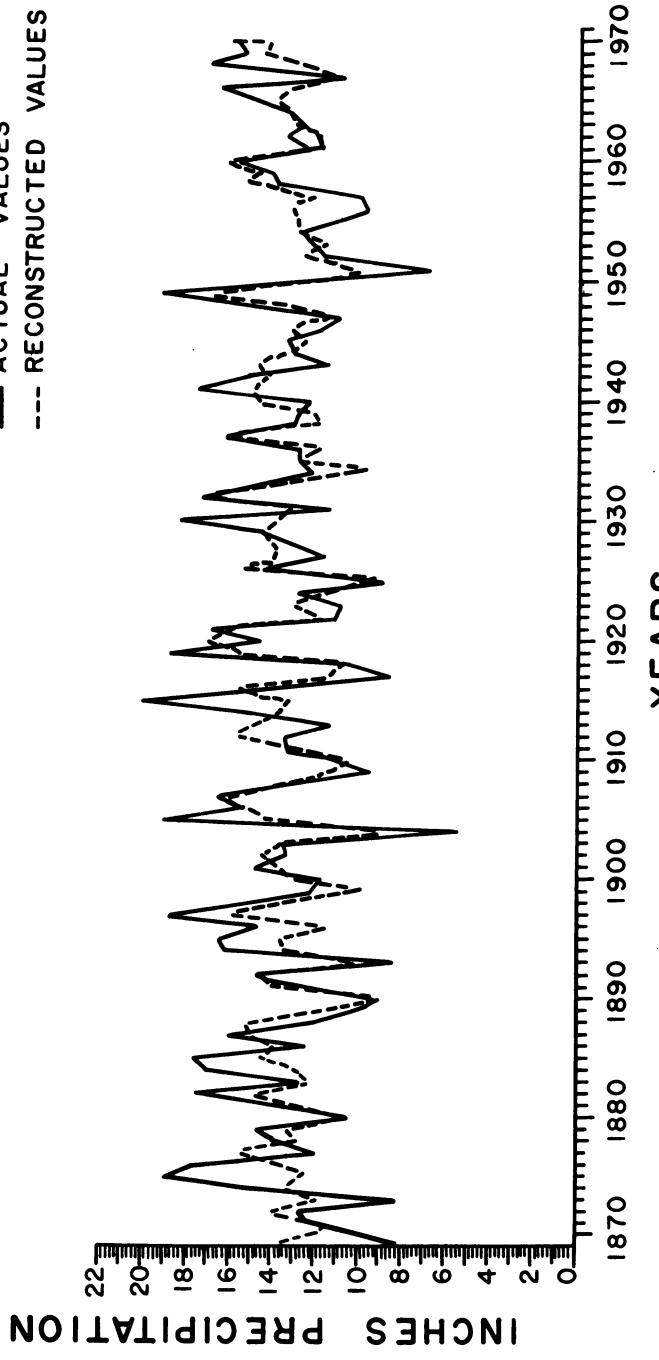

FIG. 31. Actual and reconstructed values of 12-month total precipitation for calibration and verification periods.

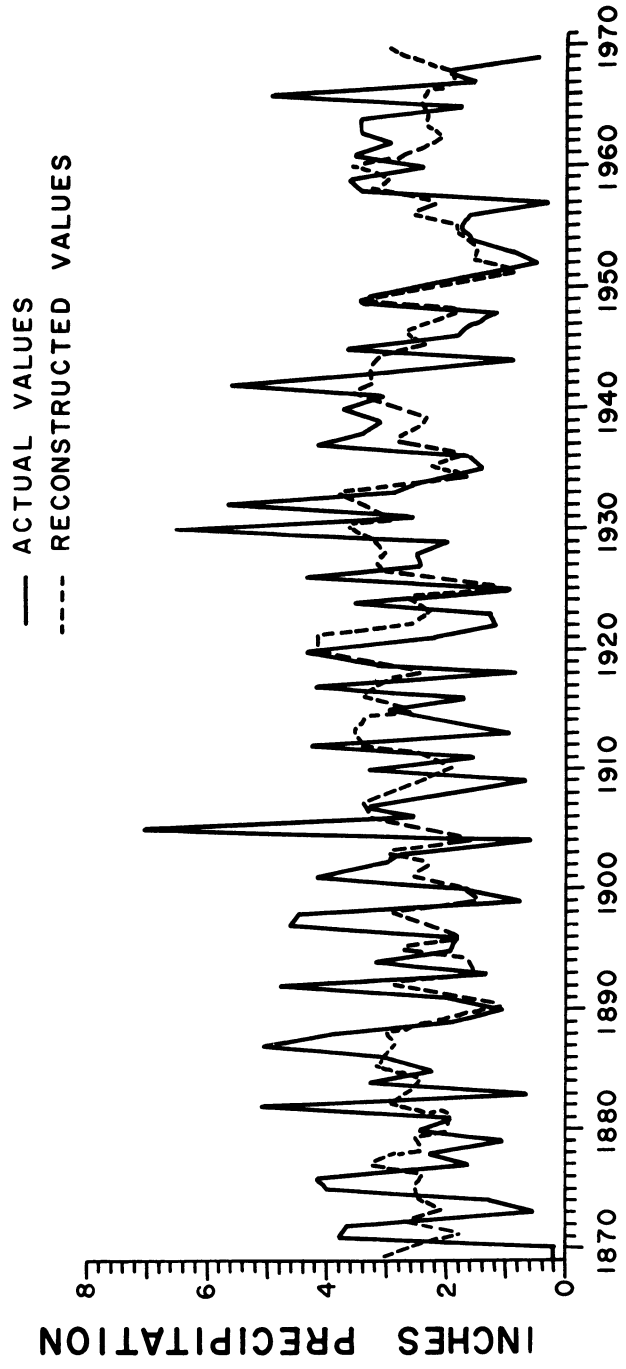

FIG. 32. Actual and reconstructed values of prior September–October precipitation for calibration and verification periods.

6
The Paleoclimate of Arroyo Hondo

The relationships between Glorieta Mesa piñon growth and the modern Santa Fe weather record, which are specified by the calibration and verification analyses, indicate that two aspects of past climate are reconstructable from the local, long-range tree-ring chronology: "annual" (August through July) and spring (March through June) precipitation. Quantitative estimates of precipitation values for these intervals are obtained by applying the transfer function to the Santa Fe paleoclimatic tree-ring series. This procedure translates ring-width variability into precipitation variability for the period of years encompassed by the tree-ring chronology. Tables 21 and 22 list reconstructed spring and annual precipitation values for each year from A.D. 985 to 1970.

Human societies usually employ behavioral buffering mechanisms (Jorde 1977) such as the storage of food surpluses, trade, "banking" (Bronitsky 1977), and so forth to offset the effects of normal, high-frequency fluctuations in climate and other environmental variables. Therefore, in order to comprehend possible relationships between the dendroclimatic reconstructions and the behavior of the people of Arroyo Hondo, paleoclimatic variations of somewhat longer duration than one year must be examined. Such longer-term fluctuations might be expected to have affected aboriginal subsistence activities and to have had some impact on the occupational history of Arroyo Hondo. Longer climatic trends, however, are difficult to segregate from the

high frequency "noise" of the yearly reconstructions presented in Tables 21 and 22. Therefore, we have converted the yearly spring and annual precipitation estimates into departure values that reflect a time interval of ten years, a duration that might be expected to have had some impact on the subsistence behavior of the inhabitants of Arroyo Hondo.

The yearly precipitation figures for the August–July year and for spring (March–June) are transformed into decade departures. For each time series (annual and spring), the values for each decade are summed to produce two new time series composed of values representing decades overlapped by five years. The mean and standard deviation of each new series are calculated, and these values are used to convert the two decade series into sequences of z-scores. In each case, the series mean is subtracted from the decade value, and the result is divided by the standard deviation of the series. Carried out for the entire lengths of the sequences of decade values, this operation produces two series of z-scores, each with a mean of zero and a standard deviation of one. Thus, the decade departure values are expressed in standard deviation units. For example, a value of +2 indicates that the decade departure is two standard deviations above the series mean. Variation that exceeds two standard deviations in either direction from the mean is considered to be significant in the sense that such departures are of sufficient rarity and magnitude to have had potential adaptive consequences for plant, animal, and human populations. Thus, we emphasize those values that lie outside the range of 95 percent of the variability about the mean.

The ten-year precipitation departures for the spring and annual reconstructions are plotted against time in Figures 33 and 34. The decades are overlapped five years (A.D. 985–994, 990–999, 995–1004, and so on), and the value for each decade is plotted on the midpoint of that interval. The figures display relative variability in spring and annual precipitation on a decade basis from A.D. 985 to 1970.

Certain constraints that apply to these dendroclimatic analyses must be made explicit before we discuss the departure plots in detail. Although we present two reconstructions, one of precipitation for a 12-month tree response year and one of spring precipitation, the variability in each reconstruction is quite similar to that of the other even though the means of the two sequences differ considerably. This similarity is due to the fact that the amount of variance explained for the 12-month year (47 percent) is not substantially greater than that explained

for spring precipitation alone (43 percent). In other words, most of the variability in the annual reconstruction can be attributed to the variability of spring precipitation. This observation suggests that the nonspring component of annual rainfall in the Santa Fe area (that is, July through February) is more stable from year to year than is the spring component. Supporting this inference is the fact that the coefficient of variation for modern Santa Fe precipitation is higher for April, May, and June than for any other time of the year except November (Table 4, Fig. 12e).

The standardization and averaging procedures used in building a composite tree-ring chronology constrain the usefulness of such chronologies for the analysis of long-term trends. Standardizing tends to remove low frequency variability from the index series (Fritts 1976: 267–68), and averaging ring records of different lengths reduces the amount of low frequency variance in the composite chronology. Because the archaeological portion of the Santa Fe paleoclimatic chronology is comprised of relatively short ring records, any analyses of these data and of paleoclimatic reconstructions derived from them are confined to the consideration of fairly short-term variability. For these reasons, the analyses discussed here are all focused on high frequency (annual) variability.

Our verification analyses indicated that the Santa Fe tree-ring chronology is a better predictor of low rainfall values than of high ones (Figs. 30 and 31). This result is consistent with our knowledge of the growth of arid site conifers. Low moisture levels inhibit growth through direct effects on the physiological processes of the trees. In contrast, high moisture levels free the trees from climatic control and allow them to respond more idiosyncratically to other variables such as competition, injury, hormone production, and so on. Thus, if the quantity of moisture available to the trees exceeds the threshold of direct control, the amount of radial growth is regulated by nonclimatic factors and may not accurately reflect the degree to which precipitation surpassed the threshold value. Therefore, the climatic signal in tree-ring series tends to be weaker for large rings than for small rings, and the latter represent weather more accurately than do the former.

Although tree-ring chronologies are excellent predictors of low moisture levels, they may not always accurately reflect the *degree* of water stress. This is so because there is an absolute limit on the minimum size of a tree ring: zero. A ring that is missing from a sample has a value of zero and indicates that in that year, moisture was insufficient to

sustain radial growth throughout the tree. But since a ring cannot be smaller than zero, there is no way of measuring how far below the zero-growth threshold moisture levels fell. Thus, dendroclimatic reconstructions of past precipitation may tend to underestimate the severity of the driest years.

Finally, the error components and variances of the reconstructed precipitation time series are high at the early ends of the two sequences because there are fewer individual tree-ring specimens in the early part of the Santa Fe paleoclimatic chronology than in the later part. This problem is minimized by increasing sample depth beyond A.D. 1000 and is negligible during the period of occupation of Arroyo Hondo.

RECONSTRUCTION OF SPRING PRECIPITATION

The yearly values for reconstructed spring (March through June) precipitation at Santa Fe are presented in Table 21. The plotted decade departures are displayed in Figure 33, which shows some interesting general trends. Between A.D. 990 and 1430, the reconstruction is characterized by oscillations of both high amplitude and high frequency. After 1430 and lasting until 1735, the values fall between +1 and −1 standard deviation units; low frequency and low amplitude variability distinguish this long interval. From 1735 to the present, the frequency of the fluctuations remains low, but the amplitudes increase somewhat. In this period, a major low centered on 1740 is followed by a substantial high interval between 1745 and 1760. The low from 1890 to 1900 represents a well-documented drought that encompassed much of the Southwest during the last third of the nineteenth century. This drought is followed by a sustained high from 1905 to 1945, with only a slight dip at 1935 to indicate the severe drought that afflicted much of the West in the 1930s. The last few years of the record are dominated by an intense low between 1950 and 1955, with average conditions prevailing from then to the end of the series at 1970.

The period from A.D. 1250 to 1450, which spans the occupational history of Arroyo Hondo Pueblo, can be examined in greater detail. Early in this interval there is no appreciable evidence for the Great Drought, traditionally dated between 1276 and 1299, in the upper Rio Grande Valley. The period between 1250 and 1255 is actually more

TABLE 21.
Reconstructed spring (current March through June) precipitation for Arroyo Hondo, A.D. 985–1970 (in inches).

Date	0	1	2	3	4	5	6	7	8	9
985						3.5	5.8	6.3	6.8	5.8
990	3.0	2.3	2.3	2.6	6.3	5.4	6.0	6.5	3.2	1.7
1000	4.3	3.4	3.3	3.3	5.3	2.7	3.4	6.0	4.5	2.4
1010	1.9	3.3	5.7	4.0	2.1	5.0	6.2	3.8	3.1	2.3
1020	5.1	4.7	3.5	4.1	4.9	6.4	6.0	0.9	4.7	5.9
1030	3.1	3.5	4.0	5.1	3.4	2.7	5.2	4.6	4.9	3.3
1040	2.7	2.9	8.8	5.2	2.6	2.2	4.8	4.3	1.7	5.8
1050	5.7	3.8	8.2	4.6	3.7	4.4	4.9	5.5	3.0	4.3
1060	5.8	3.3	3.2	4.4	4.8	6.7	4.7	2.2	2.0	4.4
1070	5.3	4.7	4.6	4.4	5.3	3.0	5.0	4.4	3.5	3.8
1080	3.9	3.3	6.1	3.9	4.5	2.5	5.0	3.4	4.5	5.9
1090	2.2	3.8	4.6	3.7	3.1	6.4	6.0	3.0	2.0	2.7
1100	4.6	5.5	4.9	3.6	4.8	4.0	6.1	3.8	3.6	4.8
1110	4.7	4.7	5.2	4.6	2.9	3.8	5.7	6.3	4.7	5.0
1120	3.1	2.0	6.4	3.9	5.8	4.1	3.4	3.0	4.3	6.9
1130	3.7	2.2	3.1	5.2	2.2	2.8	5.0	3.7	3.7	4.1
1140	2.7	5.9	4.2	2.5	4.3	5.5	2.7	2.9	3.5	5.4
1150	2.4	3.8	6.8	4.3	4.8	3.9	2.7	2.0	3.1	6.6
1160	3.9	2.7	6.4	5.7	5.9	3.2	2.1	5.4	3.1	1.9
1170	5.0	7.2	4.4	3.7	2.7	5.9	3.1	3.8	4.9	4.1
1180	3.2	4.5	4.3	4.2	6.4	4.9	1.7	3.5	3.2	2.8
1190	5.8	6.8	3.7	3.2	3.6	5.2	5.0	4.7	3.8	3.7
1200	5.6	5.4	4.7	5.7	4.2	2.1	3.4	5.3	4.3	5.4
1210	4.1	4.5	4.6	5.3	4.1	3.6	2.3	2.0	4.4	6.2
1220	3.8	2.7	4.3	4.3	4.4	5.2	4.2	2.6	4.0	5.2
1230	6.0	5.0	4.5	2.8	3.3	4.9	3.7	4.7	4.8	4.7
1240	3.9	5.2	4.3	4.0	4.6	5.2	3.0	3.7	3.5	5.2
1250	3.6	1.9	3.8	5.2	2.8	4.4	4.0	4.5	3.3	4.9
1260	3.5	3.7	4.4	3.0	3.9	4.5	4.5	5.8	5.1	3.0
1270	4.5	4.5	4.0	3.2	4.5	4.9	3.4	4.3	3.5	4.6
1280	2.8	4.4	4.0	5.5	4.0	3.6	3.3	5.7	1.9	5.6
1290	6.4	2.2	4.0	4.0	3.9	4.8	2.9	4.9	5.5	4.9

TABLE 21. *(continued)*

Date	0	1	2	3	4	5	6	7	8	9
1300	4.9	5.2	4.9	3.0	3.3	5.0	4.8	4.2	3.2	4.9
1310	5.2	3.9	2.7	6.2	5.7	3.3	2.6	5.6	5.3	4.3
1320	4.4	4.5	4.4	3.2	3.8	7.2	4.8	3.3	2.8	4.3
1330	4.5	4.4	5.2	5.1	4.2	3.0	4.3	3.4	3.5	4.4
1340	4.0	3.9	3.6	5.1	4.8	5.7	4.4	1.7	3.9	4.7
1350	5.0	4.6	2.3	5.5	5.2	4.6	4.0	3.8	5.7	4.4
1360	2.6	4.8	3.4	2.9	4.0	6.1	4.4	3.7	4.0	2.9
1370	5.3	4.8	5.6	4.2	4.2	2.9	3.3	3.6	5.2	4.6
1380	4.6	3.6	3.3	5.5	3.3	4.3	4.4	3.9	4.8	5.3
1390	2.5	3.1	4.0	4.0	5.1	6.2	3.0	2.7	5.1	2.5
1400	3.6	4.8	4.4	4.6	5.8	4.4	4.5	2.8	5.0	5.0
1410	4.3	3.3	5.0	4.4	6.1	2.6	3.5	3.8	3.9	3.8
1420	4.1	5.5	3.5	2.3	2.8	4.8	4.7	6.0	6.2	3.1
1430	3.9	4.0	3.6	5.0	5.1	5.0	3.8	3.6	3.6	5.2
1440	4.6	4.9	4.8	5.4	3.2	2.4	5.1	5.2	4.5	3.1
1450	3.1	4.4	4.0	4.7	4.7	3.1	3.1	4.6	5.0	4.1
1460	3.6	3.1	4.7	3.7	3.8	4.7	5.4	5.0	4.9	4.9
1470	2.7	2.6	5.0	4.7	3.3	2.9	4.3	3.6	5.6	4.5
1480	2.7	3.8	4.2	4.4	5.2	5.6	5.9	2.7	3.5	4.7
1490	5.1	4.6	4.3	3.7	4.4	2.2	3.5	3.7	5.3	5.2
1500	2.8	3.2	3.3	3.8	4.2	4.3	2.0	3.9	3.4	3.2
1510	4.7	4.6	3.6	4.8	5.8	4.7	1.5	3.2	4.7	4.8
1520	5.1	5.9	3.9	3.1	2.5	4.5	4.1	4.1	4.7	5.4
1530	4.7	4.4	3.2	4.3	4.5	3.3	5.2	4.4	4.0	4.4
1540	6.0	4.4	2.4	5.1	4.6	3.0	2.9	4.5	4.2	4.0
1550	4.8	3.0	4.2	5.6	5.2	5.1	4.4	3.8	3.8	4.6
1560	3.2	3.7	2.7	4.4	4.5	5.0	3.8	3.9	4.4	5.0
1570	4.2	4.0	4.1	2.6	3.9	4.2	4.8	5.6	4.4	2.4
1580	2.5	4.3	4.2	3.5	3.6	3.4	5.1	4.1	5.0	5.0
1590	3.3	4.1	4.4	3.9	5.6	5.0	6.0	5.4	3.0	3.9
1600	2.9	2.6	4.3	5.4	5.2	4.5	3.5	4.0	3.4	4.4
1610	5.4	5.2	4.9	4.3	4.2	4.3	2.8	4.6	5.4	3.9
1620	5.0	5.2	4.7	5.1	2.6	2.7	4.2	4.2	3.4	5.6
1630	4.5	4.1	4.0	4.2	5.0	5.0	5.1	4.8	2.8	5.0
1640	4.7	3.1	3.9	4.7	3.9	3.3	5.0	4.3	3.6	4.0

TABLE 21. *(continued)*

Date	0	1	2	3	4	5	6	7	8	9
1650	3.7	5.2	4.8	3.8	3.6	4.5	4.2	4.1	3.5	3.4
1660	4.4	5.3	5.9	4.1	2.9	4.2	3.3	3.6	3.8	3.8
1670	4.0	4.3	4.3	4.7	4.9	4.0	3.4	4.3	3.6	4.9
1680	5.4	3.9	4.3	5.0	3.0	2.1	4.4	4.7	5.0	5.9
1690	3.8	3.8	5.4	4.1	4.8	4.2	3.1	4.2	3.6	4.8
1700	4.4	4.6	3.6	4.9	3.6	3.4	4.8	4.1	4.6	4.0
1710	4.9	3.6	4.8	5.0	3.4	2.7	3.0	5.3	4.6	3.5
1720	5.3	4.5	4.0	4.6	4.1	4.0	5.2	5.1	3.9	1.8
1730	3.2	4.6	4.9	4.5	4.8	3.8	3.9	3.0	3.7	2.6
1740	4.0	4.2	4.6	5.0	3.9	4.7	6.6	5.8	2.3	4.3
1750	3.9	5.5	3.0	5.0	5.9	5.4	3.7	2.2	4.2	4.0
1760	3.4	5.8	5.0	3.0	4.7	3.4	4.9	4.6	5.1	4.6
1770	4.9	6.0	4.2	1.8	3.6	4.5	4.9	4.3	4.5	3.6
1780	3.0	4.1	3.8	5.3	5.6	3.2	3.5	5.6	3.6	3.1
1790	3.5	5.0	5.7	6.0	4.0	3.2	3.1	3.1	4.5	4.8
1800	4.5	3.2	4.1	4.4	5.1	3.6	3.3	4.8	4.3	3.8
1810	4.2	4.2	4.0	4.0	3.0	5.0	5.9	4.5	3.0	2.1
1820	4.4	5.0	3.0	3.4	4.4	4.5	3.5	5.0	5.3	5.1
1830	3.7	3.5	3.6	5.2	5.6	3.0	2.3	4.5	5.0	5.8
1840	6.1	4.6	2.0	4.3	4.7	4.2	4.7	2.3	4.0	7.0
1850	4.2	2.3	3.2	4.4	5.0	4.6	5.0	5.6	5.1	3.1
1860	3.2	2.9	4.0	4.0	4.0	4.6	5.9	5.4	5.2	4.6
1870	3.0	3.6	4.3	3.4	4.3	3.6	5.0	5.2	4.0	4.0
1880	2.6	4.4	4.8	3.4	4.5	4.8	4.6	5.7	4.9	2.1
1890	2.3	5.1	4.1	2.5	4.6	3.7	3.8	6.0	3.4	2.3
1900	4.2	4.5	5.1	3.5	1.9	5.3	5.5	5.8	4.1	2.8
1910	2.5	4.5	5.7	5.2	4.3	4.7	5.3	2.5	3.5	6.1
1920	6.7	5.4	3.4	4.2	2.3	2.5	5.7	4.2	5.0	4.9
1930	4.2	4.8	6.8	4.1	2.3	3.7	3.5	5.3	2.8	4.1
1940	5.2	5.2	4.9	5.1	4.1	3.9	3.9	2.8	5.1	5.9
1950	2.5	2.6	3.4	3.0	4.0	3.9	3.9	3.8	5.5	5.3
1960	5.7	2.9	3.6	3.9	4.3	4.6	3.4	2.9	4.1	5.0
1970	4.4									

Mean = 4.210 Standard Deviation = 1.81

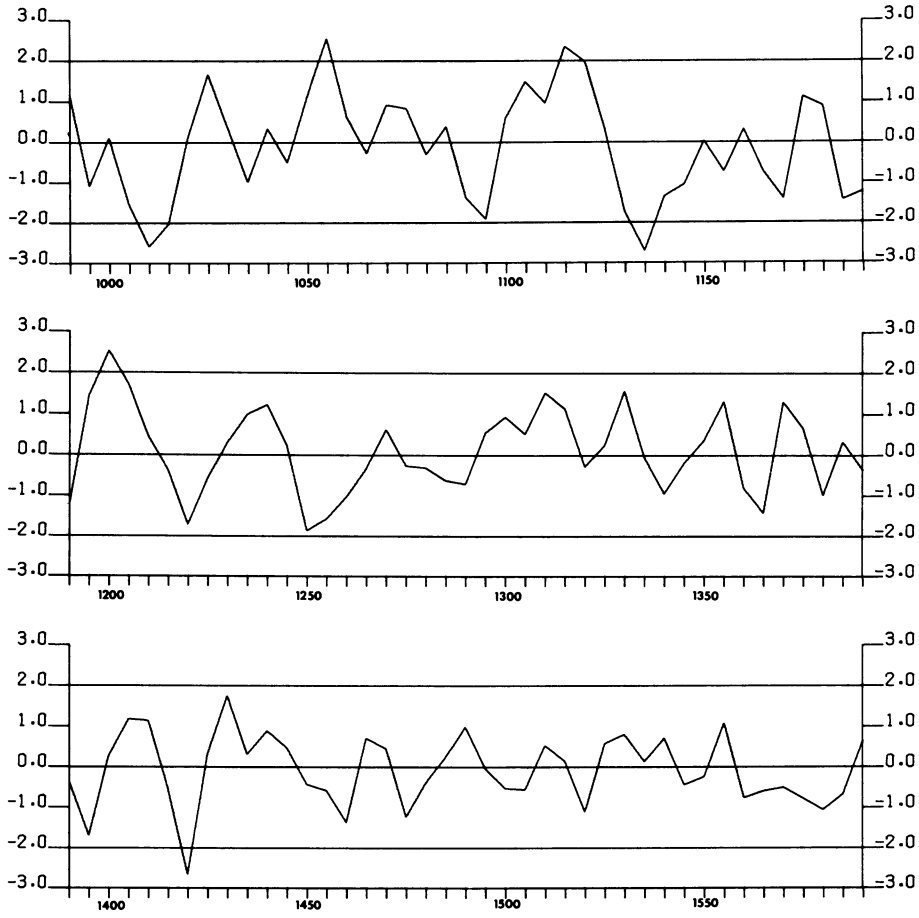

FIG. 33. Reconstruction of spring precipitation for Arroyo Hondo, A.D. 985 to 1970.

severe than the Great Drought interval itself. Spring departures for the period from 1295 to 1335 are nearly all above the long-term mean, indicating a long period of above-average precipitation. The Santa Fe area experienced a period of variable spring rainfall from 1335 to 1400, with highs centered at 1335 and 1370 and lows centered at 1365 and 1380. An extended high that prevailed from 1400 to 1415 is followed by an intense, ten-year low interval centered on 1420. This low, one of the severest in the 1,000-year spring record, was equaled only in the 1005–1014 and 1130–1139 intervals. The yearly reconstructed spring precipitation figures (Table 21) indicate that the early fifteenth-century

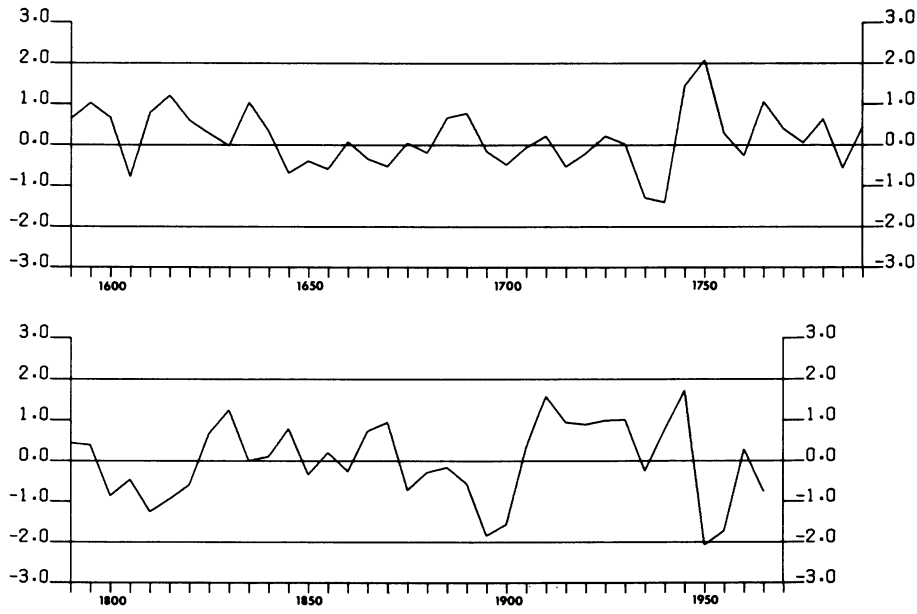

FIG. 33. Part 2.

low is due primarily to the fact that values for every year except 1421 fall below the mean. A period of high average departures carries the reconstruction beyond the abandonment of Arroyo Hondo.

In terms of individual years, the lowest value reconstructed for spring precipitation was in A.D. 1027 and the highest in 1042. Both of these years, however, are near the beginning of the tree-ring chronology where the error components and variances are high. During the period from A.D. 1250 to 1450, which includes the occupation at Arroyo Hondo, individual low years occurred in 1251, 1288, and 1347, all with reconstructed spring precipitation below two inches. An individual high in this period was reached in 1325, when precipitation exceeded seven inches.

RECONSTRUCTION OF ANNUAL PRECIPITATION

The reconstruction of precipitation for the 12-month tree response year extending from August of the previous year through July of the current year is presented in the form of yearly values (Table 22) and

plotted decade departures (Fig. 34). The general trends of the reconstructed annual precipitation are quite similar to those of the reconstructed spring rainfall. Between 990 and 1430, annual precipitation is characterized by high frequency and high amplitude. Annual precipitation during the 1430 to 1735 period is even less variable than spring precipitation during the same interval. Both reconstructions feature a low in the 1730s, followed by a high. The drought of the late nineteenth century, especially during the 1890s, appears to be a bit more pronounced in the annual reconstruction than in the spring reconstruction. The 1905 through 1945 high indicated in the spring reconstruction is present also in the annual values, as is the slight dip centered on 1935. A considerable annual low prevailed between 1950 and 1955.

During the Arroyo Hondo occupation period, the Great Drought of 1276–1299 is more severe in terms of annual precipitation than is indicated by the spring reconstruction. In addition, the annual departures are more variable, especially in the negative direction, during the Great Drought than are the spring departures for the same interval. This difference seems to indicate that nonspring precipitation was depressed more than spring rainfall during the Great Drought period in the upper Rio Grande Valley. The final step of the response function (Fig. 27) shows that the nonspring component of the annual regime is basically a fall and/or winter phenomenon rather than a late summer manifestation.

The 1295 to 1335 annual high interval is similar to that of the spring reconstruction except that the dip centered on 1320 is somewhat more pronounced in the former. The interval of high departures between 1295 and 1335 in both the annual and spring reconstructions for Santa Fe corresponds to a major, post–Great Drought maximum that is evident in tree-growth departures for much of the Colorado Plateau and that is especially pronounced in departures representing the central mountains of eastern Arizona and western New Mexico (Dean and Robinson, in press). The annual reconstruction for Santa Fe during the period from 1335 to 1400 exhibits the same high variability and the same high and low intervals as does the spring reconstruction. The sustained annual high from 1400 to 1415 is identical to that present in the spring values, as is the deep plunge centered on 1420. This low is the severest in the 1,000 years represented by the annual precipitation reconstruction, and as was the case with spring rainfall, it reflects the

TABLE 22.
Reconstructed annual (prior August through current July) precipitation for Arroyo Hondo, A.D. 985–1970 (in inches).

Date	0	1	2	3	4	5	6	7	8	9
985						11.4	15.1	16.3	16.9	16.5
990	12.4	10.0	11.2	9.8	15.9	15.8	15.2	17.0	13.7	8.4
1000	13.3	12.6	12.4	11.0	15.3	12.1	10.8	15.8	15.1	11.0
1010	9.8	11.2	15.4	14.5	9.9	12.8	17.4	13.1	12.0	10.0
1020	14.0	14.8	12.5	12.5	14.4	15.3	18.1	8.7	11.7	17.3
1030	12.4	11.5	12.8	14.6	13.4	10.0	14.6	14.0	14.9	11.9
1040	12.2	9.0	19.7	16.9	11.2	9.5	13.5	15.1	9.1	13.6
1050	17.7	11.1	18.6	15.9	11.7	13.4	14.0	15.7	12.0	12.1
1060	16.1	13.1	10.7	13.7	13.6	16.9	15.3	10.9	9.2	12.7
1070	15.5	13.8	14.3	12.9	15.8	11.4	13.9	14.2	12.7	11.9
1080	14.0	10.6	16.7	12.9	14.4	10.3	14.1	13.2	12.1	17.1
1090	11.1	11.5	14.1	13.7	10.7	15.6	17.5	12.3	9.8	10.5
1100	13.7	14.9	15.3	11.7	14.6	12.5	16.1	13.6	11.7	13.9
1110	14.4	13.9	14.4	14.7	11.5	11.9	14.8	16.9	14.4	13.9
1120	13.7	8.0	16.7	13.3	15.2	14.0	12.1	11.8	12.0	17.8
1130	13.9	10.4	10.4	15.5	11.5	9.9	14.5	13.8	11.5	14.2
1140	10.5	15.2	14.7	10.9	12.0	16.5	11.5	11.3	11.4	15.7
1150	11.8	10.6	17.6	14.3	13.7	13.6	11.3	10.4	10.3	16.6
1160	15.0	9.4	16.0	16.2	15.7	13.4	8.9	14.7	13.2	9.5
1170	12.4	19.0	14.0	13.2	9.9	16.0	12.6	11.8	14.2	14.1
1180	11.4	13.3	14.1	12.7	15.8	16.3	9.6	11.4	12.8	10.8
1190	14.1	18.4	13.3	11.5	11.8	14.7	14.8	14.1	13.1	11.9
1200	14.7	15.9	13.6	15.3	14.4	10.6	10.6	15.5	13.2	15.1
1210	13.4	13.7	13.5	15.2	13.5	12.7	10.9	9.8	12.4	16.8
1220	14.0	10.5	13.1	13.9	13.2	14.5	14.4	10.8	12.4	14.4
1230	16.3	14.6	14.0	11.9	10.8	14.7	12.7	13.7	14.1	14.7
1240	12.4	14.7	13.8	13.2	13.1	15.8	11.6	12.4	11.9	14.8
1250	13.4	10.1	11.0	16.2	11.2	13.3	13.0	14.5	11.6	14.2
1260	13.1	11.8	14.1	12.0	12.2	13.8	13.7	14.9	15.9	11.3
1270	13.2	14.1	13.4	11.8	12.9	15.4	11.7	13.8	11.8	14.7
1280	10.9	13.7	12.5	15.6	13.1	13.3	10.4	16.6	10.5	13.0
1290	18.5	11.0	11.5	14.0	12.2	14.6	11.6	13.3	15.6	14.5

TABLE 22. *(continued)*

Date	0	1	2	3	4	5	6	7	8	9
1300	14.0	14.6	14.9	12.1	11.0	14.5	14.3	13.9	11.3	13.9
1310	14.9	14.1	10.0	15.3	16.5	12.9	9.7	14.8	15.8	13.5
1320	13.3	13.9	13.6	12.5	11.1	17.7	15.4	12.2	10.8	13.0
1330	14.1	13.3	14.7	14.7	14.1	11.1	13.2	12.9	11.7	13.7
1340	13.1	13.2	11.9	14.5	14.3	15.1	15.1	9.5	11.6	14.6
1350	14.0	15.2	10.1	14.2	15.5	14.0	13.1	12.3	15.0	15.2
1360	10.2	13.8	13.0	11.3	12.0	16.3	14.7	11.8	13.9	10.7
1370	14.7	14.1	15.7	13.3	13.7	11.4	12.0	11.9	14.8	14.3
1380	13.6	13.3	10.8	15.7	12.5	12.8	13.9	13.2	13.2	15.8
1390	11.4	10.9	13.0	13.2	13.7	16.7	13.2	9.4	15.2	11.6
1400	11.7	13.9	14.4	12.9	16.2	13.4	14.4	10.8	14.0	14.5
1410	14.4	11.1	14.8	12.9	16.8	11.7	11.5	13.0	12.9	13.0
1420	12.4	15.5	13.3	10.6	10.4	14.0	14.3	14.9	17.3	12.2
1430	11.8	13.7	12.0	14.2	14.6	15.0	12.7	12.7	11.8	14.8
1440	14.0	14.2	13.9	15.3	13.0	9.7	13.9	15.4	14.2	12.1
1450	11.1	13.6	13.2	13.6	14.5	12.3	11.3	13.3	15.0	13.3
1460	12.9	11.2	14.0	13.1	12.5	13.6	15.1	14.7	14.0	14.7
1470	12.1	9.8	14.2	14.6	12.7	10.6	13.7	12.2	14.8	15.1
1480	11.1	12.1	13.7	13.2	14.8	14.6	16.8	11.6	11.3	13.7
1490	15.2	13.7	14.0	12.0	14.4	10.4	11.9	12.5	14.4	15.7
1500	12.3	12.4	15.1	13.9	11.9	15.0	10.8	13.3	13.5	12.9
1510	13.5	14.6	12.3	13.7	15.3	15.6	9.4	10.7	14.1	14.6
1520	13.9	16.3	13.4	12.2	10.2	13.6	13.5	13.2	13.5	15.4
1530	14.2	13.9	11.9	12.7	14.6	11.5	14.3	14.2	13.1	13.0
1540	15.8	15.1	9.9	13.8	14.9	12.1	10.7	13.5	14.1	12.4
1550	14.7	12.0	12.3	15.5	15.0	14.6	13.8	13.1	12.0	14.5
1560	11.8	13.0	10.9	13.4	13.6	14.8	13.0	12.6	13.3	14.6
1570	13.8	12.6	13.9	11.0	12.2	13.5	13.8	15.4	14.6	11.2
1580	10.3	13.0	14.1	12.2	12.7	11.5	14.6	13.5	13.8	15.1
1590	12.3	12.3	14.2	12.4	15.0	14.8	15.2	16.2	11.7	12.5
1600	12.2	10.6	12.7	15.3	14.8	14.3	12.2	13.1	12.3	13.0
1610	15.0	15.0	14.4	13.7	12.9	14.0	11.3	12.8	15.7	13.0
1620	13.6	15.4	13.7	15.1	11.7	10.5	12.7	14.4	11.4	15.0
1630	14.5	13.1	13.0	13.2	14.1	14.8	14.1	15.1	11.0	13.5
1640	15.0	11.8	12.1	14.1	13.7	11.3	14.1	14.4	12.1	13.2

TABLE 22. *(continued)*

Date	0	1	2	3	4	5	6	7	8	9
1650	12.4	14.4	14.6	13.1	11.9	13.7	13.6	13.3	12.6	11.8
1660	13.3	14.6	16.0	14.2	10.8	13.3	12.5	12.1	12.7	13.0
1670	12.8	13.5	13.4	13.8	14.5	13.6	11.6	13.5	12.5	13.5
1680	15.6	13.4	12.7	14.7	12.7	9.4	12.8	14.7	14.0	15.9
1690	13.6	11.5	15.2	13.6	13.6	14.2	11.3	13.3	12.2	14.2
1700	13.5	14.3	12.1	14.1	13.4	11.2	14.4	13.3	14.1	12.6
1710	14.6	12.7	13.4	15.1	12.7	11.3	10.9	14.3	15.1	11.7
1720	14.5	14.5	12.8	13.6	13.7	12.6	14.6	14.9	13.9	9.8
1730	11.1	13.7	14.9	13.3	14.6	12.7	13.3	11.4	12.9	11.0
1740	12.6	13.6	13.6	14.8	13.0	13.5	15.8	17.6	10.0	13.3
1750	12.4	15.7	11.7	13.3	16.0	15.5	13.3	10.0	12.6	14.0
1760	11.7	14.7	16.3	10.9	14.1	12.3	13.9	13.9	14.6	14.1
1770	13.8	15.8	14.8	9.6	11.6	13.7	14.5	13.5	13.7	13.1
1780	11.1	13.2	12.7	14.3	16.0	12.8	10.9	15.6	13.3	11.4
1790	11.8	14.3	15.1	16.3	13.8	11.6	12.0	11.4	13.5	14.2
1800	14.4	11.6	13.0	13.4	14.8	13.2	11.3	13.9	14.1	12.7
1810	13.0	13.7	12.8	13.5	11.4	13.4	16.3	14.4	12.2	9.8
1820	12.6	15.4	12.0	11.7	13.3	14.5	12.0	14.0	15.0	15.2
1830	12.7	12.3	12.2	14.1	15.9	12.7	9.5	13.3	14.5	15.5
1840	16.0	15.3	9.9	12.3	14.9	12.9	14.4	11.2	11.1	17.6
1850	15.2	10.1	11.2	13.5	14.7	13.9	14.3	15.0	15.5	11.8
1860	11.9	11.2	12.9	13.1	13.1	13.3	15.7	15.4	14.6	14.4
1870	11.9	11.6	14.0	12.0	13.5	12.5	13.8	15.5	12.9	13.5
1880	10.9	12.7	14.9	12.2	13.0	14.6	13.7	15.1	15.3	11.1
1890	9.3	14.2	14.8	10.3	13.4	13.7	11.6	15.9	13.8	9.7
1900	12.9	14.1	14.4	13.8	9.0	14.2	15.5	16.0	13.7	11.6
1910	10.3	13.0	15.6	15.1	13.7	13.2	15.7	11.5	10.8	15.6
1920	17.2	16.0	12.0	13.2	11.8	9.3	15.5	14.0	14.0	14.4
1930	13.7	13.1	17.1	14.9	9.5	12.7	11.7	15.4	11.7	12.2
1940	14.6	15.1	14.1	14.7	13.7	12.5	13.4	11.3	13.3	16.9
1950	11.9	10.0	12.6	11.6	13.0	12.9	13.3	12.0	15.3	14.6
1960	16.3	11.7	11.9	12.9	13.3	14.1	12.6	11.2	12.6	14.6
1970	14.2									

Mean = 13.337 Standard Deviation = 2.16

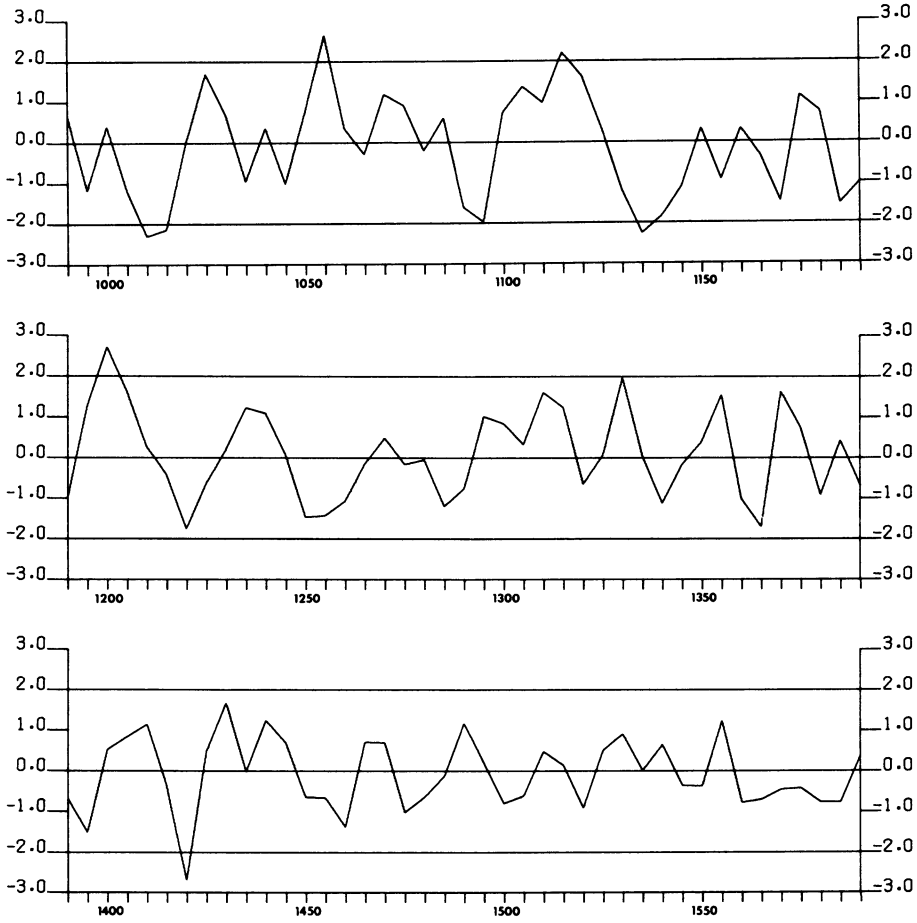

FIG. 34. Reconstruction of 12-month precipitation for Arroyo Hondo, A.D. 985 to 1970.

fact that all years in the decade but 1421 and 1422 fall below the mean. Annual precipitation for the 1425 to 1450 period is basically similar to the spring reconstruction for the same period, although a higher annual value for the 1440 decade indicates that that interval was characterized by a relatively high nonspring component coupled with a spring "drought."

The annual extremes in the total record show some interesting parallels to the spring reconstruction and some differences. The lowest individual year was 1121 and the highest 1171. Both years, again, are at the early end of the tree-ring chronology, but they do not coincide

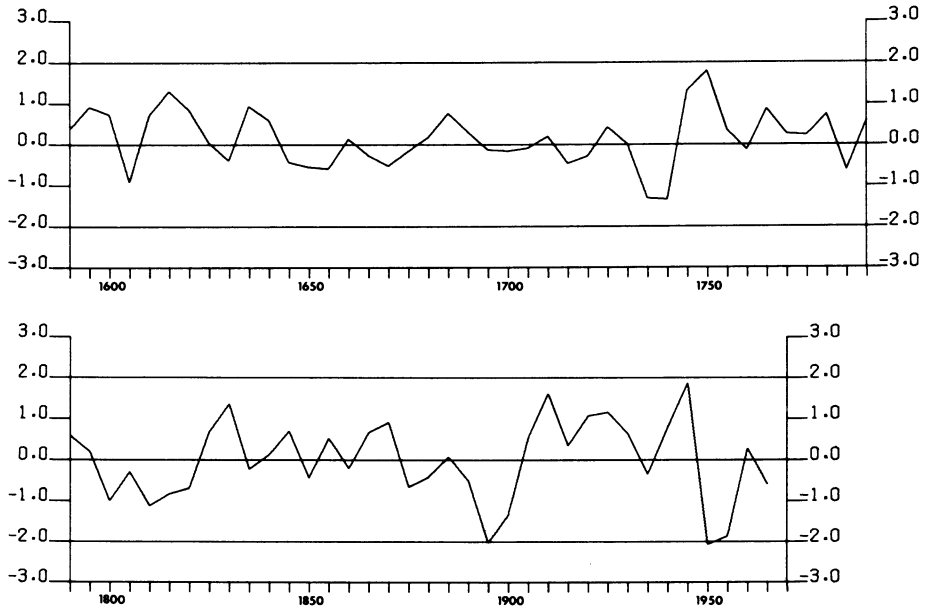

FIG. 34. Part 2.

with the spring maximum and minimum. Between A.D. 1250 and 1450, years with less than 10 inches of reconstructed annual precipitation were 1316, 1347, 1397, and 1445. The highs, exceeding 17 inches, were 1290, 1325, and 1428.

SIGNIFICANCE OF THE SANTA FE DENDROCLIMATIC RECONSTRUCTIONS

The dendroclimatic analyses isolated two elements of Santa Fe climate that account for much of the variance in local piñon growth: spring (March through June) and annual (August through July) precipitation. Late summer rainfall of the previous year appears to contribute very little to growth. This suggests that the late-summer component of the annual precipitation regime is fairly stable and less variable than other components. The low coefficients of variability of contemporary July and August rainfall at Santa Fe support this inference.

The more variable spring to early summer rainfall may have been of greater importance to Puebloan subsistence than was the more stable

late summer precipitation. Spring is the period of seed germination of the traditional Pueblo crops. Thus, we can view the Santa Fe tree-ring evidence as a relative measure of seed germination if not of crop harvest. And if late summer rainfall is as stable as suggested, germination may have been the controlling factor in successful farming at Arroyo Hondo. Unfortunately, our dendroclimatic analyses do not provide accurate reconstructions of spring temperatures, which may have been a critical factor in the agricultural equation.

The dendroclimatic reconstruction provides a detailed, synoptic picture of local climate during the occupation of Arroyo Hondo. The Great Drought, though less severe than in areas farther west, was certainly felt in the upper Rio Grande Valley. Its effects, however, were surely moderated by the perennial flow of the Rio Grande and its major tributaries. The period from A.D. 1295 to 1335 appears to represent two generations of consistently above-average precipitation, especially in the spring and early summer. Such conditions would have been extremely beneficial for seed germination. This interval coincides with the initial settlement and growth of Arroyo Hondo Pueblo. The greater variability in precipitation between 1335 and 1400 may well have required adaptive behavioral responses on the part of the residents of Arroyo Hondo. The archaeological record might be expected to produce evidence of changes in resource exploitation or even abandonment of the site during this time. The last favorable precipitation interval during the occupation of Arroyo Hondo, A.D. 1400–1415, was terminated by the most intense drought of the entire Santa Fe dendroclimatic record, A.D. 1415–1425. This drought coincides with the final abandonment of Arroyo Hondo Pueblo.

Addendum

Since this paper was first submitted to the School of American Research in March, 1978, we have produced additional dendroclimatic reconstructions for the Santa Fe area. Unlike the locality-level analysis employed in the Arroyo Hondo study, which involves relationships between a single tree-ring chronology and a single weather record, the more recent reconstructions are based on the calibration of a spatial network of tree-ring chronologies and weather stations that covers northwestern New Mexico and extreme southwestern Colorado. Lack of space precludes discussion here of the network calibration, verification, and retrodiction techniques, which differ from those employed in the Arroyo Hondo locality study. The network analyses will be fully described in a forthcoming master's thesis by Rose.

In the network study, eighteen tree-ring chronologies were used to reconstruct past climatic variables for the period from A.D. 1650 to 1970, and seven chronologies were used for the A.D. 900–1649 interval. The use of multiple sets of independent variables (the eighteen and seven tree-ring chronologies) to retrodict climatic variables is potentially superior to the matched-pair, locality technique of the Arroyo Hondo study in two ways. First, the use of several independent variables should produce better reconstructions for individual loci within the spatial grid. This is so because multiple independent variables applied to the reconstruction of climatic values for any one locus should explain more of the variance in the dependent variable than would be explained by a single independent variable. Second, the greater predictive power of several independent variables should, in most cases,

provide reconstructions for more climatic variables than can be produced by a single independent variable.

Because the Santa Fe climatic tree-ring chronology is included in both the eighteen and the seven station grids and because the Santa Fe weather data are used in the network calibration, the northwestern New Mexico study is capable of providing "point" reconstructions of various climatic variables for the Santa Fe locality. The dependent climatic variables chosen for reconstruction in the northwestern New Mexico study are average temperature and total precipitation for the hydrological year (October through the following September), winter (November through February), spring (March through June), prior summer (previous July through previous September), and current summer. Reconstructed annual and spring precipitation values based on the network analysis do not differ appreciably from those of the Arroyo Hondo locality reconstructions (Tables 21 and 22), and the former are not presented in this addendum. The two "annual" reconstructions are not directly comparable because they represent different time periods—August through July and October through September. The Arroyo Hondo and network spring reconstructions, however, cover the same interval (March through June) and are quite similar, with means of 4.21 inches and 4.12 inches and standard deviations of 1.8 inches and 1.03 inches. Correlation of the two reconstructed spring rainfall series yields a correlation coefficient of +0.87. These results provide strong confirmation of the original Arroyo Hondo locality-level reconstructions of annual and spring precipitation in the Santa Fe area.

References

AMOS, D. E., AND L. H. KOOPMANS

1963 *Tables of the Distribution of the Coefficient of Coherence for Stationary Bivariate Gaussian Processes*, Sandia Corporation Monograph SCR-483 (Albuquerque).

AYRES, FRANK, JR.

1972 *Theory and Problems of Matrices*, Schaum's Outline Series (New York: McGraw-Hill Book Company).

BLACKMAN, R. B., AND J. W. TUKEY

1958 *The Measurement of Power Spectra from the Point of View of Communication Engineering* (New York: Dover).

BLALOCK, HUBERT M., JR.

1972 *Social Statistics* (New York: McGraw-Hill Book Company).

BLASING, TERENCE JACK

1975 "Methods for Analyzing Climatic Variations in the North Pacific Sector and Western North America for the Last Few Centuries," Ph.D. diss., University of Wisconsin.

BLASING, T. J., AND HAROLD C. FRITTS

1975 "Past Climate of Alaska and Northwestern Canada as Reconstructed from Tree Rings," in *Climate of the Arctic*, ed. G. Weller and S. A. Bowling, Proceedings of the 24th Alaska Scientific Conference, pp. 48–58.

1976 "Reconstruction of Past Climatic Anomalies in the North Pacific and Western North America from Tree-Ring Data," *Quaternary Research* 6:563–79.

BOX, GEORGE E. P., AND GWILYM M. JENKINS

1976 *Time Series Analysis: Forecasting and Control* (San Francisco: Holden-Day).

BRIER, G. W.
1961 "Some Statistical Aspects of Long-Term Fluctuations in Solar and Atmospheric Phenomena," *Annals of the New York Academy of Sciences* 95:173–87.

BRILLINGER, DAVID R.
1974 *Time Series: Data Analysis and Theory* (New York: Holt, Rinehart, and Winston).

BRONITSKY, GORDON J.
1977 "An Ecological Model of Trade: Prehistoric Economic Change in the Northern Rio Grande Region of New Mexico," Ph.D. diss., University of Arizona.

BROWN, JAMES M.
1968 "The Photosynthetic Regime of Some Southern Arizona Ponderosa Pine," Ph.D. diss., University of Arizona.

BUDELSKY, CARL
1969 "Variation in Transportation and Its Relationship with Growth for *Pinus ponderosa* Lawson in Southern Arizona," Ph.D. diss., University of Arizona.

COOLEY, W. W., AND P. R. LOHNES
1971 *Multivariate Data Analysis* (New York: John Wiley and Sons).

DEAN, JEFFREY S., AND WILLIAM J. ROBINSON
1977 "Dendroclimatic Variability in the American Southwest, A.D. 680 to 1970," final report to the National Park Service, Department of the Interior, Contract CX 1595-5-0241, by the Laboratory of Tree-Ring Research, University of Arizona, Tucson.

1978 *Expanded Tree-Ring Chronologies for the Southwestern United States*, Laboratory of Tree-Ring Research, Chronology Series 3 (Tucson).

in press "Dendrochronology of Grasshopper Pueblo," in *Multidisciplinary Research at the Grasshopper Ruin*, ed. William A. Longacre, Anthropological Papers of the University of Arizona (Tucson: University of Arizona Press).

DOUGLASS, ANDREW ELLICOTT
1914 "A Method of Estimating Rainfall by the Growth of Trees," in *The Climatic Factor*, by Ellsworth Huntington, Carnegie Institution of Washington, Publication 192, pp. 101–22.

1936 *Climatic Cycles and Tree Growth, Vol. III, A Study of Cycles*, Carnegie Institution of Washington, Publication 289.

DRAPER, N. R., AND H. SMITH
1966 *Applied Regression Analysis* (New York: John Wiley and Sons).

DURBIN, J., AND G. S. WATSON
1951 "Testing for Serial Correlation in Least-Squares Regression," *Biometrika* 38: 159–78.

FREUND, JOHN E.
1969 *Statistics–A First Course* (Englewood Cliffs: Prentice-Hall).

FRITTS, HAROLD C.
1962 "An Approach to Dendroclimatology: Screening by Means of Multiple Regression Techniques," *Journal of Geophysical Research* 67:1413–20.

1965 "Tree-Ring Evidence for Climatic Changes in Western North America," *Monthly Weather Review* 93:421–43.

1966 "Growth Rings of Trees: Their Correlation with Climate," *Science* 154:973–79.

1969 *Bristlecone Pine in the White Mountains of California: Growth and Ring-Width Characteristics*, Papers of the Laboratory of Tree-Ring Research 4 (Tucson: University of Arizona Press).

1970 "Tree-Ring Analyses and Reconstruction of Past Environments," in *Tree-Ring Analysis with Special Reference to Northwest America*, ed. J. H. G. Smith and J. Worrall, University of British Columbia, Faculty of Forestry, Bulletin 7, pp. 92–98.

1971 "Dendroclimatology and Dendroecology," *Quaternary Research* 1:419–49.

1974 "Relationships of Ring Widths in Arid-Site Conifers to Variations in Monthly Temperature and Precipitation," *Ecological Monographs* 44:411–40.

1976 *Tree Rings and Climate* (London: Academic Press).

FRITTS, HAROLD C., AND DAVID J. SHATZ
1975 "Selecting and Characterizing Tree-Ring Chronologies for Dendroclimatic Analysis," *Tree-Ring Bulletin* 35:31–40.

FRITTS, HAROLD C., JAMES E. MOSIMANN,
AND CHRISTINE P. BOTTORFF
1969 "A Revised Computer Program for Standardizing Tree-Ring Series," *Tree-Ring Bulletin* 29:15–20.

FRITTS, HAROLD C., DAVID G. SMITH, AND MARVIN A. STOKES
1965 "The Biological Model for Paleoclimatic Interpretation of Mesa Verde Tree-Ring Series," in *Contributions of the Wetherill Mesa Archeological Project*, assembled by Douglas Osborne, Memoir of the Society for American Archaeology 19, pp. 101–21.

FRITTS, HAROLD C., T. J. BLASING, B. P. HAYDEN, AND JOHN KUTZBACH
1971 "Multivariate Techniques for Specifying Tree-Growth and Climate Relationships and for Reconstructing Anomalies in Paleoclimate," *Journal of Applied Meteorology* 10:845–64.

FRITTS, HAROLD C., DAVID G. SMITH, JOHN A. CARDIS, AND CARL BUDELSKY
1965 "Tree-Ring Characteristics Along a Vegetation Gradient in Northern Arizona," *Ecology* 46:393–401.

HARRIS, RICHARD J.
1975 *A Primer of Multivariate Statistics* (New York: Academic Press).

HOLLANDER, MYLES, AND DOUGLAS A. WOLFE
1973 *Nonparametric Statistical Methods* (New York: John Wiley and Sons).

HOLLOWAY, J. L., JR.
1958 "Smoothing and Filtering of Time Series and Space Fields," in *Advances in Geophysics*, vol. 4, ed. H. E. Landsberg (New York: Academic Press), pp. 351–89.

JENKINS, G. M., AND D. G. WATTS
1968 *Spectral Analysis and Its Applications* (San Francisco: Holden-Day).

JORDE, L. B.
1977 "Precipitation Cycles and Cultural Buffering in the Prehistoric Southwest," in *For Theory Building in Archaeology*, ed. Lewis R. Binford (New York: Academic Press), pp. 385–96.

JULIAN, PAUL R., AND HAROLD C. FRITTS
1968 "On the Possibility of Quantitatively Extending Precipitation Records by Means of Dendroclimatological Analysis," *Proceedings of the First Statistical Meteorological Conference* (Hartford: American Meteorological Society), pp. 76–82.

KEMRER, MEADE F., WILLIAM J. ROBINSON, AND JEFFREY S. DEAN
1971 "Tree-Rings as Indicators of Intra-Annual Climate," 1968–69 and 1969–70 annual reports to the National Park Service, Department of the Interior, by the Laboratory of Tree-Ring Research, University of Arizona, Tucson.

KERLINGER, F. N., AND E. PEDHAZER
1973 *Multiple Regression in Behavioral Research* (New York: Holt, Rinehart, and Winston).

KOHLER, M.A.
1949 "On the Use of Double-Mass Analysis for Testing the Consistency of Meteo-

rological Records and for Making Required Adjustments," *Bulletin of the American Meteorological Society* 30:188–89.

KOOPMANS, L. H.
1974 *The Spectral Analysis of Time Series* (New York: Academic Press).

LAMARCHE, VALMORE C., JR.
1974 "Frequency-Dependent Relationships between Tree-Ring Series along an Ecological Gradient and Some Dendroclimatic Implications," *Tree-Ring Bulletin* 34:1–20.

LAMARCHE, VALMORE C., JR., AND HAROLD C. FRITTS
1972 "Tree-Rings and Sunspot Numbers," *Tree-Ring Bulletin* 32:19–32.

LORENZ, E. N.
1956 *Empirical Orthogonal Functions and Statistical Weather Prediction*, M. I. T. Statistical Forecasting Project, Scientific Report 1 (Cambridge: Massachusetts Institute of Technology).

MITCHELL, J. M., JR., B. DZERDZEEVSKII, H. FLOHN, W. L. HOFMEYR, H. H. LAMB, K. N. RAO, AND C. C. WALLEN
1966 "Climatic Change," World Meteorological Organization, Technical Note 79 (Geneva).

NIE, NORMAN H., C. HADLAI HULL, JEAN G. JENKINS, KARIN STEINBRENNER, AND DALE H. BENT
1975 *SPSS Statistical Package for the Social Sciences*, 2d edition (New York: McGraw-Hill Book Company).

ROBINSON, WILLIAM J., AND JEFFREY S. DEAN
1969 "Tree-Ring Evidence for Climatic Change in the Prehistoric Southwest, A.D. 1000 to 1200," annual report to the National Park Service, Department of the Interior, Contract 14-10-7:931–8, by the Laboratory of Tree-Ring Research, University of Arizona, Tucson.

ROBINSON, WILLIAM J., BRUCE G. HARRILL, AND RICHARD L. WARREN
1973 *Tree-Ring Dates from New Mexico J–K, P, V: Santa Fe–Pecos–Lincoln Area* (Tucson: Laboratory of Tree-Ring Research, University of Arizona).

ROSCOE, JOHN T.
1969 *Fundamental Research Statistics for the Behavioral Sciences* (New York: Holt, Rinehart, and Winston).

SCHOENWETTER, JAMES
1962 "Pollen Analysis of Eighteen Archaeological Sites in Arizona and New Mexico," in *Chapters in the Prehistory of Eastern Arizona, I*, by Paul S. Martin et al., Fieldiana: Anthropology 53, pp. 168–209.

SCHULMAN, EDMUND
1956 *Dendroclimatic Changes in Semiarid America* (Tucson: University of Arizona Press).

SNEDECOR, GEORGE W., AND WILLIAM G. COCHRAN
1967 *Statistical Methods*, 6th edition (Ames: Iowa State University Press).

SPIEGEL, MURRAY R.
1961 *Theory and Problems of Statistics*, Schaum's Outline Series (New York: McGraw-Hill Book Company).

STOCKTON, CHARLES W.
1975 *Long-Term Streamflow Records Reconstructed from Tree Rings*, Papers of the Laboratory of Tree-Ring Research 5 (Tucson: University of Arizona Press).

STOCKTON, CHARLES W., AND HAROLD C. FRITTS
1971a "Augmenting Annual Runoff Records Using Tree-Ring Data," *Hydrology and Water Resouces in Arizona and the Southwest* 1:1–12, Proceedings of the 1971 meetings of the Arizona section of the American Water Resources Association and the Hydrology section of the Arizona Academy of Science, Tempe.

1971b "Conditional Probability of Occurrence for Variations in Climate Based on Width of Annual Tree Rings in Arizona," *Tree-Ring Bulletin* 31:3–24.

STOKES, MARVIN A., AND TERAH L. SMILEY
1968 *An Introduction to Tree-Ring Dating* (Chicago and London: University of Chicago Press).

TATSUOKA, MAURICE
1974 *Multivariate Analysis: Techniques for Educational and Psychological Research* (New York: John Wiley and Sons).

THOM, H. C. S.
1966 "Some Methods of Climatological Analysis," World Meteorological Organization, Technical Note 81 (Geneva).

WESOLOWSKY, GEORGE O.
1976 *Multiple Regression and Analysis of Variance: An Introduction for Computer Users in Management and Economics* (New York: John Wiley and Sons).